University of Kentucky

UKnowledge

2024

Complexity, Entanglement and Codes in Quantum Field Theory

Nikolaos Angelinos
University of Kentucky, nickangs@gmail.com
Author ORCID Identifier:
https://orcid.org/0000-0003-0246-0089
Digital Object Identifier: https://doi.org/10.13023/etd.2024.272

Right click to open a feedback form in a new tab to let us know how this document benefits you.

Complexity, Entanglement and Codes in Quantum Field Theory

—————————————

DISSERTATION

—————————————

A dissertation submitted in partial
fulfillment of the requirements for
the degree of Doctor of Philosophy
in the College of Arts and Sciences
at the University of Kentucky

By
Nikolaos Angelinos
Lexington, Kentucky

Director: Dr. Anatoly Dymarsky, Professor of Physics
Lexington, Kentucky
2024

ABSTRACT OF DISSERTATION

Complexity, Entanglement and Codes in Quantum Field Theory

In recent decades many deep connections between quantum information theory and quantum field theory have been unearthed. In this dissertation we study topics in high-energy physics through the lens of quantum information: 1) We develop connections between error-correcting codes and Narain conformal field theories. 2) We study the entanglement entropy of one-dimensional fermionic chains with long-range interactions. 3) We study the temperature dependence of Lanczos coefficients and Krylov complexity.

KEYWORDS: conformal field theory, complexity, codes, entanglement entropy

Nikolaos Angelinos

July 22, 2024

Complexity, Entanglement and Codes in Quantum Field Theory

By
Nikolaos Angelinos

Dr. Anatoly Dymarsky	
Director of Dissertation	
Dr. Anatoly Dymarsky	
Director of Graduate Studies	
July 22, 2024	
Date	

TABLE OF CONTENTS

LIST OF TABLES

LIST OF FIGURES

Chapter 1 Introduction

Quantum information has proven to be a powerful tool in advancing our understanding of physics. Besides the ability of quantum computers to efficiently simulate complex quantum systems, mathematical concepts from quantum information theory—such as entanglement, complexity, and error-correcting codes—have found significant applications in high-energy physics, offering a fresh perspective on quantum field theory and gravity.

In the quest for a theory of quantum gravity, it is often said that our classical theory of gravity is incompatible with quantum theory. However, recent developments suggest that gravity can emerge from complex patterns of quantum information, supporting the view that quantum mechanics is the fundamental theory of nature, while gravity is an emergent phenomenon.

Over the past two decades, numerous deep connections between quantum information, quantum field theory, and gravity have been uncovered, with early hints appearing even further back. One of the earliest indications emerged in 1973 when it was recognized that thermodynamics has many parallels with black holes [1]. This connection was further strengthened when the entropy of a black hole was identified with its surface area [2], which was also an early manifestation of the holographic principle.

A concrete realization of the holographic principle, the AdS/CFT correspondence [3] has played a pivotal role in discovering the connections between quantum information and gravity. This correspondence conjectures a duality between gravity in a $(d + 1)$-dimensional anti-de Sitter (AdS) space-time and a conformal field theory (CFT) existing on its d-dimensional boundary. Concepts such as quantum error-correction, entanglement entropy (EE) and complexity are crucial in understanding how information is encoded in this correspondence.

Entanglement entropy in the AdS/CFT framework acquires a concrete geometric interpretation, as the Ryu-Takayanagi (RT) formula [4] and its extensions establish a connection between the entanglement entropy of the boundary CFT and the minimal surface area within the bulk. In this context, dynamics of gravity are closely related to dynamics of entanglement [5], indicating that the space-time's geometry arises from the entanglement pattern inherent in the quantum state.

Moreover, the concept of quantum error-correction, vital for building robust quantum computers, finds application in the study of space-time. The way information is protected in a quantum code has parallels with how local bulk information is encoded in the AdS/CFT correspondence [6]. Tensor networks, which provide toy models for holography, realize the error-correcting features of AdS/CFT [7], helping us understand how space-time can emerge from a more fundamental quantum information description.

A description of Narain CFTs in terms of codes [8] opened another path for formulating gravity in terms of error-correcting codes. Recent advances suggest that low-dimensional gravity is dual not to a single boundary theory, but rather an en-

semble of theories [9]. A toy model of 3d gravity, called "$U(1)$ gravity", was found to be dual to the ensemble of Narain CFTs [10]. A generalization of the code description of Narain CFTs (see Chapter 3) has enabled our understanding of how "$U(1)$" gravity emerges from ensembles of codes [11].

Complexity is another quantity that acquires geometric meaning in holography. The complexity of an object refers to the number of "simple" objects required to build it. Specifically, for an extended quantum system, one could ask: how many local operators are needed to build a specific state starting from a fully unentangled state? This notion of complexity is known as circuit complexity. For holographic states, circuit complexity is conjectured to be related either to the volume of a maximal space-like slice [12], or the action of a region in the space-time [13].

Quantum information, under time evolution, tends to spreads across many degrees of freedom; a spreading that is governed by universal laws. Within a chaotic system, quantum information spreads rapidly throughout the entire system, transforming "simple" operators into complex multi-particle operators. This phenomenon, known as scrambling, can be described in terms of out-of-time-order correlation functions (OTOCs), which exhibit exponential growth in large-N systems. The rate of this growth, characterized by the "Lyapunov exponent" λ, is constrained by the universal Maldacena-Shenker-Stanford (MSS) bound, $\lambda \leq \frac{2\pi}{\beta}$, where β is the inverse temperature [14].

Krylov complexity, proposed as a bridge between OTOCs and traditional indicators of chaos [15] measures the average position of an operator within the Krylov basis as it evolves over time. In chaotic systems, Krylov complexity grows exponentially, with its exponent λ_K acting as an upper limit for the Lyapunov exponent ($\lambda \leq \lambda_K$) at infinite temperature, and it is conjectured to hold true at finite temperatures as well. This inequality is suggested to be part of a generalized MSS bound $\lambda \leq \lambda_K \leq \frac{2\pi}{\beta}$ [16]. Dynamics in the Krylov space are encoded by the sequence of Lanczos coefficients. The temperature-dependence of this sequence is governed by integrable Hamiltonian dynamics (see Chapter 6), and the characteristics of Krylov complexity at low temperatures exhibit universal traits.

The structure of this dissertation is as follows. In Chapter 2 we give an introduction to error-correcting codes and their generalizations, as well as a brief introduction to Narain CFTs. In Chapter 3, we construct the known (conjectured) optimal Narain CFTs for central charge up to $c = 8$ from codes. By performing an average over codes, we find that asymptotically, for large-c, the spectral gap Δ grows linearly with c, saturating the conjectured upper bound $\Delta \sim \frac{c}{2\pi e}$. In Chapter 4, we use codes to construct the RCFTs described by A, D, E affine Lie algebras at level 1. We show that classification of modular invariants is equivalent to classification of all self-dual codes with alphabets based on the discriminant groups of the A, D, E root lattices. Finally, we show how Poincaré sums can be phrased and evaluated in terms of codes.

In Chapter 5, we study the entanglement entropy of 1-dimensional fermion chains with long-range interactions, with a parameter α controlling the range of the interactions. We find that the EE in systems with a smooth IR limit obey area law, governed by the CFT at their IR fixed point. However, systems without smooth IR limit, such

as disordered systems, are not constrained to obey area law. We show, numerically, that such systems show intermediate fractal scaling of EE, as they transition from volume to area law, while α is increased.

In Chapter 6, we formulate the temperature dependence of Lanczos coefficients as an integrable Hamiltonian system. Specifically, this system is related to the Toda hierarchy. We identify two effects that cause "staggering" in the Lanczos sequence at finite temperature and illustrate them using examples.

Chapter 2 An introduction to codes and Narain CFTs

An error-correcting code is a method of introducing redundancies into a message transmitted over a noisy channel to protect against data loss or corruption. For example, consider the transmission of a single binary bit, 1, over a noisy channel. The receiver, in this case, cannot determine whether the received bit is correct or has been corrupted by noise.

To address this problem, the sender can construct a string (codeword) containing three copies of the bit:

$$c = (1, 1, 1).$$

This is known as the "repetition code." During transmission, some bits may be corrupted. The receiver can attempt to reconstruct the original message by taking a majority vote of the received message. This code can detect up to two-bit errors but can only correct single-bit errors. To provide better protection, one can send a string containing more copies of the initial bit. Clearly, there is a trade-off between efficiency and error-correcting capabilities.

A code can be defined abstractly as a subset $\mathcal{C}$ of G^n, where G is an alphabet. If G is an additive group, we can build additive codes, which have an additional structure: the sum of any two codewords is also a codeword, i.e., $\mathcal{C}$ is a $\mathbb{Z}$-module. If G is a field, we can define G-linear codes, requiring that $\mathcal{C}$ is a G-linear vector space. In this dissertation, we are not interested in the error-correcting properties of codes. Instead, we use codes to aid in the study of 2-dimensional conformal field theories.

2.1 Classical binary codes

A binary code $\mathcal{C}$ is a $\mathbb{Z}_2$-linear subspace of $\mathbb{Z}_2^n$. The elements of $\mathcal{C}$ are called **codewords**. Let G be the **generator matrix**, a $k \times n$ binary matrix ($k \leq n$) whose rows form a basis of $\mathcal{C}$. This matrix is a linear map from $\mathbb{Z}_2^k$ to $\mathcal{C}$, which maps a string x of **logical bits** into a codeword c

$$c = xG, \quad x \in \mathbb{Z}_2^k. \tag{2.1}$$

We equip the space $\mathbb{Z}_2^n$ with a bi-linear form (or inner product)

$$\langle a|b \rangle = \sum_{i=1}^{n} a_i b_i. \tag{2.2}$$

Now, for a code $\mathcal{C}$, we can define the **dual code** $\mathcal{C}^{\perp}$, as follows

$$\mathcal{C}^{\perp} = \{c' \in \mathbb{Z}_2^n : \langle c'|c \rangle = 0 \; \forall c \in \mathcal{C}\}. \tag{2.3}$$

Note that $(\mathcal{C}^{\perp})^{\perp} = \mathcal{C}$. A code $\mathcal{C}$ is **self-dual** if $\mathcal{C} = \mathcal{C}^{\perp}$. Since $|\mathcal{C}||\mathcal{C}^{\perp}| = |\mathbb{Z}_2^n| = 2^n$, it follows that a self-dual code exists only if n is even and it consists of $|\mathcal{C}| = 2^{n/2}$ codewords.

The generator H of $\mathcal{C}^{\perp}$, an $n - k \times n$ matrix, is also called the **parity check matrix** of $\mathcal{C}$. It satisfies $cH^T = 0$ if and only if $c \in \mathcal{C}$, therefore if $cH^T \neq 0$ we can be certain that an error has occurred. The converse is not true; if an error occurs, cH^T is not zero necessarily. This is because some errors may transform a codeword within the code subspace $\mathcal{C}$. Such errors change more bits than the Hamming distance of the code, which we will define next.

In order for the code to be good at detecting and correcting errors, we need to be able to easily distinguish between codewords. To make this notion more precise, define the **Hamming weight**, $w(c)$ of a codeword c as the number of its non-zero elements. The **Hamming distance** $d_{\mathcal{C}}$ of a code $\mathcal{C}$ is the minimum weight of its non-zero codewords

$$d_{\mathcal{C}} = \min_{c \in \mathcal{C}, \ c \neq 0} \{w(c)\}. \tag{2.4}$$

A code can detect errors that corrupt up to $d_{\mathcal{C}}$ bits, while it can correct errors that corrupt up to $\lfloor \frac{d_{\mathcal{C}} - 1}{2} \rfloor$ bits. A code is called **even** if the Hamming weights of all its codewords are divisible by 2.

A useful quantity that encodes important properties of a code is the **weight enumerator polynomial**. It is a homogeneous polynomial of two variables

$$W_{\mathcal{C}}(x_0, x_1) = \sum_{c \in \mathcal{C}} x_0^{n-w(c)} x_1^{w(c)} = \sum_{k=0}^{n} A_k x_1^k x_0^{n-k}, \tag{2.5}$$

where $w(c)$ is the Hamming weight of c. The coefficients A_k are positive integers that count the number of codewords of weight k and satisfy $\sum A_k = |\mathcal{C}|$. Uniqueness of the zero codeword imples $A_0 = 1$.

Two codes $\mathcal{C}, \mathcal{C}'$ are called **equivalent** if there exists a bijective map $\mathcal{C} \to \mathcal{C}'$ that preserves the bi-linear form and all Hamming weights. Clearly, equivalent codes have identical enumerator polynomials. Therefore, it is not possible, in most cases, to reconstruct the code from an enumerator polynomial. In fact, there also exist "fake" enumerator polynomials; polynomials that satisfy all properties of an enumerator polynomial, but for which no code exists.

The **MacWilliams identity** relates the weight enumerator polynomial of a code $\mathcal{C}$ to that of its dual code $\mathcal{C}^{\perp}$

$$W_{\mathcal{C}^{\perp}}(x_0, x_1) = 2^{\frac{n}{2} - k} W_{\mathcal{C}} \left(\frac{x_0 - x_1}{\sqrt{2}}, \frac{x_0 + x_1}{\sqrt{2}} \right). \tag{2.6}$$

It follows that for a self-dual code

$$W_{\mathcal{C}^{\perp}}(x_0, x_1) = W_{\mathcal{C}}(x_0, x_1). \tag{2.7}$$

To illustrate the definitions so far, consider the codes $\mathcal{C}_1, \mathcal{C}_2, \mathcal{C}_3$ with generator matrices

$$G_1 = \begin{pmatrix} 1 & 0 & 1 & 0 \\ 0 & 1 & 0 & 1 \end{pmatrix}, \ G_2 = \begin{pmatrix} 1 & 1 & 1 \end{pmatrix}, \ G_3 = \begin{pmatrix} 1 & 0 & 0 & 1 \\ 0 & 1 & 1 & 0 \end{pmatrix}. \tag{2.8}$$

The codes $\mathcal{C}_1, \mathcal{C}_3$ consists of 4 codewords each, while $\mathcal{C}_2$ consists of 2. Their Hamming distances are $d_{\mathcal{C}_1} = d_{\mathcal{C}_3} = 2$, $d_{\mathcal{C}_2} = 3$. Their dual codes are generated by

$$H_1 = \begin{pmatrix} 1 & 0 & 1 & 0 \\ 0 & 1 & 0 & 1 \end{pmatrix}, \quad H_2 = \begin{pmatrix} 1 & 1 & 0 \\ 0 & 1 & 1 \end{pmatrix}, \quad H_3 = \begin{pmatrix} 1 & 0 & 0 & 1 \\ 0 & 1 & 1 & 0 \end{pmatrix}. \tag{2.9}$$

Since $\mathcal{C}_1 = \mathcal{C}_1^\perp$ and $\mathcal{C}_3 = \mathcal{C}_3^\perp$, these codes are self-dual. Moreover, the codes $\mathcal{C}_1, \mathcal{C}_3$ are equivalent.

The codes $\mathcal{C}_1$, $\mathcal{C}_3$, being equivalent, have identical enumerator polynomials. The polynomials are given by

$$W_{\mathcal{C}_1} = W_{\mathcal{C}_1^\perp} = x_0^4 + 2x_0^2 x_1^2 + x_1^4, \quad W_{\mathcal{C}_2} = x_0^3 + x_1^3, \quad W_{\mathcal{C}_2^\perp} = x_0^3 + 3x_0 x_1^2. \tag{2.10}$$

It is straightforward to confirm that $W_{\mathcal{C}_1}$ is invariant under MacWilliams identity, while

$$\sqrt{2} W_{\mathcal{C}_2} \left(\frac{x_0 - x_1}{\sqrt{2}}, \frac{x_0 + x_1}{\sqrt{2}} \right) = W_{\mathcal{C}_2^\perp}(x_0, x_1). \tag{2.11}$$

2.1.1 Generalization

We will now generalize all the notions introduced earlier about binary codes to codes with alphabet $\mathbb{Z}_N$ (the ring of integers modulo N).

A code $\mathcal{C}$ is a $\mathbb{Z}_N$-linear subspace of $\mathbb{Z}_N^n$ (also called a $\mathbb{Z}$-module or a free Abelian group). The generator matrix G, with entries in $\mathbb{Z}_N$, is a linear map from $\mathbb{Z}_N^k$ to $\mathcal{C}$

$$c = xG, \quad x \in \mathbb{Z}_N^k. \tag{2.12}$$

Unlike binary codes, one can define many different weights on $\mathbb{Z}_N^n$. A common and straightforward generalization of the Hamming weight counts the number of non-zero entries of a codeword. For our purposes, we will need to define a more complicated weight. We will specify the choice of weight in section 2.3, but for now we mention that we require that the weight is non-degenerate, semi-positive definite and satisfies the triangle inequality.

We also need to generalize the notion of evenness in a way that is useful for our goals. We define a function wt_2, with the property that $wt_2(c) = 0$ if the codeword c is even and $wt_2(c) \neq 0$ otherwise. If all the codewords of $\mathcal{C}$ satisfy this **evenness condition**, the code $\mathcal{C}$ is even.

Given a bi-linear form $\langle a | b \rangle$ on $\mathbb{Z}_N^n$, we can define the dual code of $\mathcal{C}$

$$\mathcal{C}^\perp = \{c' \in \mathbb{Z}_N^n : \langle c' | c \rangle = 0 \ \forall c \in \mathcal{C}\}. \tag{2.13}$$

The **complete enumerator polynomial** of a code $\mathcal{C} \subseteq \mathbb{Z}_N^n$ is

$$W_{\mathcal{C}}(x_0, x_1, \ldots, x_{N-1}) = \sum_{(c_1, c_2, \ldots, c_n) \in \mathcal{C}} \prod_{i=1}^{n} x_{c_i}. \tag{2.14}$$

The **MacWilliams identity** can be straightforwardly generalized:

$$W_{\mathcal{C}^\perp}(x_0, x_1, \ldots, x_{N-1}) = N^{\frac{n}{2} - k} W_{\mathcal{C}}(\tilde{x}_0, \tilde{x}_1, \ldots, \tilde{x}_{N-1}), \tag{2.15}$$

where

$$\tilde{x}_a = \frac{1}{\sqrt{N}} \sum_{a' \in \mathbb{Z}_N} e^{-2\pi i \langle a | a' \rangle} x_{a'}. \tag{2.16}$$

The enumerator polynomial of a self-dual code is invariant under this transformation

$$W_{\mathcal{C}^\perp}(x_0, x_1, \ldots, x_{N-1}) = W_{\mathcal{C}}(x_0, x_1, \ldots, x_{N-1}). \tag{2.17}$$

2.2 Lattices

A lattice is a periodic arrangement of points in space. Lattices have many applications including cryptography, solid-state physics and sphere-packings. Here we are going to adopt an abstract mathematical description.

A lattice $\Lambda \subseteq \mathbb{R}^m$ of dimension n is a free $\mathbb{Z}$-module whose $\mathbb{R}$-span is isomorphic to the vector space $\mathbb{R}^n$. Consequently, a lattice as an additive group, is isomorphic to $\mathbb{Z}^n$. We will only consider the case $n = m$ for simplicity.

A lattice Λ inherits a bilinear form $\langle \cdot | \cdot \rangle$ from the space (usually $\mathbb{R}^n$) in which it is embedded. Using this form, we can define the **dual lattice** as follows

$$\Lambda^\perp = \{ \lambda' \in \mathbb{R}^n : \langle \lambda | \lambda' \rangle \in \mathbb{Z} \ \forall \lambda \in \Lambda \}. \tag{2.18}$$

If $\Lambda \subseteq \Lambda^\perp$, the lattice Λ is called **self-orthogonal**. If $\Lambda = \Lambda^\perp$, the lattice is **self-dual**. If $\langle \lambda | \lambda \rangle \in \mathbb{Z}$ for all $\lambda \in \Lambda$, then Λ is **integral**. If $\langle \lambda | \lambda \rangle$ is even for all $\lambda \in \Lambda$, then the lattice is **even**. Finally, an integral lattice whose unit cell has volume equal to 1 is called **unimodular**.

The **theta series** of a lattice Λ is a holomorphic function of τ in the upper-half complex plane that encodes important properties of the lattice.It is defined by

$$\Theta_\Lambda(\tau) = \sum_{\lambda \in \Lambda} e^{\pi i \tau \langle \lambda | \lambda \rangle}. \tag{2.19}$$

Consider now the case where $\langle \lambda | \lambda \rangle = \sum_{i=1}^n \lambda_i^2$ is the Euclidean inner product in $\mathbb{R}^n$. The theta series of an even, self-dual Euclidean lattice is a modular form of weight $\frac{n}{2}$. Even, self-dual Euclidean lattices are not easy to construct. In fact, they exist only in dimensions divisible by 8. The smallest example is the E_8 lattice; the root lattice of one of the exceptional Lie algebras. For $n = 16$ there are two even, self-dual lattices, while for $n = 24$ there are 24, the most important of which is the Leech lattice[17].

We will be interested in even, self-dual Lorentzian lattices (which will be defined later in section 2.4). Such lattices exist for any even integer dimension n. The theta-series is generalized to the Siegel theta series, a function of two variables $\tau, \bar{\tau}$ in the upper half complex plane. The Siegel theta series is a Siegel modular form, a type of automorphic form.

2.2.1 Lattices from binary codes: Construction A

Let $\mathcal{C}$ be a classical binary code. The construction A lattice is defined by [17]

$$\Lambda = \left\{ \frac{1}{\sqrt{2}} x \in \mathbb{R}^n : x = c \mod 2 \text{ for some } c \in \mathcal{C} \right\}. \tag{2.20}$$

If $\mathcal{C}$ is even and self-dual, then Λ is a unimodular lattice. In addition, if the weights of all codewords of $\mathcal{C}$ are divisible by 4 (doubly even), then Λ is even.

The theta series of Λ can be obtained from the enumerator polynomial of $\mathcal{C}$ by the substitutions [8]

$$x_0 \to \theta_3(q^2), \quad x_1 \to \theta_2(q^2), \tag{2.21}$$

where θ_2, θ_3 are the Jacobi theta functions

$$\theta_2(q) = \sum_{n \in \mathbb{Z} + \frac{1}{2}} q^{n^2/2}, \ \theta_3(q) = \sum_{n \in \mathbb{Z}} q^{n^2/2}, \quad q = e^{2\pi i \tau}. \tag{2.22}$$

Consider two examples: the trivial binary code $\mathcal{C}_0 = \{(0,0)\}$, as well as the code $\mathcal{C}_1$ generated by

$$G_1 = (1,1). \tag{2.23}$$

The construction A lattice of $\mathcal{C}_0$ is the square lattice of side length $\sqrt{2}$. Meanwhile, $\mathcal{C}_1$ leads to the unimodular lattice:

$$\Lambda_1 = \left\{ \begin{pmatrix} \sqrt{2} \\ 0 \end{pmatrix} p + \begin{pmatrix} \frac{1}{\sqrt{2}} \\ \frac{1}{\sqrt{2}} \end{pmatrix} q, \ \ p, q \in \mathbb{Z} \right\}. \tag{2.24}$$

Their enumerator polynomials are respectively

$$W_{\mathcal{C}_0}(x_0, x_1) = x_0^2, \ \ W_{\mathcal{C}_1}(x_0, x_1) = x_0^2 + x_1^2. \tag{2.25}$$

Explicitly, they are given by

$$\Theta_{\mathcal{L}_0} = \theta_3^2(q^2) = \sum_{n,m \in \mathbb{Z}} q^{n^2+m^2}, \ \ \Theta_{\mathcal{L}_1} = \theta_3^2(q^2) + \theta_2^2(q^2) = \sum_{n,m \in \mathbb{Z}} q^{m^2+2n^2+2nm}. \tag{2.26}$$

These examples illustrate how codes can be a powerful tool in the study of lattices. Unlike lattices, codes contain finitely many elements. The short vector of a lattice stems from the codeword with the minimum Hamming weight, therefore the short vector problem is equivalent to finding the Hamming distance of a code. Moreover, an enumerator polynomial, being a homogeneous polynomial of a finite number of variables, is much easier to handle than a theta series.

2.3 Generalized construction A

Let Λ be a self-orthogonal lattice. Then, $G = \Lambda^\perp/\Lambda$ is a finite, free Abelian group, called the **discriminant group**. We define a code $\mathcal{C}$ to be an additive subgroup of G^n. We are interested in self-dual codes with alphabet G.

Let $\phi : \Lambda^\perp \to G$ be a surjective map with $\ker(\phi) = \Lambda$. The inner product $\langle \cdot | \cdot \rangle_\Lambda$ on the lattice Λ induces an inner product $\langle \cdot | \cdot \rangle$ on the group G. Let $g_1, g_2 \in G$ and let $\lambda_1, \lambda_2 \in \Lambda^\perp$ be such that $g_1 = \phi(\lambda_1)$ and $g_2 = \phi(\lambda_2)$. We define

$$\langle g_1 | g_2 \rangle \equiv \langle \lambda_1 | \lambda_2 \rangle_\Lambda \mod \mathbb{Z}. \tag{2.27}$$

We also define the **evenness condition** wt_2 on G, which will be used to define even codes. For $g = \phi(\lambda)$:

$$wt_2(g) \equiv \langle \lambda | \lambda \rangle_\Lambda = 0 \mod 2\mathbb{Z}. \tag{2.28}$$

We extend the above definitions to G^n in the following, straightforward way. For $\boldsymbol{g} = (g_1, \ldots, g_n), \boldsymbol{g}' = (g_1', \ldots, g_n') \in G^n$:

$$\langle \boldsymbol{g} | \boldsymbol{g}' \rangle = \sum_{i=1}^{n} \langle g_i | g_i' \rangle, \tag{2.29}$$

$$wt_2(\boldsymbol{g}) \equiv \sum_{i=1}^{n} wt_2(g_i). \tag{2.30}$$

A code $\mathcal{C}$ is **even** if all $c \in \mathcal{C}$ satisfy $wt_2(c) = 0$.

Now we can define the following generalization to construction A

$$\mathcal{L}_\mathcal{C} = \{l \in \Lambda^\perp \oplus \cdots \oplus \Lambda^\perp | \phi(l) \in \mathcal{C}\}. \tag{2.31}$$

By definition, this lattice satisfies

$$\Lambda \oplus \cdots \oplus \Lambda \subseteq \mathcal{L}_\mathcal{C} \subseteq \Lambda^\perp \oplus \cdots \oplus \Lambda^\perp. \tag{2.32}$$

We define the **weight** wt on G^k as follows

$$wt(c) = \min_{l \in \Lambda^\perp \oplus \cdots \oplus \Lambda^\perp : \phi(l) = c} \langle l | l \rangle_\Lambda. \tag{2.33}$$

In words, the weight of an element of G^k is equal to the length of the shortest vector it gives rise to under construction A.

From these definitions, it follows that the lattice constructed from the dual code $\mathcal{C}^\perp$ is dual to the lattice constructed from the code $\mathcal{C}$

$$\mathcal{L}_{\mathcal{C}^\perp} = \mathcal{L}_\mathcal{C}^\perp. \tag{2.34}$$

In particular, if $\mathcal{C}$ is self-dual, the lattice $\mathcal{L}_\mathcal{C}$ is self-dual. Additionally, the minimum weight of the code is equal to the length of the short vector of the lattice, and even codes result in even lattices.

2.4 Conformal Field Theory: Narain lattices

Consider a theory of n free bosons in 2 space-time dimensions, governed by the action [18]

$$S = \frac{1}{8\pi} \int dt \int_0^{2\pi} d\sigma ((\partial_t \phi)^2 - (\partial_x \phi)^2 - 2B_{ij}\partial_t \phi^i \partial_x \phi^j). \tag{2.35}$$

We require that the bosons are compactified on a torus $\mathbb{R}^n/(2\pi\Gamma)$, where $\Gamma \subseteq \mathbb{R}^n$ is a Euclidean lattice. In practice, this means that we impose the boundary condition

$$\phi(t, x + 2\pi) = \phi(t, x) + 2\pi\boldsymbol{\alpha}, \quad \boldsymbol{\alpha} \in \Gamma. \tag{2.36}$$

The solution to the classical equation, after imposing (2.36), is

$$\phi(t, x) = \phi_0 + \boldsymbol{v}t + \boldsymbol{\alpha}x + \frac{i}{2}\sum_{n \neq 0} \frac{\boldsymbol{a}_n}{n} e^{-in(t+x)} + \frac{i}{2}\sum_{n \neq 0} \frac{\boldsymbol{b}_n}{n} e^{-in(t-x)}, \quad \boldsymbol{\alpha} \in \Gamma. \tag{2.37}$$

It can be written as a sum of left and right movers

$$\phi(t, x) = \phi_L(t + x) + \phi_R(t - x), \tag{2.38}$$

where

$$\phi_L(t + x) = \frac{1}{2}\phi_0 + \boldsymbol{p}_L(t + x) + \frac{i}{2}\sum_{n \neq 0} \frac{\boldsymbol{a}_n}{n} e^{-in(t+x)}, \tag{2.39}$$

$$\phi_R(t - x) = \frac{1}{2}\phi_0 + \boldsymbol{p}_L(t - x) + \frac{i}{2}\sum_{n \neq 0} \frac{\boldsymbol{b}_n}{n} e^{-in(t-x)} \tag{2.40}$$

and

$$\boldsymbol{p}_L - \boldsymbol{p}_R \in \Gamma, \tag{2.41}$$

$$\boldsymbol{p}_L + \boldsymbol{p}_R = \boldsymbol{v}. \tag{2.42}$$

The canonical momentum, from (2.35), is

$$P_i = \frac{1}{2}(v_i - B_{ij}\alpha_j). \tag{2.43}$$

In the quantum theory, after imposing canonical commutation relations, the canonical momentum is quantized in $\boldsymbol{P} \in \Gamma^\perp$ (the dual lattice of Γ). Therefore, we can write

$$\begin{pmatrix} \boldsymbol{p}_L \\ \boldsymbol{p}_R \end{pmatrix} = \tilde{\mathcal{L}}\boldsymbol{k}, \quad \boldsymbol{k} \in \mathbb{Z}^{2n}, \tag{2.44}$$

where

$$\tilde{\mathcal{L}} = \begin{pmatrix} \Gamma^\perp & \frac{B+I}{2}\Gamma \\ \Gamma^\perp & \frac{B-I}{2}\Gamma \end{pmatrix} \tag{2.45}$$

and by abuse of notation, we denote the lattices $\Gamma^\perp, \Gamma$ and their generator matrices by the same symbol. It is convenient to make the choice $\Gamma^\perp = (\Gamma^{-1})^T$.

We shall also use another convention, mainly in chapter 3, where we define the lattice $\mathcal{L}$ by

$$\begin{pmatrix} \frac{\boldsymbol{p}_L + \boldsymbol{p}_R}{\sqrt{2}} \\ \frac{\boldsymbol{p}_L - \boldsymbol{p}_R}{\sqrt{2}} \end{pmatrix} = \mathcal{L}\boldsymbol{k}, \quad \boldsymbol{k} \in \mathbb{Z}^{2n}, \tag{2.46}$$

from which it follows that

$$\mathcal{L} = \begin{pmatrix} \gamma^\perp & B\gamma \\ 0 & \gamma \end{pmatrix}, \quad \gamma = \Gamma/\sqrt{2}. \tag{2.47}$$

The generator matrix $\mathcal{L}$ satisfies the $O(n,n,\mathbb{R})$ relation

$$\mathcal{L}^T g \mathcal{L} = g, \quad g = \begin{pmatrix} 0 & I \\ I & 0 \end{pmatrix}, \tag{2.48}$$

where I is the $n \times n$ identity matrix. Therefore, all inner products, with respect to g are integers and all lengths are even integers. We will refer to g as the Lorentzian inner product. This means that $\mathcal{L}$ is an even, self-dual Lorentzian lattice. Lattices satisfying these conditions are also called Narain lattices [19].

The partition function of this CFT is given by

$$Z(\tau, \bar{\tau}) = \frac{1}{|\eta(\tau)|^{2n}} \sum_{(\boldsymbol{p}_L, \boldsymbol{p}_R) \in \tilde{\mathcal{L}}} q^{p_L^2/2} \bar{q}^{p_R^2/2}, \quad q = e^{2\pi i \tau}, \ \bar{q} = e^{-2\pi i \bar{\tau}}. \tag{2.49}$$

For a CFT to be well-defined, its partition function must be modular invariant. The modular group $SL(2, \mathbb{Z})$ is generated by $\tau \to \tau + 1$ and $\tau \to -1/\tau$. Evenness and self-duality of $\mathcal{L}$ automatically implies that $Z(\tau, \bar{\tau})$ is modular invariant. In chapter 3 we will see how the partition function of a CFT constructed from a code $\mathcal{C}$ is related to the enumerator polynomial of $\mathcal{C}$.

Consider now the moduli space $\mathcal{M}_c$ of all Narain CFTs of fixed central charge c. Since every Narain CFT can be described by a Narain lattice, we may want to identify $\mathcal{M}_c$ with the indefinite orthogonal group $O(c, c, \mathbb{R})$, which is the set of all self-dual Lorentzian lattices. However, the correspondence between this group and Narain CFTs is not one-to-one. First, we must quotient out the automorphism group of the lattice, which is $O(c, c, \mathbb{Z})$. Moreover, distinct Narain lattices may correspond to the same underlying CFT, due to T-duality. The group of T-dualities, $O(c, \mathbb{R}) \times O(c, \mathbb{R})$ contains the elements that preserve the Lorentzian inner product, as well as the Euclidean norms of all vectors. Hence, the moduli space of Narain CFTs at central charge c is given by [10]

$$\mathcal{M}_c = O(c, \mathbb{R}) \times O(c, \mathbb{R}) \backslash O(c, c, \mathbb{R}) / O(c, c, \mathbb{Z}). \tag{2.50}$$

Chapter 3 Optimal Narain CFTs from codes

This chapter is based on the published work "Optimal Narain CFTs from codes" co-authored with D. Chakraborty and A. Dymarsky [20] and is reproduced here with the co-authors' consent and according to the CC BY 4.0 license. Minor changes were made in order to improve consistency with other chapters and to eliminate redundancies.

3.1   Motivation: Codes and Narain CFTs

Conformal modular bootstrap program aims to establish universal constraints on two-dimensional CFTs and elucidate properties of those special theories which saturate these constraints. One of the central goals of the modular bootstrap is to study theories maximizing the value of the spectral gap for a given fixed value of central charge [21], as these theories for large central charge are expected to be dual to weakly coupled gravity [22]. To simplify this obviously challenging task one can restrict their attention to a class of Narain theories, i.e. CFTs exhibiting $U(1)^c \times U(1)^c$ symmetry. In this case, large spectral gap theories are not sparse (in the sense of [22]), and their holographic description is less clear [23]. Nevertheless, the study of such theories is well motivated by both holography and the modular bootstrap, with the latter relating solutions of spinless bootstrap constraints to densest sphere packings [24].[1] Narain theories were studied in [26] and [27] using spinless and full modular bootstrap, with the hypothetical optimal theories being identified for $c \leq 8$. Here, following [28] we say optimal to denote CFTs maximizing the spectral gap for a given c.

A relation between quantum codes and Narain CFTs, proposed in [29], generalizes the chiral constructions of [30]. Starting from a code, it constructs the corresponding Narain lattice and expresses CFT torus partition function in terms of the code enumerator polynomial. In this way constraints of modular invariance reduce to two algebraic constrains at the level of enumerator polynomial. The relation to quantum codes was recently extended and interpreted in terms of CFT Hilbert space in [31]. There are also "bottom-up" generalizations when the connection with codes is perceived as a tool to solve modular bootstrap constraints and construct interesting CFTs [8, 32], also see [33, 34] for the subsequent developments.

In this chapter, we apply the Construction A outlined in chapter 2, which generalizes and encompasses the constructions of [8, 32]. In particular, we explicitly construct all (conjecturally) optimal Narain theories for $c \leq 8$ identified in [27]. We consider self-dual codes over abelian groups $G = \mathbb{Z}_p \times \mathbb{Z}_q$, built from 2-dimensional even, Lorentzian lattices. The generalization of the code Hamming distance, modulo certain subtleties, defines CFT spectral gap Δ^* such that "better" codes with larger Hamming distance corresponds to larger Δ^*. In each case, the resulting Narain lat-

---

[1]Here we are speaking of a density of states satisfying (some subset) of modular bootstrap constraints, with no regard to whether there is an actual CFT yielding this density of states. Similarly, speaking of densest sphere packings, we in fact refer to a solution to Cohen-Elkies linear program constraints [25], with no regard to whether there are actual associated sphere packings.

tice necessarily has vectors of particular length which is independent of c. Hence any given construction can only yield CFTs with bounded spectral gap that doesn't grow with c. Nevertheless by considering a sequence of constructions parametrized by c one can obtain a family of Narain theories with the spectral gap growing linearly with c. For $c \gg 1$ finding optimal codes, i.e. those maximizing corresponding Hamming distance, is a challenging task, but one can average over a family of codes with the given c. From here we find that random code CFT, drawn from a particular ensemble, has spectral gap

$$\Delta^* = \frac{c}{2\pi e}, \qquad c \to \infty, \tag{3.1}$$

which was conjectured in [23] to be asymptotically largest possible value. Thus, we conclude that certain code CFT are optimal for $c \gg 1$ or at least give spectral gap with the conjectured maximal asymptotic value of Δ^*/c.

This chapter is organized as follows. In section 3.2 we outline our main construction mapping codes to Narain CFTs and then express their partition functions in terms of enumerator polynomials in section 3.3. We then use these results to construct optimal theories for $c \leq 8$ in section 3.4. We proceed by considering the case of asymptotically large c and a family of associated constructions in section 3.5. We conclude in section 3.6.

3.2 Additive codes and Lorentzian lattices

The main ingredient of our construction is a 2-dimensional even lattice $\Lambda \in \mathbb{R}^{1,1}$, which we call a "glue" lattice. The discriminant group of such a lattice is an additive group G, which serves as the alphabet of the code. Then Construction A (see section 2.3) maps a code $\mathcal{C} \subset G^c$ into a lattice

$$\underbrace{\Lambda \oplus \cdots \oplus \Lambda}_{c \text{ times}} \subset \Lambda_{\mathcal{C}} \subset \underbrace{\Lambda^{\perp} \oplus \ldots \Lambda^{\perp}}_{c \text{ times}} \subset \mathbb{R}^{c,c}. \tag{3.2}$$

When $\mathcal{C}$ satisfies additional conditions, the lattice $\Lambda_{\mathcal{C}}$ is even and self-dual, thus defining a Narain theory.

3.2.1 Even lattices in $\mathbb{R}^{1,1}$

We equip $\mathbb{R}^2$ with a Lorentzian metric

$$g = \begin{pmatrix} 0 & 1 \\ 1 & 0 \end{pmatrix}, \tag{3.3}$$

thus turning it into $\mathbb{R}^{1,1}$. It is convenient to parametrize a lattice by a generating matrix Λ, such that $v = \Lambda n$, $n \in \mathbb{Z}^2$ generates all lattice vectors. Again we abuse the notation by using Λ to denote both the lattice and its generating matrix. The generating matrix is not unique, obviously Λ and ΛS for $S \in SL(2, \mathbb{Z})$ generate the same lattice. So far we are only interested in the scalar product defined by (3.3), we

can identify all lattices related by $O(1,1)$, $\Lambda \sim O\Lambda$ for $O \in O(1,1)$. The dual lattice $\Lambda^\perp$, at the level of generating matrix can be expressed as $\Lambda^\perp = g(\Lambda^{-1})^T$.

We can parametrize all even lattices in $\mathbb{R}^{1,1}$ as follows. In full generality

$$g_\Lambda = \Lambda^T g \Lambda = \begin{pmatrix} 2m & k \\ k & 2n \end{pmatrix}, \quad n, m, k \in \mathbb{Z}, \tag{3.4}$$

assuming $\det(\Lambda) = \sqrt{k^2 - 4mn} > 0$. Then using $SL(2,\mathbb{Z})$ we can bring n, m, k to satisfy (see chapter 15 of [17])

$$0 < k < \sqrt{k^2 - 4nm} < \min(k + 2|n|, k + 2|m|), \tag{3.5}$$

unless $k^2 - 4nm$ is a full square, in which case one can choose new n, m, k such that

$$n = 0, \quad -k < m \le k. \tag{3.6}$$

With the help of an appropriate $O(1,1)$ transformation the corresponding generating matrix can be brought to the form

$$\Lambda = \begin{pmatrix} 1 & \frac{n}{a} \\ m & a \end{pmatrix}, \quad a = \frac{1}{2}(k + \sqrt{k^2 - 4mn}). \tag{3.7}$$

Since Λ is integral, it is contained in its dual $\Lambda^\perp \supseteq \Lambda$. Its discriminant group (which we will call "glue group" in this chapter) is

$$G = \Lambda^\perp / \Lambda = \mathbb{Z}^2 / g_\Lambda = \mathbb{Z}_p \times \mathbb{Z}_q. \tag{3.8}$$

Here

$$p = gcd(2n, 2m, k), \quad q = |G|/p, \tag{3.9}$$

where

$$|G| = |\det(\Lambda)/\det(\Lambda^\perp)| = k^2 - 4mn. \tag{3.10}$$

is the order of the group. This follows from the invariant factor decomposition of finitely generated Abelian groups.

One possible parametrization of the elements of G is as pairs $g = (a, b)$ of integer numbers $0 \le a < p$, $0 \le b < q$. Another useful parametrization is as integer vectors $\ell(g) \in \mathbb{Z}^2$ modulo columns of g_Λ. An explicit map between these two parametrizations may be nontrivial.

The Lorentzian metric on $\mathbb{R}^{1,1}$ induces a bi-linear form (or scalar product) $\langle \cdot | \cdot \rangle$ on G, which is then extended to G^c (see section 2.3). We are interested in codes $\mathcal{C} \subseteq \mathcal{G}^c$ that are even and self-dual with respect to this inner product.

3.2.2 Narain lattices from Construction A

Starting from a code $\mathcal{C} \subset G^c$, Construction A (2.31) associates to it a lattice $\Lambda_{\mathcal{C}}$ in $\mathbb{R}^{c,c}$. Then it is straightforward to see that an even $\mathcal{C}$ would give rise to an even lattice $\Lambda_{\mathcal{C}}$ and a self-dual $\mathcal{C}$ to a self-dual $\Lambda_{\mathcal{C}}$, both understood with respect to Lorentzian scalar product $g_L = g \oplus \cdots \oplus g$ in $\mathbb{R}^{c,c}$.

To define a Narain theory, besides Lorentzian scalar product, even self-dual lattice should also be equipped with the Euclidean scalar product. For each Λ defined in previous section there is $O(1,1)$ ambiguity how it can be embedded in $\mathbb{R}^2$. Thus, very explicitly we can write

$$v = \begin{pmatrix} O(\Lambda^\perp \ell_1 + \Lambda k_1) \\ \vdots \\ O(\Lambda^\perp \ell_c + \Lambda k_c) \end{pmatrix} \in \Lambda_{\mathcal{C}}, \quad (\ell_1, \dots, \ell_c) \in \mathcal{C}, \quad k_i \in \mathbb{Z}^2, \tag{3.11}$$

where in (3.11) we parametrize elements of $G = \mathbb{Z}^2/g_\Lambda$ by vectors ℓ. Matrix O is an arbitrary element from $O(1,1)$. In principle we can introduce c different transformations $O_i \in O(1,1)$ acting in each $\mathbb{R}^2$ plane. In this case most of the construction remains intact, but the permutation of factors of G in $\mathcal{C} \subset G^c$, which is conventionally considered to be a code equivalence, would no longer yield physically equivalent lattices. In what follows we assume that all factors O are the same.

The main result of this section is as follows. For any discriminant group G defined via (3.8) with the help of an appropriate even lattice $\Lambda \subset \mathbb{R}^{1,1}$, any even self-dual code $\mathcal{C} \subset G^c$ via Construction A defines Narain lattice $\Lambda_{\mathcal{C}}$ (3.11) and hence a Narain CFT. We will call such CFTs code theories.

3.2.3 Example: square glue lattice

Consider the following glue lattice generating matrix

$$\Lambda = \sqrt{p}\, g, \quad p \in \mathbb{N}. \tag{3.12}$$

The dual lattice is generated by $\Lambda^\perp = I/\sqrt{p}$. Clearly this is the case of $n = m = 0, k = p$ and the glue group $G = \mathbb{Z}_p \times \mathbb{Z}_p$ is parametrized by $g = (a,b) \in G$, $0 \le a, b < p$ and

$$\ell(g) = (a, b)^T. \tag{3.13}$$

It is convenient to write codewords $c = (g_1, \dots, g_c) \in \mathcal{C} \subset G^c$ as

$$c = (a_1, \dots, a_c | b_1, \dots, b_c) \in \mathbb{Z}_p^{2c}. \tag{3.14}$$

A code can be defined with a $2c \times d$ generating matrix $G_{\mathcal{C}}$ such that

$$c = G_{\mathcal{C}}\, r, \quad r \in \mathbb{Z}_p^d, \tag{3.15}$$

where d depends on p. For prime p generating matrix is $2c \times c$ and using permutations can always be brought to the form

$$G_{\mathcal{C}} = \left(I \,|\, B^T \right), \tag{3.16}$$

15

where B is an integer values antisymmetric $c \times c$ matrix defined mod p,

$$B^T = -B \mod p, \tag{3.17}$$

and $B_{ii} = 0$. Applying Construction A to such codes leads to Narain lattices generated by

$$\Lambda_{\mathcal{C}} = \begin{pmatrix} pI_c & B \\ 0 & I_c \end{pmatrix} / \sqrt{p}, \qquad g_L = \begin{pmatrix} 0 & I_c \\ I_c & 0 \end{pmatrix}, \tag{3.18}$$

associated with the Lorentzian scalar product g_L. Here I_c is a c-dimensional identity matrix.

The form of $\Lambda_{\mathcal{C}}$ provides a clear interpretation – corresponding Narain theory describes c scalars compactified on a c-dimensional cube of size $1/\sqrt{p}$ in presence of B-field B.

The construction of [8, 29], which considered the case of $p = 2$, is a special case of the construction described in this section. A similar generalized construction has been recently introduced independently in [33].

3.2.4 Generalization: isodual codes

Permutation of factors $S : G^c \to G^c$

$$S : (g_1, \ldots, g_c) \to (g_{i_1}, \ldots, g_{i_c}) \tag{3.19}$$

is the simplest example of code equivalences, defined as a linear transformation $S : G^c \to G^c$ which preserves scalar product $\langle \cdot | \cdot \rangle$. Provided dual code is equivalent to the original one

$$\mathcal{C}^\perp = S(\mathcal{C}), \tag{3.20}$$

such a code is called isodual. From this follows $S^2 = 1$, i.e. when S is a permutation, it is a pair-wise permutation, with the corresponding matrix satisfying $S^T = S$.

We can introduce evenness as the condition for all codewords $(g_1, \ldots, g_c) \in \mathcal{C} \subset G^c$ to have even scalar product with its permuted self,

$$\sum_{i=1}^{c} \langle g_i | g_{S(i)} \rangle \in 2\mathbb{Z}. \tag{3.21}$$

An even, isodual code $\mathcal{C}$ with respect to some pairwise permutation S, via Construction A (3.11) gives rise to an even lattice, which is self-dual with respect to Lorentzian scalar product

$$g_L = g \otimes S. \tag{3.22}$$

In this way isodual codes also can be used to define Narain lattices and code CFTs.

3.2.5 CFT spectral gap and code modified Hamming distance

Construction A (3.11) relates each codeword $c \in \mathcal{C}$ to a family of vectors $l(c)$. We define the weight of c to be the minimal length squared among all such l, according to (2.33). Define the generalized Hamming distance $d(\mathcal{C})$ to be the minimum non-zero weight of the code $\mathcal{C}$.

From this definition follows that the code theory spectral gap Δ^*, defined as the length-squared of the shortest non-zero vector divided by two, is simply related to code's generalized Hamming distance $\Delta^* = \frac{d(\mathcal{C})}{2}$. This relation is transparent, but there is one caveat: zero codeword $c = 0$ is mapped into the origin of $\Lambda_{\mathcal{C}}$, as well as many vectors of the form $\Lambda(k_1, \ldots, k_c)$. The origin is excluded from the consideration, while minimizing over k_i yields shortest vector of Λ. We thus have

$$\Delta^* = \frac{1}{2} \min \left(d(\mathcal{C}), |v_\Lambda|^2 \right), \tag{3.23}$$

where by $|v_\Lambda|$ we denoted the length of shortest non-trivial vector of Λ. This length depends non-trivially on the choice of n, m, k and the $O(1,1)$ factor (which we absorbed into the definition of Λ), but an upper bound (3.26) is readily available, see below.

For the square lattice of subsection 3.2.3 we find that $wt(c)$ is given by

$$wt(c) := \min_{k \in Z} (c + pk)^2, \tag{3.24}$$

and $|v_\Lambda|^2 = p$.

To obtain the upper bound on the length, in the sense of Euclidean norm, of the shortest vector v_Λ belonging to (3.11) we consider all $\ell_i = 0$, arbitrary k_1 and $k_i = 0$ for $i > 1$. Then the Euclidean norm of corresponding two-dimensional vectors is

$$|v|^2 = k_1^T \Lambda^T O^T O \Lambda k_1, \tag{3.25}$$

which defines a positive-definite scalar product in $\mathbb{R}^2$. The shortest vector will necessarily be shorter than $|v_\Lambda|^2 \leq 2|G|^{1/2}/\sqrt{3}$, see Appendix A, and therefore corresponding code CFT would have the spectral gap not exceeding

$$\Delta^* \leq \frac{\sqrt{k^2 - 4nm}}{\sqrt{3}}. \tag{3.26}$$

This is a standard weakness of the Construction A lattices; they always include short vectors of a certain length, which does not increase with c. Therefore to construct large spectral gap CFTs with Δ^* scaling linearly with c we would need to consider a cascade of different constructions by adjusting k, n, m together with c.

3.3 Torus partition function of code theories

3.3.1 Enumerator polynomial and theta-series

One of the central properties of code theories which make them interesting is that their torus partition function can be expressed in a compact way in terms of the

so-called code enumerator polynomial which characterizes the corresponding code. Generalization of this result to higher genus partition function is also possible [35, 36].

We use the complete enumerator polynomial of a code $\mathcal{C}$ (2.14) as a vehicle to count how many times each element $g \in G$ appears in each codeword of $\mathcal{C}$,

$$W_{\mathcal{C}}(\{x_g\}) = \sum_{(g_1,\ldots,g_c)\in\mathcal{C}} \prod_{i=1}^{c} x_{g_i}. \tag{3.27}$$

The torus partition function of a code CFT, associated with $\Lambda_{\mathcal{C}}$ obtained by Construction A, is given in terms of $W_{\mathcal{C}}$,

$$\mathcal{Z}_{\mathcal{C}}(\tau) = W_{\mathcal{C}}(\{\psi_g(\tau)\}), \tag{3.28}$$

where

$$\psi_\ell(\tau) = \frac{1}{|\eta(\tau)|^2} \sum_{k\in\mathbb{Z}^2} \exp(i\pi v^T \Omega v), \tag{3.29}$$

$$v = \Lambda^\perp \ell + \Lambda\, k, \quad \Omega = \begin{pmatrix} i\tau_2 & \tau_1 \\ \tau_1 & i\tau_2 \end{pmatrix}, \tag{3.30}$$

$\tau = \tau_1 + i\tau_2$ is the torus modular parameter and in (3.29) we parametrize elements of G with help of vectors $\ell \in \mathbb{Z}^2/g_\Lambda$. We also absorbed $O \in O(1,1)$ into the definition of Λ.

The modular group, generated by $T : \tau \to \tau + 1$ and $S : \tau \to -1/\tau$, transforms Ω as follows

$$T \circ \Omega = \Omega + g, \tag{3.31}$$

$$S \circ \Omega = -\Omega^{-1}. \tag{3.32}$$

Functions ψ_ℓ transform accordingly

$$T \circ \psi_\ell(\tau) = \psi_\ell(\tau + 1) = \exp(i\pi v^T g_\Lambda v)\psi_\ell(\tau), \quad v = \Lambda^\perp \ell, \tag{3.33}$$

$$S \circ \psi_\ell(\tau) = \psi_\ell(-1/\tau) = \frac{1}{\sqrt{|G|}} \sum_{\ell'\in G=\mathbb{Z}^2/g_\Lambda} \exp(-2\pi i u^T g_\Lambda v)\psi_{\ell'}(\tau), \quad u = \Lambda^\perp \ell' \tag{3.34}$$

Evenness and self-duality of $\mathcal{C}$ ensure that $\mathcal{Z}_{\mathcal{C}}(\tau)$ is invariant under T and S respectively. Indeed, since the code is even, for any $(\ell_1,\ldots,\ell_n) \in \mathcal{C}$ we have $\sum_i \ell_i^T g_\Lambda^{-1} \ell_i \in 2\mathbb{Z}$, and therefore T is a symmetry of $P_{\mathcal{C}}(\{\psi_\ell\})$, while it is invariant under (3.34) because of self-duality.

3.3.2 Example: theta series for square glue lattice

For the lattice (3.12) functions ψ_g defined in (3.29) read

$$\psi_{ab} = \frac{1}{|\eta|^2} \sum_{k_1,k_2\in\mathbb{Z}} q^{\frac{p}{4}(\frac{a+b}{p}+k_1+k_2)^2} \bar{q}^{\frac{p}{4}(\frac{a-b}{p}+k_1-k_2)^2}, \tag{3.35}$$

18

where $(a, b) \in G = \mathbb{Z}_p \times \mathbb{Z}_p$. This can be written as follows

$$|\eta|^2 \psi_{ab} = \Theta_{a+b,p} \bar{\Theta}_{a-b,p} + \Theta_{a+b-p,p} \bar{\Theta}_{a-b-p,p}, \tag{3.36}$$

where

$$\Theta_{m,p} = \sum_{n \in \mathbb{Z}} q^{p(n+\frac{m}{2p})^2}. \tag{3.37}$$

These functions are the chiral algebra characters of free boson compactified at radius $R = \sqrt{2k}$.

Note, if we perform $O(1,1)$ rotation on the lattice Λ, functions ψ_{ab} will change. Let

$$\Lambda' = O\sqrt{p}g, \ O = \begin{pmatrix} \lambda & 0 \\ 0 & \lambda^{-1} \end{pmatrix}. \tag{3.38}$$

Then

$$|\eta|^2 \psi_{ab} = \sum_{k_1,k_2 \in \mathbb{Z}} q^{\frac{p}{4}(\frac{\lambda a + \lambda^{-1}b}{p} + \lambda k_1 + \lambda^{-1}k_2)^2} \bar{q}^{\frac{p}{4}(\frac{\lambda a - \lambda^{-1}b}{p} + \lambda k_1 - \lambda^{-1}k_2)^2}. \tag{3.39}$$

For $\lambda = \sqrt{q}$ with $q \in \mathbb{N}$, we can again decompose ψ_{ab} as follows

$$|\eta|^2 \psi_{ab} = \sum_{k=0}^{q-1} \Theta_{qa+b+kp,qp} \bar{\Theta}_{qa-b-kp,qp} + \Theta_{q(a-p)+b+kp,qp} \bar{\Theta}_{q(c_1-p)-c_2-kp,qp}, \tag{3.40}$$

where the functions $\Theta_{m,pq}$ above are now characters of compactified boson at radius $R = \sqrt{2pq}$.

Finally, if $\lambda = \sqrt{q/r}$ with q, r are co-prime, we can again perform the same decomposition to obtain a more general result

$$|\eta|^2 \psi_{ab} = \sum_{v_1=0}^{r-1} \sum_{v_2=0}^{q-1} \Theta_{q(a+pv_1)+r(b+pv_2),pqr} \bar{\Theta}_{q(a+pv_1)-r(b+pv_2),pqr} + \tag{3.41}$$

$$\Theta_{q(a+pv_1)+r(b+pv_2)-pqr,pqr} \bar{\Theta}_{q(a+pv_1)-r(b+pv_2)-pqr,pqr},$$

where the functions $\Theta_{m,pqr}$ above are characters of compactified boson at radius $R = \sqrt{2pqr}$.

3.3.3 Partition function in case of isodual codes

In case of isodual codes satisfying (3.20) with pairwise permutation S, the codeword $c = (g_1, \ldots, g_c) \in \mathcal{C}$ should be understood as consisting of r pairs (g_i, g_j) with S mapping $i \leftrightarrow j$, while the remaining $c - 2r$ "letters" remain intact. It is convenient to introduce new notation for c which is related to the previous one by permutation,

$$c = ((g_{i_1}, g_{j_1}), \ldots, (g_{i_r}, g_{j_r}), g_{2r+1}, \ldots, g_c) \in \mathcal{C}. \tag{3.42}$$

With this notation we define an extended enumerator polynomial, which will depend on both $\mathcal{C}$ and S. It is a function of $|G|^2$ variables $y_{g_1 g_2}$ and $|G|$ variables x_g,

$$W_{\mathcal{C}}^S(\{y_{g_1 g_2}\}, \{x_g\}) = \sum_{((g_{i_1}, g_{j_1}), \ldots, (g_{i_r}, g_{j_r}), g_{2r+1}, \ldots, g_c) \in \mathcal{C}} \prod_{k=1}^{r} y_{g_{i_k} g_{j_k}} \prod_{i=2r+1}^{c} x_{g_i}. \tag{3.43}$$

The CFT partition function is given by

$$\mathcal{Z}_{\mathcal{C}}(\tau) = W_{\mathcal{C}}^{S}(\{\psi_{g_1 g_2}(\tau)\}, \{\psi_g(\tau)\}), \tag{3.44}$$

where

$$\psi_{\ell_1 \ell_2}(\tau) = \frac{1}{|\eta(\tau)|^4} \sum_{k_1, k_2 \in \mathbb{Z}^2} \exp\Big(i\pi(v_1, v_2)^T \tilde{\Omega}(v_1, v_2)\Big), \tag{3.45}$$

$$\tilde{\Omega} = \begin{pmatrix} i\tau_2 I_2 & \tau_1 g \\ \tau_1 g & i\tau_2 I_2 \end{pmatrix}, \qquad v_i = \Lambda^{\perp}\ell_i + \Lambda k_i. \tag{3.46}$$

Under modular transformations $T : \tau \to \tau + 1$ and $S : \tau \to -1/\tau$, this function changes as follows

$$T \circ \tilde{\Omega} = \tilde{\Omega} + g \otimes g, \tag{3.47}$$
$$S \circ \tilde{\Omega} = -\tilde{\Omega}^{-1}. \tag{3.48}$$

and

$$T \circ \psi_{\ell_1 \ell_2} = \exp\big(2i\pi v_1^T g v_2\big)\psi_{\ell_1 \ell_2}, \quad v_i = \Lambda^{\perp}\ell_i, \tag{3.49}$$

$$S \circ \psi_{\ell_1 \ell_2} = \frac{1}{|G|} \sum_{\ell_1', \ell_2' \in G = \mathbb{Z}^2/g_\Lambda} \exp\big(2i\pi(u_1^T g v_1 + u_2^T g v_2)\big)\psi_{\ell_1' \ell_2'}, \quad u_i = \Lambda^{\perp}\ell_i'. \tag{3.50}$$

Clearly when $\mathcal{C}$ is even in the sense of (3.21) and isodual in the sense of (3.20), the identities (3.49,3.50) respectively ensure modular invariance of (3.44).

3.4 Examples: optimal Narain theories for small c

In this section we consider a number of explicit examples of code theories. In particular we discuss optimal theories, i.e. those with the largest spectral gap, for $c \leq 8$ identified in [27], and show they all are codes theories, in the sense defined in this chapter.

3.4.1 $c = 1$

We first consider the simplest case of $n = m = 0$, when

$$g_\Lambda = \begin{pmatrix} 0 & k \\ k & 0 \end{pmatrix}. \tag{3.51}$$

In this case the group $G = \mathbb{Z}_k \times \mathbb{Z}_k$ is parametrized by vectors $\ell = (a, b)$ for $0 \leq a, b < k$. Let's consider a self-dual code $\mathcal{C} = \mathcal{C}^{\perp}$ and demand it to be even and self-dual. When k is prime the only such two codes consist or vectors $(a, 0)$ and $(0, a)$ for $0 \leq a < k$ correspondingly. Using appropriate $O(1,1)$ transformation we can bring corresponding Narain lattice to the form

$$\Lambda_{\mathcal{C}} \ni \begin{pmatrix} a/\sqrt{k} \\ b\sqrt{k} \end{pmatrix}, \qquad a, b \in \mathbb{Z}. \tag{3.52}$$

At this point we recognize Narain lattice of a compact boson of radius $R^2 = 2k$. Choosing $k = 1$ will yield boson at self-dual radius, which has largest possible spectral gap

$$\Delta^* = \frac{1}{2}. \qquad (3.53)$$

The corresponding enumerator polynomial is simply $P = x_{00}$, giving rise to torus partition function via (3.28) and (3.29),

$$\mathcal{Z}_{\mathcal{C}}(\tau, \bar{\tau}) = \Psi_{0,0} = \frac{1}{|\eta|^2} \sum_{n,m \in Z} q^{\frac{(m+n)^2}{4}} \bar{q}^{\frac{(m-n)^2}{4}} = \frac{|\theta_3(2\tau)|^2 + |\theta_2(2\tau)|^2}{|\eta|^2}. \qquad (3.54)$$

Clearly, an appropriate $O(1,1)$ transformation will turn $\Lambda_{\mathcal{C}}$ to any other Narain lattice in $\mathbb{R}^{1,1}$, or, equivalently, change the compact boson radius R to any desired value. In other words, together with the $O(1,1)$ factor our code construction is versatile enough such that any $c = 1$ Narain theory is a code theory. This emphasizes the bottom-up nature of our approach. While codes are expected to reflect some algebraic properties of the underlying CFTs in the top-down constructions [31], in our construction certain non-rational CFTs without obvious algebraic properties which would make them "finite" also can be obtained from codes.

3.4.2 $c = 2$

We start with $m = 2, n = -1, k = 2$, which satisfies (3.5) and the glue lattice generated by

$$g_\Lambda = \Lambda^T g \Lambda = \begin{pmatrix} 4 & 2 \\ 2 & -2 \end{pmatrix}, \quad \Lambda = R\, 2 \begin{pmatrix} 1 & 1/2 \\ 0 & \sqrt{3}/2 \end{pmatrix}, \quad R = \begin{pmatrix} 1 & -1 \\ 1 & 1 \end{pmatrix} / \sqrt{2}. \qquad (3.55)$$

From the Euclidean point of view this is a hexagonal (triangular) lattice with the lattice vectors of length 2, rotated by $\pi/2$. Using equivalence transformation

$$P = \begin{pmatrix} 0 & 1 \\ -1 & 1 \end{pmatrix} \in SL(2, \mathbb{Z}) \qquad (3.56)$$

we can bring $g_\Lambda = \Lambda^T g \Lambda$ to the diagonal form

$$\begin{pmatrix} -2 & 0 \\ 0 & 6 \end{pmatrix} = P^T g_\Lambda P, \qquad (3.57)$$

which makes decomposition $G = \mathbb{Z}_2 \times \mathbb{Z}_6$ manifest, with the map

$$g = (a, b) \in G, \quad 0 \le a < 2, 0 \le b < 6, \qquad \ell(g) = (P^T)^{-1} \begin{pmatrix} a \\ b \end{pmatrix} \in \mathbb{Z}^2 / g_\Lambda.$$

We consider a code $\mathcal{C}$ generated by the following three codewords

$$c_1 = ((0, 3), (1, 0)), \qquad (3.58)$$
$$c_2 = ((1, 0), (0, 1)), \qquad (3.59)$$
$$c_3 = ((0, 0), (0, 2)), \qquad (3.60)$$

21

in the notations $c = (g_1, g_2) = ((a_1, b_1), (a_2, b_2))$. This codes is iso-dual, $\mathcal{C}^\perp = S(\mathcal{C})$, where S is the permutation of two elements. Corresponding lattice $\Lambda_{\mathcal{C}}$ obtained via (3.11)

$$\Lambda_{\mathcal{C}} = \begin{pmatrix} \Lambda^\perp (P^T)^{-1} & 0 \\ 0 & \Lambda^\perp (P^T)^{-1} \end{pmatrix} \left(\ell + \begin{pmatrix} 2k_1 \\ 6k_2 \\ 2k_3 \\ 6k_4 \end{pmatrix} \right), \quad \ell^T = \sum_{i=1}^{3} n_i c_i, \quad n_i \in \mathbb{Z}, \quad k_i \in \mathbb{Z}.$$

In this expression above we should understand codewords c_i as regular vectors in $\mathbb{Z}^4$. This lattice is a Narain lattice with respect to the Lorentzian metric (3.22)

$$g_L = \begin{pmatrix} 0 & S \\ S & 0 \end{pmatrix}, \qquad S = \begin{pmatrix} 0 & 1 \\ 1 & 0 \end{pmatrix}. \tag{3.61}$$

By an orthogonal transformation g_L can be brought to conventional form

$$O g_L O^T = \begin{pmatrix} 0 & I_2 \\ I_2 & 0 \end{pmatrix}, \qquad O = \frac{1}{\sqrt{2}} \begin{pmatrix} 1 & 1 & 0 & 0 \\ 0 & 0 & 1 & -1 \\ 0 & 0 & 1 & 1 \\ -1 & 1 & 0 & 0 \end{pmatrix}, \tag{3.62}$$

such that $\Lambda_{\mathcal{C}}$ becomes equivalent to the Narain lattice $\Lambda_{c=2}$ defining $SU(3)_1$ WZW theory

$$\Lambda_{c=2} \sim O\Lambda_C, \quad \Lambda_{c=2} = \begin{pmatrix} (\gamma^{-1})^T & B\gamma \\ 0 & \gamma \end{pmatrix}, \quad \gamma = \sqrt{\frac{b_2}{t_2}} \begin{pmatrix} 1 & t_1 \\ 0 & t_2 \end{pmatrix}, \quad B = \frac{b_1}{b_2} \begin{pmatrix} 0 & 1 \\ -1 & 0 \end{pmatrix},$$

where $t_1 + it_2 = b_1 + ib_2 = (1 + i\sqrt{3})/2$.

The code enumerator polynomial of $\mathcal{C}$ is

$$\begin{aligned} W_{\mathcal{C}}^S = {} & y_{00,00} + y_{00,02} + y_{00,04} + y_{10,01} + y_{10,03} + y_{10,05} \\ & + y_{03,10} + y_{03,12} + y_{03,14} + y_{13,11} + y_{13,13} + y_{13,15}, \end{aligned}$$

which yields partition function via (3.44). Shortest lattice vector with $\ell^T = c_2$ or $\ell^T = c_3$ and $k_i = 0$ has length $|v|^2 = 4/3$, hence corresponding CFT has spectral gap $\Delta^* = 2/3$.

3.4.3 $c = 3, 4, 5$

Optimal theories for $c = 3, 4, 5$ were constructed from codes in [8]. They correspond to $k = 2$ and $n, m = 0$ with

$$\Lambda = \sqrt{2} \begin{pmatrix} 0 & 1 \\ 1 & 0 \end{pmatrix}, \qquad g_\Lambda = 2 \begin{pmatrix} 0 & 1 \\ 1 & 0 \end{pmatrix}, \qquad \Lambda^\perp = I_2/\sqrt{2}. \tag{3.63}$$

In this case $G = \mathbb{Z}_2 \times \mathbb{Z}_2$ which as an additive group is equivalent to F_4. As discussed in section 3.2.3 these codes are parametrized by B-matrix controlling the B-field of

the Narain compactification, $B^T = B \mod 2$, see (3.18). The case of $k = 2$ is special because antisymmetric $B^T = -B \mod 2$ and symmetric matrices B are equivalent.

For the optimal theories with $c = 3, 4, 5$ the symmetric B-matrices, which can be interpreted as graph adjacency matrix , describes the maximally connected graph

$$B_{ij} = \begin{cases} 1, & i \neq j, \\ 0, & i = j. \end{cases} \tag{3.64}$$

Their enumerator polynomials and partition functions can be found in [8]. Here we only point out that for $p = 2$ and $0 \leq a, b < p$

$$\psi_{a,b} = \frac{1}{|\eta|^2} \sum_{n,m \in \mathbb{Z}} q^{(\tilde{a}+\tilde{b})^2/8} \bar{q}^{(\tilde{a}-\tilde{b})^2/8}, \qquad \tilde{a} = a + 2n, \quad \tilde{b} = b + 2m, \tag{3.65}$$

$$\psi_{0,0} = \frac{|\theta_3(\tau)|^2 + |\theta_4(\tau)|^2}{2|\eta|^2}, \tag{3.66}$$

$$\psi_{1,1} = \frac{|\theta_3(\tau)|^2 - |\theta_4(\tau)|^2}{2|\eta|^2}, \tag{3.67}$$

$$\psi_{0,1} = \psi_{1,0} = \frac{|\theta_2(\tau)|^2}{2|\eta|^2}. \tag{3.68}$$

in full agreement with [8]. The spectral gaps are $\Delta^* = 3/4, 1, 1$ for $c = 3, 4, 5$ correspondingly.

3.4.4 $c = 6, 7$

Optimal theories for $c = 6, 7$ were found in [32] to be related to codes, where a construction, different from [8, 29], relating codes over F_4 to CFTs was introduced. Here we show this construction is a particular case of the glue construction introduced in this chapter.

Let us consider the glue matrix

$$\Lambda = \frac{1}{3^{1/4}} \begin{pmatrix} 1 & -1 \\ -\sqrt{3} & -\sqrt{3} \end{pmatrix}. \tag{3.69}$$

This corresponds to $m = -1, n = 1, k = 0$ case as follows from

$$g_\Lambda = \begin{pmatrix} -2 & 0 \\ 0 & 2 \end{pmatrix}. \tag{3.70}$$

Clearly $G = \mathbb{Z}_2 \times \mathbb{Z}_2$ which can be parametrized by $\ell^T = (a, b)$, $0 \leq a, b < 2$. As in the previous section we can identify G with F_4 via the Gray map

$$(a, b) \to c(a, b) := a\,\omega + b\,\bar{\omega}, \tag{3.71}$$

where $F_4 = \{0, \omega, \bar{\omega}, 1\}$.

The scalar product inherited from on G from (3.3) reads

$$\langle (a_1, b_1), (a_2, b_2) \rangle = \ell_1^T g_\Lambda^{-1} \ell_2 = \frac{b_1 b_2 - a_1 a_2}{2}. \tag{3.72}$$

Since the scalar product is defined up to integer shits, orthogonality with respect to $\langle \cdot | \cdot \rangle$ is equivalent to orthogonality with respect to

$$a_1 a_2 + b_1 b_2 \mod 2 = c_1 c_2 + \bar{c}_1 \bar{c}_2, \tag{3.73}$$

where the right-hand-side uses notations (3.71). This is different from the conventional Hermitian scalar product on F_4

$$(c_1, c_2) = c_1 \bar{c}_2 + \bar{c}_1 c_2, \tag{3.74}$$

by an additional conjugation. Thus a code $\mathcal{C} \in G^c$ iso-dual with respect to scalar product on G inherited from (3.3) and pairwise permutation S, $\mathcal{C}^\perp = S(\mathcal{C})$, will be isodual to its conjugate, $\mathcal{C}^\perp = S(\bar{\mathcal{C}})$, with respect to Hermitian scalar product (3.74). This is exactly the isoduality condition outlined in [32].

Similarly, the evenness condition (3.21), written in coordinates

$$\sum_{i=1}^{c} \frac{b_i b_{S(i)} - a_i a_{S(i)}}{2} \mod 2 = 0, \tag{3.75}$$

matches precisely with the evenness condition of [32].

To complete the comparison with [32] we note that under Construction A (3.11) group elements $\ell^T = (a, b)$ will be mapped to

$$v = \Lambda \ell, \quad \Lambda = \begin{pmatrix} -\frac{1}{2} & -\frac{1}{2} \\ \frac{\sqrt{3}}{2} & \frac{-\sqrt{3}}{2} \end{pmatrix}, \tag{3.76}$$

which is exactly the map from $c = a\omega + b\bar{\omega} \in F_4$ to $\mathbb{R}^2$ used in [32]. In other words, we have shown that the construction of [32] is exactly the construction of this chapter with the glue matrix taken to be (3.69).

We notice the choice $m = -1, n = 1, k = 0$ is not the canonical one. By an appropriate $GL(2, \mathbb{Z})$ transformation we can bring it to $m = 1, n = 0, k = 2$, satisfying (3.6). The new form of the glue lattice generating matrix is then

$$\Lambda = \frac{2}{3^{1/4}} \begin{pmatrix} \frac{1}{2} & 1 \\ \frac{\sqrt{3}}{2} & 0 \end{pmatrix}, \tag{3.77}$$

which is a hexagonal (triangular) lattice with the basic vector length $2/3^{1/4}$.

The codes leading to optimal $c = 6$ and $c = 7$ theories, the hexacode and the "septacode" are rather bulky and we do not repeat them here. Let us just mention that in both cases the resulting spectral gap is $\Delta^* = \sqrt{4/3}$.

3.4.5 $c = 8$

We consider the $n = m = 0, k = 4$ case with the glue lattice

$$\Lambda = 2 \begin{pmatrix} 0 & 2^{1/4} \\ 2^{-1/4} & 0 \end{pmatrix}, \quad g_\Lambda = \begin{pmatrix} 0 & 4 \\ 4 & 0 \end{pmatrix}, \quad \Lambda^\perp = \begin{pmatrix} 2^{1/4} & 0 \\ 0 & 2^{-1/4} \end{pmatrix} /2. \tag{3.78}$$

In this case $G = \mathbb{Z}_4 \times \mathbb{Z}_4$ parametrized by $g = (a, b)$, $0 \le a, b < 4$ and $\ell^T = (a, b)$. Let us consider the code $\mathcal{C} \in G^8$ generated by rows of the following matrix

$$
G_{\mathcal{C}} = \begin{pmatrix}
0 & 0 & 0 & 2 & 2 & 0 & 0 & 0 & 0 & 0 & 0 & 0 & 0 & 0 & 0 & 0 \\
0 & 0 & 0 & 0 & 2 & 2 & 0 & 0 & 0 & 0 & 0 & 0 & 0 & 0 & 0 & 0 \\
0 & 0 & 0 & 0 & 0 & 2 & 2 & 0 & 0 & 0 & 0 & 0 & 0 & 0 & 0 & 0 \\
1 & 1 & 1 & 1 & 1 & 1 & 1 & 1 & 0 & 0 & 0 & 0 & 0 & 0 & 0 & 0 \\
2 & 0 & 0 & 0 & 2 & 0 & 0 & 0 & 0 & 0 & 0 & 0 & 0 & 0 & 0 & 0 \\
3 & 1 & 0 & 0 & 3 & 1 & 0 & 0 & 2 & 2 & 0 & 0 & 0 & 0 & 0 & 0 \\
0 & 3 & 1 & 0 & 0 & 3 & 1 & 0 & 0 & 2 & 2 & 0 & 0 & 0 & 0 & 0 \\
0 & 0 & 3 & 1 & 0 & 0 & 3 & 1 & 0 & 0 & 2 & 2 & 0 & 0 & 0 & 0 \\
3 & 0 & 0 & 3 & 1 & 0 & 0 & 3 & 0 & 0 & 0 & 2 & 2 & 0 & 0 & 0 \\
1 & 3 & 0 & 0 & 3 & 1 & 0 & 0 & 0 & 0 & 0 & 0 & 2 & 2 & 0 & 0 \\
0 & 1 & 3 & 0 & 0 & 3 & 1 & 0 & 0 & 0 & 0 & 0 & 0 & 2 & 2 & 0 \\
0 & 0 & 0 & 0 & 1 & 1 & 1 & 1 & 1 & 1 & 1 & 1 & 1 & 1 & 1 & 1
\end{pmatrix} \tag{3.79}
$$

in the notation $c = (a_1, \ldots, a_8 | b_1, \ldots, b_8) \in \mathcal{C}$. This code is even and self-dual with respect to

$$
\langle (\boldsymbol{a}|\boldsymbol{b})|(\boldsymbol{a}'|\boldsymbol{b}') \rangle = \frac{\boldsymbol{a} \cdot \boldsymbol{b}' + \boldsymbol{a}' \cdot \boldsymbol{b}}{4}. \tag{3.80}
$$

Accordingly the lattice

$$
\Lambda_{\mathcal{C}} = \frac{1}{2} \begin{pmatrix} 2^{1/4} I_8 & 0 \\ 0 & 2^{-1/4} I_8 \end{pmatrix} (G_{\mathcal{C}}^T z + 4k), \quad z \in \mathbb{Z}^{12}, \quad k \in \mathbb{Z}^{16}, \tag{3.81}
$$

is a Narain lattice with respect to

$$
g_L = \begin{pmatrix} 0 & I_8 \\ I_8 & 0 \end{pmatrix}. \tag{3.82}
$$

The lattice shortest vector has length $|v|^2 = 2\sqrt{2}$ yielding $\Delta^* = \sqrt{2}$. This follows from the lattice theta series, which can be readily obtained from the code enumerator polynomial. The code in question has 2^{16} codewords and enumerator polynomial $P_{\mathcal{C}}(x_{ab})$ is too large to be written explicitly here. Upon substituting $x_{ab} \to \psi_{ab}$ where

$$
\psi_{ab} = \sum_{k \in \mathbb{Z}^2} q^{|v|^2/2}, \quad v = \Lambda^\perp (\ell + 4k), \quad \ell^T = (a, b). \tag{3.83}
$$

(this definition is different from (3.29) in two ways: i) there is no $|\eta(\tau)|$ in the denominator because we are interested in the lattice theta-function rather than the CFT partition function ii) ψ_{ab} depends on q but not $\bar{q}$ as we are interested in the Euclidean structure only), we obtain

$$
W_{\mathcal{C}}(\psi_{ab}) = 1 + 4320t^2 + 61440t^3 + 522720t^4 + 2211840t^5 + O\left(t^6\right), \quad t = q^{2^{-1/2}},
$$

which is exactly the theta-function of the Barnes-Wall lattice. This is in agreement with [37] who identified optimal $c = 8$ theory to be based on a rescaled Barnes-Wall lattice, equipped with the Lorentzian metric and understood as a Narain lattice.

3.5 Asymptotically large c

When $c \gg 1$ asymptotic behavior of spectral gap is not known. Spinless modular bootstrap bounds Δ^*/c to be less than or equal to $1/\pi^2$ (with this value being obtained numerically) [26], while the full set of bootstrap constraints is likely to significantly decrease this value. Averaging over the whole moduli space of Narain theories provides a lower bound on Δ^*/c to be $1/(2\pi e)$ [37]. Ref. [23] conjectured this value to be asymptotically saturated,

$$\lim_{c \to \infty} \frac{\Delta^*}{c} = \frac{1}{2\pi e}. \tag{3.84}$$

For this to be true, i.e. for the mean value to (asymptotically) be the largest possible value, the distribution of spectral gaps on the Narain moduli space for large c must be very sharply peaked around the mean without outliers. Thus, for consistency, as a necessary condition, variance should be very small. Using the ensemble of code CFTs, as well as chiral cousins of Narain theories, ref. [23] has shown the variance of density of states distribution to be exponentially suppressed $\sim e^{-\mathcal{O}(c)}$, the conclusion consequently confirmed for the Narain theories in [38]. This does not constitute a proof of (3.84) as variance is not sensitive to possible outliers.

The conjecture of [23] is based on similarity between the ensemble of codes, ensemble of sphere packings, and the ensemble (space) of CFTs, and the problems of maximizing code Hamming distance, density of sphere packing and CFT spectral gap. Specifically for codes, there is an expectation that the Gilbert-Varshamov bound (the value resulting from averaging over all codes) would asymptotically yield the best value of Hamming distance to code size ratio [39, 40]. Similar expectation holds for the maximal density of lattice sphere packing: the densest packing to asymptotically saturate the Minkowski bound, which is simply averaged value over all possible lattices. (For sphere packings of general kind stronger asymptotic value is expected [41].) While we leave validity of (3.84) for future studies, here we show there are codes theories achieving this value of Δ^* for large c.

The Construction A used in this chapter has a fundamental limitation: the corresponding lattices have vectors of certain length no matter how big the dimension c is. This is formalized in equation (3.26), which provides an upper bound on Δ^*. Thus, to obtain Δ^* scaling linearly with c one has to adjust n, m, k together with c such that $|G|$ grows as or faster than c. Here for simplicity we focus on the square gluing lattice $n = m = 0$, with prime $k = p$, discussed in sections 3.2.3, 3.3.2. The spectral gap is given by (3.23) with $|v_\Lambda| = \sqrt{p}$,

$$\Delta^* = \frac{1}{2} \min\left(d(\mathcal{C}), p\right). \tag{3.85}$$

The best (maximal) generalized Hamming distance d beyond small c values is not known. One nevertheless can bound d from below by consider ensemble averaging, the so-called Gilbert-Varshamov bound. Then, similarly to the case of binary linear codes one may expect best d/c to asymptotically approach the bound when $c \to \infty$.

By averaged polynomial $\bar{P}(\{x_{ab}\})$ we mean enumerator polynomial averaged over all $p^{c(c-1)/2}$ possible codes parametrized by B, see (3.16). From the CFT point of view this is the calculation of averaged torus partition function. So far we are interested only in d, or alternatively only in mass but not spin of the lightest non-trivial state, we can consider torus parameter to be purely imaginary $\tau = i\tau_2$. Then function (3.3.2) factorizes

$$\psi_{ab}(i\tau_2) = \frac{1}{|\eta(\tau)|^2}\psi_a\psi_b, \qquad \psi_a = \Theta_{2a,p}(i\tau_2/2) = \sum_{k\in\mathbb{Z}} e^{-\pi\tau_2(a+kp)^2/p}. \qquad (3.86)$$

Going back to enumerator polynomial, instead of variables x_{ab} we use

$$x_{ab} = t_a t_b, \qquad t_a = t_{-a}, \qquad (3.87)$$

where the last property reflects $\psi_a = \psi_{-a}$. We conjecture the form of corresponding averaged enumerator polynomial based on invariance under MacWilliams identity and explicit checks for sufficiently small n and prime p, for which direct evaluation of $\bar{P}(\{t_a t_b\})$ using computer algebra is feasible,

$$\bar{P}(\{t_a t_b\}) = \frac{1}{p^{c(c-1)/2}}\sum_B P_{\mathcal{C}(B)}(\{t_a t_b\}) =$$

$$t_0^{2c} + \frac{\sum\limits_{k=0}^{p=1}\left(\sum\limits_{a=0}^{p-1}\sum\limits_{b=0}^{p-1}\cos\left(\frac{2\pi kab}{p}\right)t_a t_b\right)^c - p\, t_0^c \left(\sum\limits_{a=0}^{p-1} t_a\right)^c}{p^c}. \qquad (3.88)$$

Now we are ready to analyze this expression to deduce the lower bound on Δ^*. For large c, the main contribution to (3.88) comes from $k = 0$, leading to the averaged partition function

$$\bar{Z} \approx \frac{1}{|\eta|^{2c}}\frac{\left(\sum\limits_{a=0}^{p-1}\psi_a\right)^{2c}}{p^c} = \frac{1}{|\eta|^{2c}}\frac{\left(\sum\limits_{n\in\mathbb{Z}} e^{-\pi\tau_2 n^2/p}\right)^{2c}}{p^c}. \qquad (3.89)$$

Interpreted as sum over lattice points, the numerator is simply the sum over $2c$-dimensional square lattice of size $1/\sqrt{p}$. On the length scales of $\sim 1/\sqrt{p}$ or larger this is just the homogeneous distribution of points with the averaged density $1/(1/\sqrt{p}^{2c}) = p^c$. This factor exactly cancels p^c in the denominator of (3.89) and we find density of states

$$\rho(\Delta) = \frac{(2\pi)^c \Delta^{c-1}}{\Gamma(c)} \qquad (3.90)$$

valid on scales $\Delta \gtrsim 1/\sqrt{p}$. This is exactly the density of states of "$U(1)$-gravity" – Narain theory averaged over the whole moduli space. Accordingly, the threshold for the density to become of order one is $\Delta = c/(2\pi e)$, which is our Gilbert-Varshamov bound. For this result to be valid we must require $p/2 > c/(2\pi e)$, otherwise shortest vector of $\Lambda_{\mathcal{C}}$ would have length $\sqrt{p}$.

To conclude, for sufficiently large p we find that the averaged density of states (with zero chemical potential for spin) of $n = m = 0$, and prime $k = p$ code theories is the same as the averaged density of states for all Narain theories. In particular in the limit $c \to \infty$, for $p > c/(\pi e)$ there are code theories with $\Delta^*/c = 1/(2\pi e)$. Provided the conjecture of [23] is correct, it would mean similar conjecture applies to $n = m = 0$, prime $k = p$ codes, in the sense that their averaged Hamming distance is asymptotically the best one.

3.6   Summary: Optimal and large-c Narain theories

In this chapter, we proposed a family of constructions mapping additive codes over abelian groups $G = \mathbb{Z}_p \times \mathbb{Z}_q$ to Narain lattices and hence Narain CFTs. Each construction is parametrized by a triplet of integer numbers n, m, k and an element from $O(1,1)$ parameterizing an even "glue" lattice $\Lambda \subset \mathbb{R}^{1,1}$. The resulting Narain lattice $\Lambda_{\mathcal{C}}$ associated with a code $\mathcal{C} \subset G^c$ obeys

$$\underbrace{\Lambda \oplus \cdots \oplus \Lambda}_{c \text{ times}} \subset \Lambda_{\mathcal{C}} \subset \underbrace{\Lambda^\perp \oplus \cdots \oplus \Lambda^\perp}_{c \text{ times}} \subset \mathbb{R}^{c,c}. \tag{3.91}$$

We call this glue construction following [17]. This construction generalizes and encompasses those of [8, 29], [32] and [33]. We call the CFTs obtained from codes "code theories." Their torus partition functions $Z_{\mathcal{C}}$ are given in terms of the code enumerator polynomials, which are multi-variable polynomials satisfying certain algebraic identities, which guarantee modular invariance of $Z_{\mathcal{C}}$. In this way one can construct many new solutions to modular bootstrap constraints.

We have provided explicit code constructions for all conjectural optimal Narain theories for $c \leq 8$ identified in [27]. Furthermore we have shown there are code theories with the spectral gap Δ^* scaling linearly with $c \gg 1$, $\Delta^* \propto c/(2\pi e)$, with the coefficient which has been conjectured in [23] to be maximal possible.

An important direction would be to connect the bottom-up approach of this chapter with the top-down approach of [31] where quantum codes were given an interpretation in terms of CFT Hilbert space extended by defect operators. Another direction would be to develop our approach into a systematic and practical way of constructing optimal theories with $c > 8$, thus complementing conventional modular bootstrap. This would be an important but challenging task because there is no known efficient methods to construct "good" codes with largest or even large (generalized) Hamming distance. And though there is a finite number of codes for any given G and c, their number grows exponentially with c. Furthermore, there is an infinite number of constructions, i.e. infinite number of different G and Λ, making the problem seemingly incomprehensible. This pessimistic assessment could be too naive, we expect only finite number of constructions to be relevant for any given c. The inequality (3.26) as well as the results of section 3.5 clearly indicate $|G|$ can not be too small, $|G|^{1/2} \geq ac$, for $c \gg 1$ with some positive constant a. We also strongly suspect large generalized Hamming distance, for given c, would require $|G|$ not be too large. We conjecture this may come from the linear programming constraints stemming from the algebraic

identities satisfied by code enumerator polynomial (the MacWilliam identity and the condition due to code evenness), i.e. generalization of Delsarte's bounds [42] to the types of codes of interest. For $c \gg 1$ we expect the bound to have the form $|G|^{1/2} \leq bc$ with some $b > a$. Thus for large but finite c we expect large but finite number of glue groups satisfying $bc \geq |G|^{1/2} \geq ac$. This form of the bound on $|G|$ is merely a guess; the important point here is the expectation that the problem of identifying the code with largest generalized Hamming distance can be reduced to an optimization problem over a finite set. Of course even for moderate c naive brute-force approaches such as going through all possible codes very quickly becomes unfeasible. The resulting optimization problem over a discrete set would be NP-hard, but novel quantum platforms promise an exciting hope of solving medium-sized discrete optimization problems in real time, the avenue we hope to pursue in the future [43].

To conclude this chapter, we would like to point out another very important direction for future work – to extend the connection between codes and CFTs beyond the Narain theories.

Chapter 4 Rational CFTs and Poincaré sums from codes

4.1 Narain CFTs with enhanced symmetry and Poincaré sums

In recent years, there is an understanding that AdS gravity in low dimensions is not dual to a single theory, but rather an ensemble average of CFTs. In [44] the path integral for 3d Einstein gravity with AdS boundary conditions was evaluated, but the result does not make sense as a CFT partition function, as it cannot be expressed in the form $\operatorname{tr} e^{-\beta H}$. Results from 2d gravity, [9], indicate that gravity may be dual to an ensemble of boundary theories. However, it is not known how to average over *all* 2d CFTs, or how they should be weighted in this average. A more realistic goal is to average over a known family of CFTs, such as the Narain family. This was achieved in [10], resulting not in 3d Einstein gravity, but rather an exotic theory, dubbed "$U(1)$ gravity".

Any Narain CFT can be constructed from codes (see section 3). However, the space of codes of a given alphabet and length is finite, therefore by averaging over codes it is not possible to cover the Narain moduli space. In [11] it was shown that averaging a family of code Narain CFTs and subsequently taking the limit where the size of the alphabet grows to infinity, the partition function of "$U(1)$ gravity" is reproduced.

In this chapter we use codes to study Narain CFTs at the points of enhanced symmetry, described by affine Lie algebras of type A,D,E at level 1. Such CFTs are rational, meaning that they contain a finite number of primary fields. The A,D,E, are the three families of simply-laced classical Lie algebras. A_n, D_n are infinite families, corresponding to the Lie groups $SU(n+1)$, $SO(2n)$ respectively, while E_6, E_7, E_8 are exceptional Lie algebras.

The theories with A Lie symmetry at level 1 were classified and their Poincaré sums were evaluated in [45]. We show that this problem can be formulated in terms of codes and the results can be straightforwardly reproduced. We proceed to apply the code formalism to theories with Lie symmetries D and E at level 1.

Let Λ denote the root lattice of a simply-laced Lie algebra. The discriminant group $G = \Lambda^\perp/\Lambda$ is a finite Abelian group. The elements of G are in one-to-one correspondence with the highest-weight representations of the affine Lie algebra at level 1. The fusion rules of the full (non-chiral) CFT are described by the group $G \times \bar{G}$, where the two factors correspond to the holomorphic and anti-holomorphic sectors. We start by classifying all their modular invariants using codes. Subsequently, we calculate their Poincaré series.

4.2 Codes based on the root lattice A_{N-1}

4.2.1 The $su(N)_1 \times su(N)_1$ CFT

The chiral $su(N)_1$ theory has central charge $c = N - 1$ and N primary fields whose conformal dimensions are given by

$$h_i = \frac{i(N-i)}{2N}, \quad i = 0, 1, \ldots, N-1. \tag{4.1}$$

The root lattice of $su(N)$ is $\Lambda = A_{N-1}$. A generator matrix is given by (we will abuse notation to denote lattices, as well as their generator matrices by the same symbol):

$$\Lambda_{ij} = \begin{cases} \sqrt{\frac{i+1}{i}} & i = j \\ -\sqrt{\frac{i}{i+1}} & j = i+1 \\ 0 & \text{otherwise} \end{cases}, \quad i, j = 1, 2, \ldots, N-1 \tag{4.2}$$

or in matrix form

$$\Lambda = \begin{pmatrix} \sqrt{2} & -\frac{1}{\sqrt{2}} & 0 & 0 & \cdots & 0 & 0 \\ 0 & \sqrt{\frac{3}{2}} & -\sqrt{\frac{2}{3}} & 0 & \cdots & 0 & 0 \\ 0 & 0 & \sqrt{\frac{4}{3}} & -\sqrt{\frac{3}{4}} & \cdots & 0 & 0 \\ \vdots & \vdots & \vdots & \vdots & \vdots & \vdots & \vdots \\ 0 & 0 & 0 & 0 & \cdots & \sqrt{\frac{N-1}{N-2}} & -\sqrt{\frac{N-2}{N-1}} \\ 0 & 0 & 0 & 0 & \cdots & 0 & \sqrt{\frac{N}{N-1}} \end{pmatrix}. \tag{4.3}$$

The determinant is

$$\det(\Lambda) = \prod_{i=1}^{N-1} \sqrt{\frac{i+1}{i}} = \sqrt{N}. \tag{4.4}$$

A convenient generator matrix for the dual lattice Λ is

$$\Lambda^\perp = (\Lambda^T)^{-1}. \tag{4.5}$$

The order of the discriminant group $G = \Lambda^\perp/\Lambda$ can be found by dividing the volumes of the unit cells $|G| = \det(\Lambda)/\det(\Lambda^\perp) = \det(\Lambda)^2 = N$, hence the discriminant group has order N and is the following

$$G = \Lambda^\perp/\Lambda \cong \mathbb{Z}_N. \tag{4.6}$$

Let us choose the map $\phi : \Lambda^\perp \to \mathbb{Z}_N$ such that ϕ^{-1} acting on an element of $\mathbb{Z}_N$ results to the following set of vectors in $\Lambda^\perp \subseteq \mathbb{R}^{N-1}$:

$$a \mapsto \left\{ \Lambda m + a\lambda, \ \lambda = \begin{pmatrix} 0 \\ \vdots \\ 0 \\ \sqrt{\frac{N-1}{N}} \end{pmatrix} : m \in \mathbb{Z}^{N-1} \right\}. \tag{4.7}$$

The group G is induced with the following bi-linear form (stemming from Euclidean inner product of $\mathbb{R}^{N-1}$)

$$\langle a_1, a_2 \rangle = a_1 a_2 |\lambda|^2 = \frac{N-1}{N} a_1 a_2 \mod \mathbb{Z}. \tag{4.8}$$

Note that the choice of λ is not unique; we may choose any element of $\Lambda^\perp/\Lambda$ that has order N. However, the inner product (4.8) is independent of the choice of λ. The group G is also equipped with the weight

$$wt(a) \equiv \min_{k \in \mathbb{Z}^{N-1}} ||\Lambda k + a\lambda|| = \frac{a(N-a)}{N}, \quad a = 0, 1, \ldots, N-1. \tag{4.9}$$

For each $a \in \mathbb{Z}_N$ define the holomorphic function in the upper half-plane

$$\chi_a(\tau) = \frac{1}{\eta^{N-1}} \sum_{n \in \mathbb{Z}^{N-1}} e^{\pi i \tau (\Lambda n + a\lambda)^T (\Lambda n + a\lambda)}. \tag{4.10}$$

The functions $\chi_a(\tau)$ are precisely the chiral characters of $su(N)_1$. They transform as follows[1] under the modular T, S transformations

$$\chi_a(\tau + 1) = e^{-\frac{(N-1)\pi i}{12}} \sum T_{aa'} \chi_{a'}(\tau), \quad T_{aa'} = \delta_{aa'} e^{\pi i (N-1) \frac{a^2}{N}} \tag{4.11}$$

$$\chi_a(-1/\tau) = \sum_{a \in \mathbb{Z}_N} S_{aa'} \chi_{a'}(\tau), \quad S_{aa'} = \frac{1}{\sqrt{N}} e^{-2\pi i \frac{aa'}{N}}. \tag{4.12}$$

Now consider codes $\mathcal{C} \subseteq G \times \bar{G}$. We equip $G \times \bar{G}$ with a Lorentzian bi-linear form by extending (4.8) to $G \times \bar{G}$ as follows

$$\langle (a_1, b_1) | (a_2, b_2) \rangle = \langle a_1 | a_2 \rangle - \langle b_1 | b_2 \rangle = \frac{N-1}{N} (a_1 a_2 - b_1 b_2) \mod \mathbb{Z}. \tag{4.13}$$

The evenness condition on $G \times \bar{G}$ is

$$wt_2((a, b)) = \frac{N-1}{N} (a^2 - b^2) = 0 \mod 2\mathbb{Z}. \tag{4.14}$$

From wt_2 it is obvious that if N is odd, any self-dual code is even. However, for even N not all self-dual codes are even. This will have consequences in our enumeration of even self-dual codes.

We define the enumerator polynomial of a code $\mathcal{C}$ as follows

$$W_{\mathcal{C}}(x_0, \bar{x}_0, \ldots, x_{N-1}, \bar{x}_{N-1}) = \sum_{(a,b) \in \mathcal{C}} x_a \bar{x}_b. \tag{4.15}$$

The partition function is obtained by the substitution

$$x_a \to \chi_a(\tau), \quad \bar{x}_b \to \bar{\chi}_b(\bar{\tau}), \tag{4.16}$$

---

[1]We do not include the constant phase $e^{-\frac{(N-1)\pi i}{12}}$ in the definition of $T_{aa'}$, since it always cancels out upon combining holomorphic and antiholomorphic characters.

where χ_a are defined in (4.10). The MacWilliams transformation acts on the x_i in the same way as the modular S transformation acts on the characters (4.12). We may also define T acting on code variables in the same manner as (4.11). In this way, the variables x_i form a representation of $SL(2, \mathbb{Z})$, with the generators given by

$$T(x_a) = \sum_{b=0}^{N-1} T_{ab} x_b, \quad T_{ab} = e^{\pi i (N-1)\frac{a^2}{N}} \delta_{ab}, \tag{4.17}$$

$$S(x_a) = \sum_{b=0}^{N-1} S_{ab} x_b, \quad S_{ab} = \frac{1}{\sqrt{N}} e^{-2\pi i \frac{ab}{N}}. \tag{4.18}$$

Let us now enumerate all even, self-dual codes. Their number depends on the factors of N

$$\text{number of self-dual codes} = \begin{cases} \sigma_0(N) & N \text{ odd} \\ \sigma_0(N/2) & N \text{ even,} \end{cases} \tag{4.19}$$

where $\sigma_0(m)$ denotes the number of divisors of m. To make this more precise, define

$$\kappa_N = \begin{cases} N, & N \text{ odd} \\ \frac{N}{2}, & N \text{ even.} \end{cases} \tag{4.20}$$

The number of even self-dual codes is $\sigma_0(\kappa_N)$. The characters (4.10) have the property $\chi_i = \chi_{N-i}$. Therefore, not all codes lead to distinct modular invariants. On the code side, this means that the operation sending a codeword (a, b) to $(a, -b)$ is a code equivalence. The number of inequivalent codes, or linearly independent partition functions, in agreement with [45], is given by

$$\text{number of inequivalent codes} = \begin{cases} \frac{\sigma_0(\kappa_N)}{2}, & \sigma_0(\kappa_N) \text{ even} \\ \frac{\sigma_0(\kappa_N)+1}{2}, & \sigma_0(\kappa_N) \text{ odd} \end{cases}. \tag{4.21}$$

To show (4.19), consider the prime factorization of $N = \Pi_i p_i^{n_i}$. By the Chinese Remainder Theorem, there exists an isomorphism

$$\pi : \mathbb{Z}_N \to \bigotimes_{i=1}^{l} \mathbb{Z}_{p_i^{n_i}}, \, l \in \mathbb{N}. \tag{4.22}$$

Explicitly, this isomorphism may be chosen as follows

$$\pi(x) = (x \bmod p_1^{n_1}, x \bmod p_2^{n_2}, \ldots, x \bmod p_l^{n_l}). \tag{4.23}$$

Its inverse is given by

$$\pi^{-1}(a_1, a_2, \ldots, a_l) = m_1 a_1 \frac{N}{p_1^{n_1}} + m_2 a_2 \frac{N}{p_2^{n_2}} + \cdots + m_l a_l \frac{N}{p_l^{n_l}}, \tag{4.24}$$

where $m_1, m_2, \ldots, m_l$ are integers that satisfy

$$m_1 \frac{N}{p_1^{n_1}} + m_2 \frac{N}{p_2^{n_2}} + \cdots + m_l \frac{N}{p_l^{n_l}} = 1. \tag{4.25}$$

The existence of these integers is guaranteed by Bezout's lemma.

An even, self-dual code $\mathcal{C}$ with alphabet $\mathbb{Z}_N$ exists if and only if even, self-dual codes with each factor alphabet $\mathbb{Z}_{p_i^{n_i}}$ exist. Moreover, given a collection of self-dual codes with alphabets $\mathbb{Z}_{p_i^{n_i}}$ a self-dual code with alphabet $\mathbb{Z}_N$ can be constructed by applying the map π^{-1}.

Consider now the codes over a single factor $\mathbb{Z}_{p_i^{n_i}}$, where p_i is odd. We shall drop the subscript i in this and the following paragraph, to reduce clutter in the notation. Each self-dual code with alphabet $\mathbb{Z}_{p^n}$ is isomorphic, as an additive group, to $\mathbb{Z}_{p^{n-k}} \times \mathbb{Z}_{p^k}$ for $k = 0, 1, \ldots, n$, resulting in $\sigma_0(p^n) = n + 1$ self-dual codes. Explicitly, the codes are generated by[2]

$$
\mathcal{C}_0^i = (1, 1), \ \mathcal{C}_n^i = (1, -1), \ \mathcal{C}_k^i =
\begin{cases}
\begin{pmatrix} p^k & p^k \\ 0 & p^{n-k} \end{pmatrix} & 1 \leq k \leq \frac{n}{2}, \\[2ex]
\begin{pmatrix} p^{n-k} & -p^{n-k} \\ 0 & p^k \end{pmatrix} & \frac{n}{2} < k \leq n - 1
\end{cases}
\tag{4.27}
$$

For $p = 2$, there is a small, but important modification of (4.27). If n is even, the code $\mathcal{C}_{n/2}$ is not even, therefore must be excluded. If n is odd, the codes $\mathcal{C}_{(n-1)/2}$ and $\mathcal{C}_{(n+1)/2}$ are identical. In either case, this decreases the number of even, self-dual codes to $\sigma_0(2^{n-1}) = n$.

Now, since the divisor function has the multiplicative property $\sigma_0(m)\sigma(k) = \sigma(mk)$ for co-prime m, k, and every factor $\mathbb{Z}_{p_i^{n_i}}$ contributes $\sigma(p_i^{n_i}) = n_i + 1$ to the number of even self-dual codes (except for $p = 2$ which contributes $\sigma(2^{n_i-1}) = n_i$, the counting (4.19) immediately follows.

The enumerator polynomial of a factor code (4.27) can be written explicitly as

$$
W_k^i = \sum_{a=0}^{p_i^{n_i-k}-1} \sum_{b=0}^{p_i^k-1} x_{ap_i^k} \bar{x}_{ap_i^k + bp_i^{n-k}}, \quad 0 \leq k \leq n_i.
\tag{4.28}
$$

Let l be the number of factors in (4.22) and define the linear map ξ, acting on the enumerator polynomial variables by combining them as follows

$$
\xi(x_{a_1}^1 \bar{x}_{b_1}^1, \ldots, x_{a_l}^l \bar{x}_{b_l}^l) = x_{\pi^{-1}(a_1, \ldots, a_l)} \bar{x}_{\pi^{-1}(a_1, \ldots, a_l)}.
\tag{4.29}
$$

Making a choice of a self-dual code $\mathcal{C}_k^i$ for each factor in (4.22) and applying the map π^{-1} we construct the code $\mathcal{C}_{k_1,\ldots,k_l}$ with alphabet $\mathbb{Z}_N$. The enumerator polynomials of the code $\mathcal{C}_{k_1,\ldots,k_l}$ of alphabet $\mathbb{Z}_N$ can be expressed as

$$
W_{k_1,\ldots,k_l} = \xi(W_{k_1}^1, \ldots, W_{k_l}^l).
\tag{4.30}
$$

---

[2]An interesting fact is that for even n and odd prime p, $p^n - 1$ is a multiple of 8, a dimension where even, self-dual Euclidean lattices exist (see section 2.2). In particular, this implies the existence of chiral bosonic CFTs. The code with $k = \frac{n}{2}$ decomposes into a direct sum of two lower-dimensional codes, resulting in a product of two chiral CFTs, with partition function

$$
Z_{\frac{n}{2}} = \sum_{a=0}^{N-1} \chi_a \sum_{a=0}^{N-1} \bar{\chi}_a.
\tag{4.26}
$$

Finally, the partition functions are obtained by replacing the code variables $x_i, \bar{x}_j$ by the characters $\chi_i, \bar{\chi}_j$

$$Z_{k_1,\ldots,k_l}(\tau,\bar{\tau}) = W_{k_1,\ldots,k_l}(\chi_0,\bar{\chi}_0,\ldots,\chi_{N-1},\bar{\chi}_{N-1}). \tag{4.31}$$

4.2.2 Poincaré series

We are now ready to evaluate the Poincaré series, $\bar{Z}$; a sum over modular images of the vacuum character

$$\bar{Z} \propto \sum_{\gamma \in SL(2,\mathbb{Z})} \gamma(\chi_0\bar{\chi}_0). \tag{4.32}$$

This series is manifestly modular invariant. The space of modular invariants is spanned by the (finitely many) partition functions (4.31), therefore $\bar{Z}$ is a linear combination of the functions (4.31).

Under a general modular transformation, the character $\chi_0\bar{\chi}_0$ is mapped to a linear combination of characters $\chi_i\bar{\chi}_j$. Since there are finitely many characters and the group $SL(2,\mathbb{Z})$ is infinite, the sum in the right-hand side of (4.32) is divergent, however it can be easily regularized, as this infinity is an overall factor. We first identify an (infinite) subgroup of $SL(2,\mathbb{Z})$ that leaves the vacuum character invariant. This subgroup is $\Gamma_0(N)$, a congruence subgroup of level N (note that this is not a normal subgroup). It is defined by:

$$\Gamma_0(N) = \left\{ \begin{pmatrix} a & b \\ c & d \end{pmatrix} \in SL(2,\mathbb{Z}) : c = 0 \mod N \right\}, \tag{4.33}$$

and its index is finite

$$[SL(2,\mathbb{Z}) : \Gamma_0(N)] = N \prod_{p|N,\ p\text{ prime}} \left(1 + \frac{1}{p}\right), \tag{4.34}$$

where the product is over the prime divisors of N. The sum on the right-hand side of (4.32) can be replaced by a sum over the quotient $SL(2,\mathbb{Z})/\Gamma_0(N)$, which is a finite set:

$$\bar{Z} = \sum_{\gamma \in SL(2,\mathbb{Z})/\Gamma_0(N)} \gamma(\chi_0\bar{\chi}_0). \tag{4.35}$$

Equivalently, we can consider the Poincaré series of the "vacuum" code enumerator variable $x_0\bar{x}_0$

$$\bar{W} = \sum_{\gamma \in SL(2,\mathbb{Z})/\Gamma_0(N)} \gamma(x_0\bar{x}_0). \tag{4.36}$$

Now consider a single $\mathbb{Z}_{p_i^{n_i}}$ factor from the decomposition (4.22). Let $\{x_a^i, \bar{x}_b^i\}$ denote its enumerator polynomial variables and $\bar{W}^i$ its Poincaré sum

$$\bar{W}^i = \sum_{\gamma \in SL(2,\mathbb{Z})/\Gamma_0(p_i^{n_i})} \gamma(x_0^i\bar{x}_0^i). \tag{4.37}$$

The index of the congruence subgroup $\Gamma_0(p_i^{n_i})$ is

$$[SL(2,\mathbb{Z}) : \Gamma_0(p_i^{n_i})] = p_i^{n_i} + p_i^{n_i-1}. \tag{4.38}$$

We make a choice of representatives in this quotient and perform the sum

$$\bar{W}^i = \left(\sum_{k=0}^{p_i^{n_i}-1} T^k S + \sum_{k=0}^{p_i^{n_i-1}-1} ST^{p_i k} S \right) x_0^i \bar{x}_0^i = W_0^i + W_{n_i}^i + \frac{p_i - 1}{p_i} \sum_{k=1}^{n_i-1} W_k^i. \tag{4.39}$$

This formula is in agreement with [45].

Combining all factors of (4.22), we obtain

$$\bar{W} = \xi(\bar{W}^1, \ldots, \bar{W}^l). \tag{4.40}$$

Finally, to obtain the Poincaré series in terms of characters, we make the substitution

$$\bar{Z}(\tau, \bar{\tau}) = \bar{W}(\chi_0, \bar{\chi}_0, \ldots, \chi_{N-1}, \bar{\chi}_{N-1}). \tag{4.41}$$

In the special case, where N is square-free, $\bar{W}$ is a sum of all polynomials in (4.30) with coefficients equal to 1, leading to

$$\bar{W} = \frac{x_0 \bar{x}_0 + \frac{1}{N^2} \sum_{r=0}^{N-1} \sum_{a,b=0}^{N-1} x_a \bar{x}_b e^{-2\pi i r \frac{a^2 - b^2}{N}}}{1 + \frac{1}{N}}. \tag{4.42}$$

4.3   Codes based on the root lattice D_n

4.3.1   The $so(2n)_1 \times so(2n)_1$ CFT

The $so(2n)_1$ chiral CFT has central charge $c = n$. In contrast to the A_n case, the number of highest-weight representations is independent of n. There are 4 highest-weight representations, which we denote by $1, v, c, s$. Their conformal weights are

$$h_1 = 0, \ h_v = \frac{1}{2}, \ h_c = h_s = \frac{n}{8}. \tag{4.43}$$

Let $\Lambda = D_n$ be the root lattice of the Lie algebra $so(2n)$. A generator matrix is given by

$$\Lambda_{ij} = \begin{cases} 1 & i = j \\ -1 & i = j + 1 \\ 1 & i = n - 1 \wedge j = n \\ 0 & \text{otherwise} \end{cases}. \tag{4.44}$$

For example, the generators of D_4, D_5 are the following

$$D_4 = \begin{pmatrix} 1 & 0 & 0 & 0 \\ -1 & 1 & 0 & 0 \\ 0 & -1 & 1 & 1 \\ 0 & 0 & -1 & 1 \end{pmatrix}, \ D_5 = \begin{pmatrix} 1 & 0 & 0 & 0 & 0 \\ -1 & 1 & 0 & 0 & 0 \\ 0 & -1 & 1 & 0 & 0 \\ 0 & 0 & -1 & 1 & 1 \\ 0 & 0 & 0 & -1 & 1 \end{pmatrix}. \tag{4.45}$$

The discriminant group depends on the parity of n

$$G = D_n^\perp / D_n \cong \begin{cases} \mathbb{Z}_4 & n \text{ odd} \\ \mathbb{Z}_2 \times \mathbb{Z}_2 & n \text{ even} \end{cases}. \tag{4.46}$$

4.3.2 Odd n

For **odd** n, G is cyclic and we choose the map $\phi : \Lambda^\perp \to \mathbb{Z}_N$, such that ϕ^{-1} from $\mathbb{Z}_4$ to $\Lambda^\perp \subseteq \mathbb{R}^n$:

$$a \mapsto \left\{ \Lambda m + a\lambda, \ \lambda = \begin{pmatrix} \frac{1}{2} \\ \vdots \\ \frac{1}{2} \\ \frac{1}{2} \\ \frac{1}{2} \end{pmatrix} : m \in \mathbb{Z}^n \right\}. \tag{4.47}$$

This induces the inner product on G

$$\langle a_1 | a_2 \rangle = \frac{n}{4} a_1 a_2 \mod \mathbb{Z}. \tag{4.48}$$

The weights on $\mathbb{Z}_4$, defined by

$$wt(g) = \min_{k \in \mathbb{Z}^n} ||\Lambda k + g\lambda||, \tag{4.49}$$

are the following

$$wt(0) = 0, \ wt(1) = \frac{n}{4}, \ wt(2) = 1, \ wt(3) = \frac{n}{4}. \tag{4.50}$$

We can make the following identifications between $G \cong \mathbb{Z}_4$ and the highest-weight representations

$$0 \mapsto 0, \ 1 \mapsto c, \ 2 \mapsto v, \ 3 \mapsto s. \tag{4.51}$$

The conformal dimension h_g is half of the group weight $wt(g)$. This correspondence is summarized in table (4.1).

Addition in $\mathbb{Z}_4$ reproduces the fusion rules, which are the following

$$v \times v = 1, \ v \times s = c, \tag{4.52}$$

$$s \times s = c \times c = v, \tag{4.53}$$

$$s \times c = 1. \tag{4.54}$$

For each $a \in G$, define the following functions, which are the holomorphic characters of $so(2n)_1$

$$\chi_a = \frac{1}{(\eta(\tau))^n} \sum_{k \in \mathbb{Z}^n} e^{\pi i \tau (a\lambda + \Lambda k)^2}. \tag{4.55}$$

In terms of Jacobi theta functions, they read

$$\chi_0 = \frac{1}{2} \frac{\theta_3^n + \theta_4^n}{\eta^n}, \ \chi_1 = \chi_3 = \frac{1}{2} \frac{\theta_2^n}{\eta^n}, \ \chi_2 = \frac{1}{2} \frac{\theta_3^n - \theta_4^n}{\eta^n}. \tag{4.56}$$

Under modular T, S transformations, we have

$$\chi_a(\tau + 1) = e^{-\frac{\pi i}{12}n} \sum_{a' \in \mathbb{Z}_4} T_{aa'} \chi_{a'}(\tau), \quad T_{aa'} = e^{\pi i \frac{a^2 n}{4}} \delta_{aa'}, \tag{4.57}$$

$$\chi_a(-1/\tau) = \sum_{a' \in \mathbb{Z}_4} S_{ab} \chi_{ab}(\tau), \quad S_{ab} = \frac{1}{2} e^{-2\pi i \frac{naa'}{4}}. \tag{4.58}$$

Now we construct codes $\mathcal{C} \subseteq G \times \bar{G}$. We extend (4.48) to a Lorentzian bi-linear form on $G \times \bar{G}$ as follows

$$\langle (a_1, b_1) | (a_2, b_2) \rangle = \langle a_1 | a_2 \rangle - \langle b_1 | b_2 \rangle = \frac{n}{4}(a_1 a_2 - b_1 b_2) \mod \mathbb{Z}. \tag{4.59}$$

The evenness condition is

$$wt_2((a, b)) = \frac{n}{4}(a^2 - b^2) = 0 \mod 2\mathbb{Z}. \tag{4.60}$$

There exist 2 even self-dual codes, which are equivalent, with generators

$$C_0 = (11), \quad C_1 = (13). \tag{4.61}$$

The characters χ_1, χ_3 being equal, at the level of codes, means that the operation that sends a codeword (a, b) to $(a, -b)$ is a code equivalence. Therefore, these two codes are equivalent and lead to the same modular invariant partition function

$$Z_0 = \sum_{i=0}^{3} \chi_i \bar{\chi}_i, \quad Z_1 = \sum_{i=0}^{3} \chi_i \bar{\chi}_{-i}, \quad Z_1 = Z_0. \tag{4.62}$$

Similarly to section 4.2.2, we now consider the Poincaré series of the vacuum character

$$\bar{Z} \propto \sum_{\gamma \in SL(2,\mathbb{Z})} \gamma(\chi_0 \bar{\chi}_0). \tag{4.63}$$

An (infinite) subgroup of $SL(2, \mathbb{Z})$ that leaves the vacuum character invariant is $\Gamma_0(8)$, of index 12. We replace the sum on the right-hand side of (4.63) by:

$$\bar{Z} = \frac{1}{2} \sum_{\gamma \in SL(2,\mathbb{Z})/\Gamma_0(8)} \gamma(\chi_0 \bar{\chi}_0). \tag{4.64}$$

In terms of code enumerator polynomial variables it reads

$$\bar{W} = \frac{1}{2} \sum_{\gamma \in SL(2,\mathbb{Z})/\Gamma_0(8)} \gamma(x_0 \bar{x}_0) = \frac{1}{2} \left(\sum_{k=0}^{7} T^k S + \sum_{k=0}^{3} ST^{2k} S \right) x_0^i \bar{x}_0^i = W_0 + W_1. \tag{4.65}$$

Therefore, the Poincaré series leads to

$$\bar{Z} = Z_0 + Z_1 = 2Z_0. \tag{4.66}$$

38

Table 4.1: The correspondence between chiral primaries and elements of the discriminant group G for odd n (left) and even n (right).

field	$G \cong \mathbb{Z}_4$	wt	h	field	$G \cong \mathbb{Z}_2 \times \mathbb{Z}_2$	wt	h
1	0	0	0	1	(00)	0	0
v	2	1	$\frac{1}{2}$	v	(11)	1	$\frac{1}{2}$
s	3	$\frac{n}{4}$	$\frac{n}{8}$	s	(10)	$\frac{n}{4}$	$\frac{n}{8}$
c	1	$\frac{n}{4}$	$\frac{n}{8}$	c	(01)	$\frac{n}{4}$	$\frac{n}{8}$

4.3.3 Even n

For **even** n, we choose the map $\phi : \Lambda^{\perp} \to \mathbb{Z}_2 \times \mathbb{Z}_2$ such that ϕ^{-1} takes elements of $\mathbb{Z}_2 \times \mathbb{Z}_2$ to the lattice vectors

$$(a,b) \mapsto \left\{ \Lambda m + a\lambda_- + b\lambda_+, \ \lambda_{\pm} = \begin{pmatrix} \frac{1}{2} \\ \vdots \\ \frac{1}{2} \\ \pm\frac{1}{2} \end{pmatrix} : m \in \mathbb{Z}^n \right\}. \tag{4.67}$$

The induced inner product on the group G is

$$\langle (a,b) | (a',b') \rangle = \frac{n}{4}(aa' + bb') + \frac{n-2}{4}(ab' + a'b) \mod \mathbb{Z}. \tag{4.68}$$

The weights are

$$wt(0,0) = 0, \ wt(1,1) = 1, \ wt(1,0) = wt(0,1) = \frac{n}{4}. \tag{4.69}$$

We make the following identifications between $G \cong \mathbb{Z}_2 \times \mathbb{Z}_2$ and the highest-weight representations

$$(0,0) \mapsto 1, \ (1,0) \mapsto c, \ (1,1) \mapsto v, \ (0,1) \mapsto s. \tag{4.70}$$

This identification is summarized in table 4.1.

Addition in $\mathbb{Z}_2 \times \mathbb{Z}_2$ reproduces the fusion rules for even n, which are the following

$$v \times v = 1, \ v \times s = c, \tag{4.71}$$

$$s \times s = c \times c = 1, \tag{4.72}$$

$$s \times c = v. \tag{4.73}$$

The holomorphic characters of $so(2n)_1$ are given by

$$\chi_{(ab)} = \frac{1}{(\eta(\tau))^n} \sum_{k \in \mathbb{Z}^n} e^{\pi i \tau (a\lambda_- + b\lambda_+ + \Lambda k)^2}. \tag{4.74}$$

In terms of Jacobi theta functions, they read

$$\chi_{(00)} = \frac{1}{2} \frac{\theta_3^n + \theta_4^n}{\eta^n}, \ \chi_{(10)} = \chi_{(01)} = \frac{1}{2} \frac{\theta_2^n}{\eta^n}, \ \chi_{(11)} = \frac{1}{2} \frac{\theta_3^n - \theta_4^n}{\eta^n}. \tag{4.75}$$

Under T, S, they transform as

$$\chi_{(ab)}(\tau) = e^{-\frac{\pi}{12}n} \sum_{(a',b') \in \mathbb{Z}_2 \times \mathbb{Z}_2} T_{(a,b),(a',b')} \chi_{(a'b')}(\tau), \quad T_{(a,b),(a',b')} = e^{\pi i ((a^2+b^2)\frac{n}{4} + ab\frac{n-2}{2})} \delta_{aa'} \delta_{bb'},$$

(4.76)

$$\chi_{(ab)}(-1/\tau) = \sum_{(a'b') \in \mathbb{Z}_2 \times \mathbb{Z}_2} S_{(a,b),(a',b')} \chi_{(a'b')}(\tau), \quad S_{(a,b),(a',b')} = \frac{1}{2} e^{-2\pi i \langle (a,b)|(a',b')\rangle}. \quad (4.77)$$

We now construct even, self-dual codes $\mathcal{C} \subseteq G \times \bar{G}$, by extending the bilinear form (4.68) to

$$\langle (a,b)|(a',b')\rangle = \langle a|a'\rangle - \langle b|b'\rangle. \tag{4.78}$$

The evenness condition for $((a,b),(a',b')) \in G \times \bar{G}$ is

$$wt_2(((a,b),(a',b'))) = \frac{n}{4}(a^2 + b^2 - a'^2 - b'^2) + \frac{n-2}{2}(ab - a'b') = 0 \mod 2\mathbb{Z}. \tag{4.79}$$

The equality of characters $\chi_{(10)} = \chi_{(01)}$ means that the operation acting on a codeword as $((a,b),(a',b')) \to ((a,b),(b',a'))$ is a code equivalence. Due to the nature of (4.68), we need to consider different cases in order to classify the modular invariants and calculate the Poincaré series.

$n = 2 \mod 4$

There are two even, self-dual codes, generated by

$$C_0 = \begin{pmatrix} (10) & (10) \\ (01) & (01) \end{pmatrix}, \quad C_1 = \begin{pmatrix} (01) & (10) \\ (10) & (01) \end{pmatrix}, \tag{4.80}$$

giving rise to the modular invariants

$$Z_0 = \chi_0 \bar{\chi}_0 + \chi_s \bar{\chi}_s + \chi_c \bar{\chi}_c + \chi_v \bar{\chi}_v, \tag{4.81}$$

$$Z_1 = \chi_0 \bar{\chi}_0 + \chi_s \bar{\chi}_c + \chi_c \bar{\chi}_s + \chi_v \bar{\chi}_v. \tag{4.82}$$

These two codes are equivalent, leading to $Z_1 = Z_0$.

We now calculate the Poincaré series of the vacuum character. An (infinite) subgroup of $SL(2, \mathbb{Z})$ that leaves the vacuum character invariant is $\Gamma_0(4)$. In terms of code enumerator polynomial variables, the sum can be performed as follows

$$\bar{W} = (\sum_{i=0}^{3} T^i S + \sum_{i=0}^{2} ST^{2i}S) x_{(00)} \bar{x}_{(00)} = W_0 + W_1, \tag{4.83}$$

leading to the linear combination of the two partition functions with equal weights

$$\bar{Z} = Z_0 + Z_1 = 2Z_0. \tag{4.84}$$

40

$n = 4 \mod 8$

There are six even, self-dual codes

$$C_0 = \begin{pmatrix} (10) & (10) \\ (01) & (01) \end{pmatrix}, \; C_1 = \begin{pmatrix} (01) & (10) \\ (10) & (01) \end{pmatrix}, \tag{4.85}$$

$$C_2 = \begin{pmatrix} (10) & (11) \\ (11) & (10) \end{pmatrix}, \; C_3 = \begin{pmatrix} (01) & (11) \\ (11) & (10) \end{pmatrix}, \tag{4.86}$$

$$C_4 = \begin{pmatrix} (10) & (11) \\ (11) & (01) \end{pmatrix}, \; C_5 = \begin{pmatrix} (01) & (11) \\ (11) & (01) \end{pmatrix}, \tag{4.87}$$

giving rise to the modular invariants

$$Z_0 = \chi_0 \bar{\chi}_0 + \chi_s \bar{\chi}_s + \chi_c \bar{\chi}_c + \chi_v \bar{\chi}_v, \tag{4.88}$$

$$Z_1 = \chi_0 \bar{\chi}_0 + \chi_s \bar{\chi}_c + \chi_c \bar{\chi}_s + \chi_v \bar{\chi}_v, \tag{4.89}$$

$$Z_2 = \chi_0 \bar{\chi}_0 + \chi_c \bar{\chi}_v + \chi_v \bar{\chi}_c + \chi_s \bar{\chi}_s, \tag{4.90}$$

$$Z_3 = \chi_0 \bar{\chi}_0 + \chi_c \bar{\chi}_s + \chi_s \bar{\chi}_v + \chi_v \bar{\chi}_c, \tag{4.91}$$

$$Z_4 = \chi_0 \bar{\chi}_0 + \chi_c \bar{\chi}_v + \chi_s \bar{\chi}_c + \chi_v \bar{\chi}_s, \tag{4.92}$$

$$Z_5 = \chi_0 \bar{\chi}_0 + \chi_c \bar{\chi}_c + \chi_s \bar{\chi}_v + \chi_v \bar{\chi}_s. \tag{4.93}$$

Due to $\chi_s = \chi_c$, only two of them are distinct,

$$Z_0 = Z_1, \; Z_2 = Z_3 = Z_4 = Z_5. \tag{4.94}$$

We now calculate the Poincaré series of the vacuum character. The representation of S, T matrices satisfy the relations of the dihedral group D_6: $S^2 = T^2 = (ST)^3 = 1$, which is a finite group of order 6. We can perform the sum over all elements of this group

$$\bar{W} = (1 + T + S + TS + STS + TSTS)x_{(00)}\bar{x}_{(00)} = W_0 + W_3 + W_4, \tag{4.95}$$

leading to the linear combination of the partition functions

$$\bar{Z} = Z_0 + Z_3 + Z_4 = Z_0 + 2Z_2. \tag{4.96}$$

$n = 0 \mod 8$

There are six even, self-dual codes[3]

$$C_0 = \begin{pmatrix} (10) & (10) \\ (01) & (01) \end{pmatrix}, \; C_1 = \begin{pmatrix} (01) & (10) \\ (10) & (01) \end{pmatrix}, \tag{4.97}$$

---

[3]Here we note again the existence of factorizable partition functions, due to the existence of Euclidean even, self-dual lattices in dimensions divisible by 8.

$$C_2 = \begin{pmatrix} (01) & (00) \\ (00) & (01) \end{pmatrix}, \ C_3 = \begin{pmatrix} (01) & (00) \\ (00) & (10) \end{pmatrix}, \tag{4.98}$$

$$C_4 = \begin{pmatrix} (10) & (00) \\ (00) & (01) \end{pmatrix}, \ C_5 = \begin{pmatrix} (10) & (00) \\ (00) & (10) \end{pmatrix}, \tag{4.99}$$

giving rise to the modular invariants

$$Z_0 = \chi_0 \bar{\chi}_0 + \chi_s \bar{\chi}_s + \chi_c \bar{\chi}_c + \chi_v \bar{\chi}_v, \tag{4.100}$$

$$Z_1 = \chi_0 \bar{\chi}_0 + \chi_s \bar{\chi}_c + \chi_c \bar{\chi}_s + \chi_v \bar{\chi}_v, \tag{4.101}$$

$$Z_2 = |\chi_0 + \chi_s|^2, \tag{4.102}$$

$$Z_3 = (\chi_0 + \chi_s)(\bar{\chi}_0 + \bar{\chi}_c), \tag{4.103}$$

$$Z_4 = (\chi_0 + \chi_c)(\bar{\chi}_0 + \bar{\chi}_s), \tag{4.104}$$

$$Z_5 = |\chi_0 + \chi_c|^2. \tag{4.105}$$

Again, due to $\chi_s = \chi_c$ only two of them are distinct

$$Z_0 = Z_1, \ Z_2 = Z_3 = Z_4 = Z_5. \tag{4.106}$$

We calculate the Poincaré series of the vacuum character similarly to the $n = 4$ mod 8 case:

$$\bar{W} = (1 + T + S + TS + STS + TSTS)x_{(00)}\bar{x}_{(00)} = W_0 + W_3 + W_4, \tag{4.107}$$

leading to the linear combination

$$\bar{Z} = Z_0 + Z_3 + Z_4 = Z_0 + 2Z_3. \tag{4.108}$$

4.4 Codes based on the root lattices E_6, E_7, E_8

4.4.1 E_6

The $(E_6)_1$ CFT has central charge $c = 6$. It has 3 chiral primary fields with dimensions $0, \frac{2}{3}, \frac{2}{3}$.

The $\Lambda = E_6$ latice is generated by

$$\Lambda = \begin{pmatrix} 1 & 0 & 0 & 0 & -\frac{1}{2} & 0 \\ -1 & 1 & 0 & 0 & -\frac{1}{2} & 0 \\ 0 & -1 & 1 & 0 & -\frac{1}{2} & 0 \\ 0 & 0 & -1 & 1 & -\frac{1}{2} & 1 \\ 0 & 0 & 0 & 1 & -\frac{1}{2} & -1 \\ 0 & 0 & 0 & 0 & \frac{\sqrt{3}}{2} & 0 \end{pmatrix}. \tag{4.109}$$

The discriminant group is $G \cong \mathbb{Z}_3$. Choose the function $\phi : \Lambda^\perp \to \mathbb{Z}_3$, such that ϕ^{-1} maps an element a of $\mathbb{Z}_3$ to the following vectors

$$a \mapsto \left\{ a\lambda + \Lambda m, \ \lambda = (1, 0, 0, 0, 0, 1/\sqrt{3})^T : m \in \mathbb{Z}^6 \right\}. \tag{4.110}$$

This induces the inner product on G

$$\langle a_1 | a_2 \rangle = \frac{4}{3} a_1 a_2 \quad \mathrm{mod} \ \mathbb{Z}. \tag{4.111}$$

The weights on $\mathbb{Z}_3$ are the following

$$wt(0) = 0, \ wt(1) = wt(2) = \frac{4}{3}. \tag{4.112}$$

For each $a \in \mathbb{Z}_3$, define the following functions, which are the holomorphic characters of the CFT

$$\chi_a = \frac{1}{(\eta(\tau))^6} \sum_{k \in \mathbb{Z}^6} e^{\pi i \tau (a\lambda + \Lambda k)^2}. \tag{4.113}$$

Under modular T, S transformations, we have

$$\chi_a(\tau + 1) = e^{\pi i \frac{4}{3} a^2} \chi_a(\tau), \tag{4.114}$$

$$\chi_a(-1/\tau) = \frac{1}{\sqrt{3}} \sum_{a' \in \mathbb{Z}_3} e^{-2\pi i \frac{4}{3} a a'} \chi_{a'}(\tau). \tag{4.115}$$

We define the Lorentzian bi-linear form on $G \times \bar{G}$

$$\langle (a_1, b_1) | (a_2, b_2) \rangle = \langle a_1 | a_2 \rangle - \langle b_1 | b_2 \rangle = \frac{4}{3}(a_1 a_2 - b_1 b_2) \quad \mathrm{mod} \ \mathbb{Z}. \tag{4.116}$$

The evenness condition is

$$wt_2((a, b)) = \frac{4}{3}(a^2 - b^2) = 0 \quad \mathrm{mod} \ 2\mathbb{Z}. \tag{4.117}$$

It follows that any self-dual code is also even.

There exist 2 even self-dual codes, generated by

$$C_0 = (11), \ C_1 = (12). \tag{4.118}$$

This leads to the modular invariants, which are not distinct, due to $\chi_1 = \chi_2$

$$Z_0 = \sum_{i=0}^{2} \chi_i \bar{\chi}_i, \ Z_1 = \sum_{i=0}^{2} \chi_i \bar{\chi}_{-i}, \ Z_1 = Z_0. \tag{4.119}$$

The Poincaré series of the vacuum character can be written as

$$\bar{W} = \sum_{\gamma \in SL(2,\mathbb{Z})/\Gamma_0(3)} \gamma(x_0 \bar{x}_0) = (1 + \sum_{i=0}^{2} T^i S) x_0 \bar{x}_0 = W_0 + W_1, \tag{4.120}$$

leading to

$$\bar{Z} = Z_0 + Z_1 = 2Z_0. \tag{4.121}$$

4.4.2 E_7

The $(E_7)_1$ CFT has central charge $c = 7$. It has two chiral primary fields of conformal weights $0, \frac{3}{4}$.

A generator of the root lattice E_7 is

$$\Lambda = \begin{pmatrix} 1 & 0 & 0 & 0 & 0 & -\frac{1}{2} & 0 \\ -1 & 1 & 0 & 0 & 0 & -\frac{1}{2} & 0 \\ 0 & -1 & 1 & 0 & 0 & -\frac{1}{2} & 0 \\ 0 & 0 & -1 & 1 & 0 & -\frac{1}{2} & 0 \\ 0 & 0 & 0 & -1 & 1 & -\frac{1}{2} & 1 \\ 0 & 0 & 0 & 0 & 1 & -\frac{1}{2} & -1 \\ 0 & 0 & 0 & 0 & 0 & \frac{1}{\sqrt{2}} & 0 \end{pmatrix}. \tag{4.122}$$

The discriminant group is $G = \Lambda^\perp / \Lambda = \mathbb{Z}_2$. Choose $\phi : \Lambda^\perp \to \mathbb{Z}_2$ such that ϕ^{-1} maps an element $a \in \mathbb{Z}_2$ to the vectors

$$a \mapsto \left\{ a\lambda + \Lambda m, \ \lambda = (1, 0, 0, 0, 0, 0, 1/\sqrt{2})^T : m \in \mathbb{Z}^7 \right\}. \tag{4.123}$$

The induced inner product in the group G is

$$\langle a_1 | a_2 \rangle = \frac{3}{2} a_1 a_2 \quad \mathrm{mod} \ \mathbb{Z}. \tag{4.124}$$

The weights are

$$wt(0) = 0, \ wt(1) = \frac{3}{2}. \tag{4.125}$$

For each $a \in \mathbb{Z}_2$, define the following functions, which are the holomorphic characters of the CFT

$$\chi_a = \frac{1}{(\eta(\tau))^7} \sum_{k \in \mathbb{Z}^7} e^{\pi i \tau (a\lambda + \Lambda k)^2}. \tag{4.126}$$

Under modular T, S transformations, we have

$$\chi_a(\tau + 1) = e^{\pi i \frac{3}{2} a^2} \chi_a(\tau), \tag{4.127}$$

$$\chi_a(-1/\tau) = \frac{1}{\sqrt{2}} \sum_{a' \in \mathbb{Z}_2} e^{-2\pi i \frac{3}{2} aa'} \chi_{a'}(\tau). \tag{4.128}$$

We extend the bi-linear form on $G \times \bar{G}$ as follows

$$\langle (a_1, b_1) | (a_2, b_2) \rangle = \frac{3}{2} (a_1 a_2 - b_1 b_2) \quad \mathrm{mod} \ \mathbb{Z}. \tag{4.129}$$

The evenness condition is

$$wt_2((a, b)) = \frac{3}{2} (a^2 - b^2) = 0 \quad \mathrm{mod} \ 2\mathbb{Z}. \tag{4.130}$$

There exists 1 even self-dual code, generated by

$$C_0 = (11), \tag{4.131}$$

leading to the diagonal modular invariant

$$Z = \chi_0 \bar{\chi}_0 + \chi_1 \bar{\chi}_1. \tag{4.132}$$

Since there is a unique modular invariant, the Poincaré series of the vacuum character is a multiple of Z.

4.4.3 E_8

We conclude this chapter with the E_8 lattice. The analysis of this theory is trivial, but it is included for completeness. The $(E_8)_1$ CFT has central charge $c = 8$ and a single chiral primary of conformal weight 0.

A generator of the root lattice E_8 is

$$\Lambda = \begin{pmatrix} 2 & -1 & 0 & 0 & 0 & 0 & 0 & \frac{1}{2} \\ 0 & 1 & -1 & 0 & 0 & 0 & 0 & \frac{1}{2} \\ 0 & 0 & 1 & -1 & 0 & 0 & 0 & \frac{1}{2} \\ 0 & 0 & 0 & 1 & -1 & 0 & 0 & \frac{1}{2} \\ 0 & 0 & 0 & 0 & 1 & -1 & 0 & \frac{1}{2} \\ 0 & 0 & 0 & 0 & 0 & 1 & -1 & \frac{1}{2} \\ 0 & 0 & 0 & 0 & 0 & 0 & 1 & \frac{1}{2} \\ 0 & 0 & 0 & 0 & 0 & 0 & 0 & \frac{1}{2} \end{pmatrix}. \tag{4.133}$$

This lattice is unimodular, hence the discriminant group is trivial. There is a single chiral character

$$\chi_0 = \frac{1}{(\eta(\tau))^8} \sum_{\lambda \in E_8} e^{\pi i \tau \lambda}. \tag{4.134}$$

There is a unique modular invariant partition function, which is factorizable

$$Z = |\chi_0|^2. \tag{4.135}$$

The vacuum character $\chi_0 \bar{\chi}_0$ is already modular invariant, hence the Poincaré series is equal to Z.

4.5 Summary

Using codes based on the root lattices A,D,E, we studied the Poincaré series of the vacuum characters of RCFTs described by affine Lie algebras A,D,E at level 1. The A_n theories at level 1 were studied in [45]. Here we formulated the problem in terms of codes and reproduced these results. We proceeded to apply our formalism to the families D, E at level 1.

For the E_i, D_{2i+1}, D_{4i+2} and A_j (with j square-free) lattices, the Poincaré series of the vacuum returns a linear combinations of all partition functions with equal weights. For the D_{4i} cases, the Poincaré series results in a linear combination of the partition functions with unequal weights. The A_n case, where n is not square-free, is much richer, with coefficients depending on the prime factors of n.

The code formalism paves the way to study, in a systematic way, CFTs with more general chiral symmetries. A straightforward generalization is to consider theories with chiral symmetry described by products $g_1^{\otimes k}$, where g is one of the A, D, E algebras, by classifying codes of larger length. Another interesting generalization would be to consider levels higher than 1. There is no obvious way to accomplish this, as the operator product expansions of these CFTs do not exhibit an additive structure at higher levels.

Chapter 5 Entanglement Entropy in Ground States of Long-Range Fermionic Systems

This chapter is based on the work "Entanglement Entropy in Ground States of Long-Range Fermionic Systems" co-authored with D. Chakraborty [46] and is reproduced here with the co-author's consent.

5.1 Entanglement entropy beyond local systems

Locality severely constrains the features of commonly studied physical systems. Such local systems show special features that are absent in generic quantum-mechanical models. A crucial property is the relative suppression of long-range correlations in the ground states of local Hamiltonians [47] compared to random states in the Hilbert space [48]. Besides exhibiting exponential decay of correlation functions, such ground states obey an area law for entanglement entropy along spatial bi-partitions, in the presence of an energy gap. For $d = 1$ critical systems, entanglement entropy may be enhanced by a logarithmic term, whose coefficient is proportional to the central charge of the conformal field theory (CFT) describing the critical point. Similarly, in $d = 2$ topological phases of matter can be understood in terms of the presence of certain universal terms in the entanglement entropy [49]. Entanglement entropy also plays a central role in providing quantum mechanical interpretations for geometric data in theories of quantum gravity [50]. Entanglement entropy has been a powerful tool to characterize phases of matter and their low-temperature physics. These properties of entanglement entropy have been exploited to efficiently study ground states of many-body systems with the help of various tensor network methods [51].

In this chapter, we study the geometric scaling of ground-state entanglement entropy as a function of a continuous parameter which controls the degree of non-locality of interactions. We do this by considering various setups involving fermions with long-range power-law couplings that decay with the exponent α. There is a number of reasons for considering such a setup. Experimental progress has led to the possibility of realizing controlled Ising-type power-law interactions in trapped ion systems with tunable exponent α. Such systems carry several signatures of exotic phases of matter, partially reflected by anomalous entanglement scaling. An example of this is the known logarithmic violation of the area-law behavior in the presence of a gap [52], [53].

The theoretical analysis of long-range models has independent interest. Long-range interactions often show up in continuum theories upon partially integrating out degrees of freedom in local models. While the vacua of such models, in terms of appropriate degrees of freedom, are not expected to be qualitatively different, there are field theories with nonlocal UV descriptions that show novel structures, such as critical points with conformal symmetry without the existence of a local stress-energy tensor [54], and unusual symmetry-breaking patterns [55]. In the context of holography, highly non-local quantum theories with volume-law scaling of entanglement

entropy have been proposed as candidate duals to asymptotically flat theories of gravity [56].

In [57] it was shown that there exists an area law for general gapped systems having bounded local Hilbert spaces with few-body interactions falling off as a power $\alpha > 2$ in $d = 1$ spatial dimensions generalizing previously known bounds for local models [58], [59]. For fermions with long-range hopping or pairing, the bound is tighter and an area law is expected for $\alpha > \frac{3}{2}$ in the presence of a gap. We are interested in understanding the transition to conventional scaling of entanglement entropy as α is varied. The conventional scaling in $d = 1$ is an area law (i.e bounded entanglement on increasing subsystem size) for gapped systems and possible logarithmic dependence on subsystem size for gapless systems. There are constructions designed to break these conventional expectations [60], [61]. We ask the following questions:

1. For sufficiently small α, what kind of scaling of EE do generic models show?

2. Is there any *universality* in the transition of EE to conventional scaling as a function of α? In other words, does there exist a common α_c controlling the behavior of ground state correlations across a variety of models?

3. How does EE scale for models with a well-defined continuum limit?

We study these questions with several numerical calculations in quadratic models of spinless fermions on a lattice in $d = 1$. Despite the simplicity of these models, their detailed study in the local case has paved the way for understanding interacting and higher-dimensional systems. The numerical flexibility to study large subsystem sizes is a bonus for examining subtleties in the scaling behavior.

We postulate:

1. Systems with a smooth IR continuum limit will have their long-range entanglement scaling constrained by the scaling of entanglement in their continuum theory. For this reason, such systems will typically have only logarithmic violations of area-law behavior in the presence of a gap for the few-body interactions we consider.

2. Systems that have large gradients at the microscopic scale, like disordered systems will violate the area law by a power-law correction that may transition to a volume-law at small enough α.

3. The exponent α_c at which the transition to conventional scaling occurs depends on features of the system. One may identify α_c for particular ensembles of random Hamiltonians. For translationally invariant models in the infinite system limit technical considerations and examples suggest $\alpha_c = 1$ though for $\alpha > 1$ the saturation of EE could set in for very large subsystem sizes.

We illustrate all three of the points using numerical examples in free systems that are expected to generalize to the interacting systems. We also support point 1) using some qualitative RG arguments that we hope to make more precise in the future. Section 5.2 deals with models with particle number conservation and discusses the

48

translationally invariant 5.2.1 and disordered cases 5.2.2 separately. Section 5.3 considers translationally invariant models with long-range hopping and pairing. Section 5.4 summarizes the key points along with a conceptual discussion.

5.2 Models with particle number conservation

We begin by reviewing some preliminary definitions. The reduced density matrix ρ_A of a contiguous spatial subsystem A with linear size L_A is obtained from tracing out the complement $\bar{A}$ from the global state ρ of a lattice of fermion of length L as $\rho_A = \mathrm{Tr}_{\bar{A}} \, \rho$. The von Neumann entropy of ρ_A is defined as:

$$S(\rho_A) = -\mathrm{Tr}(\rho_A \log(\rho_A)) \tag{5.1}$$

When ρ is a pure state, $S(\rho_A)$ is a genuine measure of quantum entanglement and is called the entanglement entropy. The entanglement entropy of eigenstates of lattice models quadratic in fermionic operators can be efficiently computed because the subsystem is specified entirely by two-point functions [62]. The reduced density matrix of a subsystem is proportional to the exponential of a modular Hamiltonian quadratic in fermionic operators. The lattice fermionic degrees of freedom are identified with creation operators $c_i^\dagger$. We consider Hamiltonians of the form:

$$H = \sum_{i,j} V_{ij} c_i^\dagger c_j \tag{5.2}$$

Here V_{ij} is the Hermitian matrix with entries such that V_{ij} falls of as $|i-j|^{-\alpha}$ at long distances. This Hamiltonian is diagonalized with a unitary rotation of the operators c_i. We adopt the convention that the many-body ground state $|\Omega\rangle$ is the state occupied by the negative-energy modes of the Hamiltonian, without fixing particle number. This means that once we diagonalize V_{ij} as follows,

$$H = \sum_{i,j} V_{ij} c_i^\dagger c_j = \sum_{k=1}^{L} \lambda_k \eta_k^\dagger \eta_k \tag{5.3}$$

the ground-state is given by

$$|\Omega\rangle = \prod_{k:\lambda_k<0} \eta_k^\dagger |0\rangle \,. \tag{5.4}$$

We restrict attention to cases without degenerate ground states. The entanglement entropy of a subsystem A is computed using the eigenvalues of the correlation matrix $(C_A)_{ij} = \langle\Omega| c_i^\dagger c_j |\Omega\rangle$ with $i,j \in A$ as:

$$S(\rho_A) = -\mathrm{Tr}(C_A \log(C_A)) - \mathrm{Tr}((\mathbb{I} - C_A)\log(\mathbb{I} - C_A)) \tag{5.5}$$

It follows that empty ground states will have zero entanglement entropy.

5.2.1 Translationally invariant models

Translationally invariant models have V_{ij} as a function of $|i - j|$ alone, which means that the matrix V is Toeplitz. We suppose V_{ij} can be written in the form

$$V_{ij} = \frac{f(d_{O/P}(i,j)))}{g(d_{O/P}(i,j))}, \tag{5.6}$$

where $f(r)$ is a function that remains bounded and does not decay with r and $g(r)$ is a function that grows as r^α. For finite systems one may consider open boundary conditions $d_O(i,j) = |i - j|$, or periodic boundary conditions with distance $d_P(i,j) = \min(L - |i - j|, |i - j|)$ such that V is circulant. In the thermodynamic limit, the spectrum of the Toeplitz matrix coincides with that of the circulant matrix. The latter can be diagonalized even at finite L using a Fourier unitary. The choice of open or periodic boundary condition does affect the entanglement entropy but not its scaling in the thermodynamic limit, see for example [63]. For finite L, the open boundary condition is the physical choice. For $\alpha \leq 1$ in 1D, the spectrum may develop isolated divergences in the thermodynamic limit, related to the nonconvergence of the generalized harmonic sum. The ground-state energy-density may still remain well defined.

Let us consider the large L limit of these models. Our claim is that for a generic translationally invariant V_{ij} which *also has a smooth continuum limit*, the entanglement entropy is at most $\log(L_A)$ for any α. This well-understood point for short-ranged models generalizes in a simple way and has important implications. We briefly review the mathematical and conceptual underpinnings of this result.

In the thermodynamic limit, the eigenvalues become a smooth function of quasi-momenta k taking values in $[0, 2\pi)$, in units of inverse lattice spacing

$$\lambda(k) = \sum_{r=-\infty}^{\infty} V(r)e^{ikr}, \tag{5.7}$$

where $V(r) = V(i - j)$. The correlation submatrix C_A of the subsystem of interest is given by

$$C_A(i - j) = \left\langle c_i^\dagger c_j \right\rangle = \frac{1}{2\pi} \int_0^{2\pi} dk \quad e^{-ik(i-j)}\Theta(-\lambda(k)), \tag{5.8}$$

where we used the important fact that C_A is Toeplitz to write $C_A(i - j)$. The formula (5.5) can be rewritten as a contour integral involving $\log(\det(C_A - \mathbb{I}_A))$ and model independent functions. On using the Fisher-Hartwig conjecture and certain assumptions [64], the leading answer is proportional to $\log(L_A)$. The prefactor of the log is given by $\frac{1}{6}$ times the number of discontinuities of the "symbol", $\Theta(-\lambda(k))$. These discontinuities are precisely at the Fermi points k_i^* where the dispersion changes sign. The 1D answer for free fermions was generalized to higher-dimensions in [65] and seen to be consistent with a conjecture due to Widom.

There is a physical argument based on RG for the results explained above as discussed in [63], [66] that we expand on. The long distance entanglement properties

of such free fermion models under consideration should match the predictions from the effective IR theory. Despite the potentially complicated nature of the dispersion $\lambda(k)$, assuming analytic behavior about c Fermi points k_i^*, the IR theory in momentum space will look like:

$$H \propto \sum_{i=1}^{c} \int dk \, v_{F_i} k (\psi_i^\dagger \psi_i - \chi_i^\dagger \chi_i) + \dots, \tag{5.9}$$

where $v_{Fi} = \lambda'(k_i^*)$ is the local Fermi velocity and ψ_i and χ_i are the right and left-movers corresponding to low energy excitations and holes. We omit the higher powers of k, which are irrelevant at low energies. Thus the entanglement entropy can be understood as being the sum of contributions from c decoupled chiral and anti-chiral modes. The CFT answer is $\frac{n_L + n_R}{6} \log(L_A)$ which gives a contribution of $\frac{1}{6} \log(L_A)$ from each mode. On summing them we get $S(\rho_A) = \frac{c}{3} \log(L_A) + \dots$ where the ellipsis stands for subleading contributions. The answer for open boundary condition can be derived within the CFT formalism and is given by halving the prefactor of the logarithm $S(\rho_A) = \frac{c}{6} \log(L_A) + \dots$.

The low-energy theory written in (5.9) has an emergent Lorentz invariance but lacks conformal invariance unless all the v_{Fi} are equal. In that case conformal symmetry arises from a spacetime rescaling, in addition to the internal symmetry between different chiral fields. An interesting manifestation of the emergent conformal symmetry is found in examining the finite-size correction to ground state energy:

$$F_L = f_0 L - \frac{\pi c v_F}{6L} + O(\frac{1}{L^2}), \tag{5.10}$$

where f_0 is the ground state energy density in the thermodynamic limit and F_L is the ground state energy at finite size L. This relation is obtained applying the Euler-Maclaurin formula to an arbitrary dispersion on the lattice. The leading order answer precisely matches the correction to vacuum energy density of a CFT on mapping a theory from infinite plane to a cylinder of radius L and setting $v_F = 1$. The lack of scale invariance of (5.9) is not a problem from the RG perspective, because the v_{F_i}'s get renormalized and the theory flows to the one with all v_F's the same. This expected behavior is illustrated with the agreement between finite-size results and the thermodynamic limit of

$$V_{ij} = \begin{cases} \frac{1}{d_P(i,j)^{0.6}} \sum_{l=-3}^{l=3} \cos\left(\frac{2\pi l}{7} d_P(i,j)\right) & i \neq j \\ 0 & i = j \end{cases}. \tag{5.11}$$

The function $\lambda(k)$ can be computed in the thermodynamic limit as a linear combination of polylogs. The periodic modulation that picks out every seventh site in the numerator gives rise to $c = 7$ pairs of Fermi points and emergent species of fermions. The EE for $L = 1200$ with open boundary conditions is presented in Fig. 5.1c. This example illustrates how predictions from the effective theory give an accurate answer for the EE when there are no obvious means to an exact answer: for finite L and open boundary conditions.

The nontrivial implication of the argument in [66] was that it predicted, in d dimensions, the same $L_A^{d-1} \log(L_A)$ scaling of EE for interacting theories that can be described in terms of a deformed Fermi surface. This discussion generalizes to our setting: for fermionic systems with a continuum limit, provided the Fermi surface is stable, the leading piece of EE will continue to scale at most as $L_A^{d-1} \log(L_A)$ even if the microscopic degrees of freedom have long-range interactions. The stability of the Fermi surface is a more subtle matter, but it is unlikely that long-range hopping terms alone affect the conventional kinematical arguments provided at least that $\alpha > d$, though long-range density interactions might. The hopping model ground states considered above are simple and non-generic, but they illustrate the utility of effective theory for understanding entanglement.

Lattice models without a continuum limit however, are not constrained in this manner. By this we mean models which lack a gradient expansion or equivalently, a smooth momentum-space Hamiltonian which can be expanded around low-energy points. Disordered hopping models are known to exhibit volume law entanglement in the limit of small α, [67], and are expected to show area law for large α. We study this transition in EE for disordered models in Section 5.2.2.

However, disorder is not necessary to go beyond $\log(L_A)$ scaling as has been appreciated in [68], [69]. To illustrate this point, we first construct an example of V_{ij} with translation invariance weakly broken only due to open boundary conditions, that we numerically show to saturate the maximal possible growth of entanglement for fermionic models at $\alpha = 0$, see Fig 5.1a. This is given by the highly oscillatory sequence of models:

$$V_{ij} = \begin{cases} \frac{1}{d_O(i,j)^\alpha} \frac{\sin\left(\left(L+\frac{1}{2}\right)d_O(i,j)\right)}{\sin\left(\frac{1}{2}d_O(i,j)\right)} & i \neq j \\ 0 & i = j \end{cases} \tag{5.12}$$

The transition to bounded EE is seen in this model through the appearance of a plateau at large fractions $f = \frac{L_A}{L}$ and the appearance of fractal scaling L_A^γ with $0 < \gamma < 1$ for $0.8 < \alpha < 1.6$, see Fig. 5.1b. The intermediate fractal scaling L_A^γ is an interesting feature that shows up robustly for disordered models. We expand on this in Section 5.2.2. Note that this sequence of models has couplings explicitly dependent on L and therefore its scaling properties might differ from conventional models.

Another example of a translationally invariant model without disorder with a ground state which saturates the maximal growth of entanglement entropy is the following

$$H = \sum_{j=1}^{\frac{L}{2}} c_{j+\frac{L}{2}}^\dagger c_j + \sum_{j=1}^{\frac{L}{2}} c_j^\dagger c_{\frac{L}{2}+j}, \tag{5.13}$$

where we assume that the system size L is even. The entanglement entropy for $L_A \leq L/2$ is $S(L_A) = L_A \log 2$ (see appendix C).
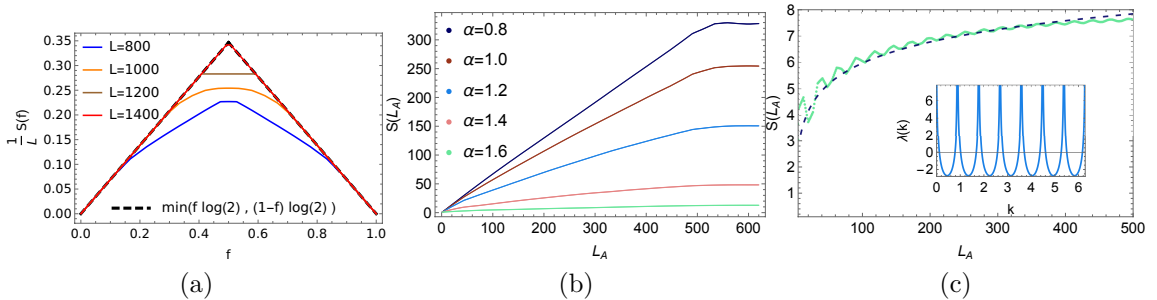
Figure 5.1: Fig 5.1a shows maximal volume-law growth of entanglement in ground state of the model specified by (5.12) at $\alpha = 0$, shown for sequence of L starting from 800 to 1400. To compare across system sizes, the entropy density $\frac{1}{L}S$ is expressed as a function of subsystem fraction $f = \frac{L_A}{L}$. Fig 5.1b shows the intermediate EE scaling regime for the same model for different α at $L = 1200$. Fig 5.1c shows the agreement between the EE of a long-ranged hopping model with $\alpha = 0.6$ of $L = 1200$ and OBC, with the CFT predictions (dashed lines). The inset shows the dispersion relation of this model for $L \to \infty$ limit with seven pairs of Fermi points giving rise to $c = 7$ in the CFT formula.

5.2.2 Universality in Disordered Models

Volume-law scaling of EE in random hopping models has been studied across the entirety of spectrum in [70],[71] and for ground states in [72], [73], [67], the latter in the context of the SYK_2 model. SYK_q models are generally interpreted as being N flavors of fermions embedded in a quantum dot, with all-to-all interaction in flavor space. Here we consider a disordered hopping model that interpolates between a complex SYK_2 model embedded on a 1D wire at $\alpha \to 0$ to a disordered local model for $\alpha \to \infty$. We examine the nature of the transition of EE scaling and the value α_c that controls the transition to bounded EE.

For our numerical study we consider the ensemble:

$$V_{ij} = \frac{R_{ij}}{1 + (d_O(i,j))^\alpha}, \tag{5.14}$$

where R_{ij} are elements of a symmetric Gaussian random matrix with zero mean. The variance of R_{ij} needs to be chosen as a function of both L and α to retain extensivity of total energy, but the overall scale does not affect the ground state or entanglement properties. The single particle Hamiltonian is an example of a power-law banded random matrix of the type studied in [74]. This model is known to exhibit an Anderson localization transition at $\alpha = 1$, as diagnosed through inverse participation ratios [74], [75]. The random matrix model in (5.14) retains a lack of correlation between matrix elements akin to Gaussian random matrix models, but loses invariance under a change of basis.

The ensemble averaged EE $\overline{S}(L_A)$ displays the following properties:

1. Self-averaging, meaning that a randomly picked member of the ensemble gives

$S(L_A)$ similar to $\overline{S}(L_A)$ for fixed α and L. The distribution of $S(L_A)$ about the mean increases with α.

2. L-independent behavior for L_A/L small compared to $\frac{1}{2}$.

3. Leading order fractal scaling $L_A^{\gamma(\alpha)}$ with $0 < \gamma(\alpha) < 1$ with $\gamma(\alpha)$ continuously decreasing from 1 as $\alpha \to 0$.

We numerically checked that other choices of random ensembles of V_{ij} preserve the features mentioned above as long as the V_{ij}'s are identically distributed and uncorrelated. For example, a sign-randomized ensemble with $R_{ij} = \pm 1$ will show similar features. The exponent $\gamma(\alpha)$ as well as the coefficient of the term $L_A^{\gamma(\alpha)}$ are dependent on the choice of ensemble; see Figure 5.2b.

To account for finite-size effects we use the following fitting function:

$$\bar{S}(L_A) = aL_A^{\gamma} + \frac{b}{L}L_A^{\gamma+1}. \tag{5.15}$$

This fitting function is chosen for two reasons. First, the Page curve for free fermions is known to be susceptible to considerable finite size effects. In the $\alpha \to 0$ limit, $\gamma = 1$ and the leading order correction to volume-law behavior is of the form $\frac{L_A^2}{L}$ [71]. Second, the best-fit $a(\alpha)$ and $b(\alpha)$ are $O(1)$ numbers roughly independent of system size. Therefore, at least for $f = \frac{L_A}{L} \ll 1$ and α not too large, this fit should capture the correct behavior.

The fit gives accurate behavior, see the inset in Fig 5.2a. For small α, say 0.01, we checked that the answer for ground state EE matches the average answer for EE across the spectrum valid for arbitrary subsystem fractions derived in [71]. This fractal scaling is consistent with the results of scaling of entanglement for typical eigenstates in a disordered ensemble studied in [72]. The rate of change of $\gamma(\alpha)$ sharply increases at about $\alpha \approx 0.5$, see Fig 5.2b. The transition to bounded entanglement at larger α seems to be continuous. That makes it difficult to pin down a precise α_c where the ensemble-averaged $\overline{S}$ saturates as for short-ranged disordered hopping models. We estimate that $\alpha_c \approx 1.3$ where according to our numerics, $\overline{S}$ saturates for a sequence of L. We note that for the range of powers we consider, there is no indication of an emerging gap. Although the localization of entanglement and Anderson localization arise due to similar mechanisms in the considered model, C_A and therefore entropy depends on the correlations between distinct single-particle eigenvectors. Therefore without contradiction, the EE continues to show slow fractal growth for $\alpha > 1$ when the model has undergone a localization-transition as diagnosed through inverse participation ratios. See Fig 5.2c for the slowly growing $\overline{S}$ at $\alpha = 1.05$ for different system sizes expressed as a function of f.

We do not give a first-principles derivation of the behavior of the EE. However, we make the observation that the α-dependent falloff in the Hamiltonian gives rise to localization of the correlation functions. The two-point function develops a power-law decay of exponent β with a stochastic envelope, which means for $i \neq j$:

$$\sqrt{\overline{C_{ij}^2}} = \frac{\kappa}{d_O(i,j)^{\beta}}. \tag{5.16}$$

In the free fermion case, the scaling of entanglement entropy is severely constrained by particle-number fluctuations [65], [68], given by $\Delta N_A^2 = \mathrm{Tr}(C_A(\mathbb{I} - C_A))$ using the inequality

$$2\Delta N_A^2 \leq S(L_A) \leq \Delta N_A^2 O(\log(L_A)). \tag{5.17}$$

Using (5.16), neglecting correlations and using the constraint that the ground state will generically be at half-filling, we give a non-rigorous estimate of the scaling of $\overline{S}(L_A)$ using the behavior of $\Delta \overline{N}_A^2$ in Appendix B as a function of β, see (A.5). The scaling (5.15) is controlled by the exponent β. This point of view suggests that the onset of area-law behavior in disordered hopping models is linked to the the exponent β becoming larger than 1. See Figure 5.3a for an example of β dependence of root-mean square of the two-point functions and 5.3b for the prediction generated by $\Delta \overline{N}_A^2$.

(a) (b) (c)
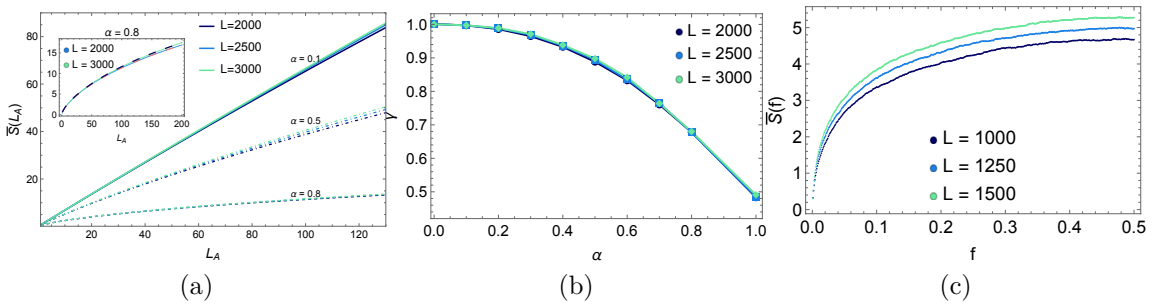
Figure 5.2: Fig 5.2a shows the behavior of the ensemble averaged $\overline{S}(L_A)$ for different α's and its L independent collapse, for L_A smaller than a certain fraction of L. Inset shows $\overline{S}(L_A)$ for $\alpha = 0.8$ and $L = 2000, 3000$ along with the fit (5.15) indicated by dashed lines. Fig 5.2b shows numerically obtained best-fit $\gamma(\alpha)$ for system sizes $L = 2000, 2500, 3000$. To compare across system sizes best fit parameters were obtained by fitting $\overline{S}$ for L_A up to 200. The collapse for different system sizes over the range of α indicates γ for this range may be well-defined in thermodynamic limit for finite L_A. For $\alpha > 1$, extracting the value of γ becomes difficult, though the EE still shows growth. Fig 5.2c shows that for numerically accessible L, $\overline{S}$ now expressed as function of $f = \frac{L_A}{L}$ continues to slowly increase at $\alpha = 1.05$. Between 400 to 500 samples were used to generate the plots above.

5.3 Models without particle number conservation

Here we consider translationally invariant free models of the form:

$$H = \sum_{\substack{i,j \\ i \neq j}} A_{ij} c_i^\dagger c_j + \sum_{i,j} \frac{1}{2}(B_{ij} c_i^\dagger c_j^\dagger + h.c.) + \mu \sum_i c_i^\dagger c_i \tag{5.18}$$

B is antisymmetric, with entries falling off with the exponent α_p whereas the entries of A can decay with a different exponent α_h. Such Hamiltonians are diagonalized

using a combination of Fourier and Bogoliubov transformations, or in the absence of translation invariance through the singular value decomposition of $A + B$. The ground-state reduced density matrix is characterized in terms of $\left\langle c_i^\dagger c_j^\dagger \right\rangle$ for $i, j \in A$ in addition to the matrix C_A. The formula for the EE in terms of correlation matrices is a generalization of (5.5), see [62] for details. These models will generically contain singular excitations, though the ground state energy density is still well-defined. Refs [53], [76], [77] studied models of the form above as extensions of Kitaev's model of a superconducting wire hosting Majorana modes at the edge. For sufficiently slowly decaying couplings, these models show several exotic features such as massive edge modes, anomalous decay of correlation functions and logarithmic violations of the area law, despite a gap in the thermodynamic limit. The latter two are related: the algebraic decay of two-point functions is a necessary but not sufficient condition for the entanglement entropy to not saturate. This point is particularly transparent for free fermion systems where Renyi entropies are directly expressed in terms of traces of powers of correlation matrices.

The exponents α_h and α_p have different roles in controlling the physics, which may be understood from considering the Hamiltonian in momentum space (after dropping an additive constant):

$$H = \frac{1}{2} \sum_{k=-\pi}^{\pi} \begin{pmatrix} c_k^\dagger & c_{-k} \end{pmatrix} \begin{pmatrix} a(k) + \mu & ib(k) \\ -ib(k) & -a(k) - \mu \end{pmatrix} \begin{pmatrix} c_k \\ c_{-k}^\dagger \end{pmatrix}. \qquad (5.19)$$

The functions $a(k)$ and $ib(k)$ are the symbols of the matrices A and B respectively, which when smooth, allow rewriting (5.19) as an integral in the thermodynamic limit. Both $a(k)$ and $b(k)$ are 2π periodic, but $a(k)$ is even about 0 (assuming reflection symmetry) while $b(k)$ is odd. The spectrum of single-particle excitations is given by $\lambda(k) = \sqrt{(a(k) + \mu)^2 + b(k)^2}$.

We examine two instances of models (5.18) in the $L \to \infty$ limit that highlight the important features in the scaling of EE:

$$(i) \quad A_{ij} = \frac{1}{d_P(i,j)^{\alpha_h}} \quad \text{and} \quad B_{ij} = \frac{\text{sgn}(i-j)}{d_P(i,j)^{\alpha_p}} \qquad (5.20)$$

In this case $a(k) = \text{ReLi}_{\alpha_h}(e^{ik})$ and $b(k) = \text{ImLi}_{\alpha_p}(e^{ik})$, where $\text{Li}_\alpha(z)$ stands for polylogarithm of order α. For large α_h and α_p, on tuning μ to criticality, the system falls under the $c = \frac{1}{2}$ Ising universality class. This follows from the low-energy behavior of (5.19) by taking the continuum limit, using a procedure similar to the one used in 5.2.1, see [78] for more details. When $\alpha_p > 2$, for any α_h, this model continues to show similar behavior to the Ising model at criticality, but shows deviations away from it. Driving $\alpha_p \leq 2$ alone, while keeping a local hopping term, alters the critical behavior [53] and results in an additive logarithmic term in the EE that persists in the presence of a gap. This additive term quickly jumps to about $\frac{1}{6} \log(L_A)$ for $\alpha < 1$. In [79], studying the same model, an effective field theory description of this phenomenon was developed, using modes away from the low-energy points in momentum space that remain relevant, arising from an expansion of the form: $b(k) = v(\alpha)k^{\alpha-1} + \dots$. These

terms correspond to fractional spatial derivatives and for $\alpha < 2$ may dominate low-energy behavior over the standard kinetic and mass terms. Such expansions also exist for $a(k)$, and indeed, even for dispersion of the model considered in (5.11). However these contributions may develop divergent masses and get gapped out. We leave to the future the task of systematically studying these excitations and a field-theoretic derivation of their contribution to entanglement entropy.

We discuss now the numerical results with $\alpha_h = \alpha_p = \alpha$, which is an instance of model studied in [76]. This model can be tuned to criticality by choosing $\mu_c = -a(\pi)$, in which case the spectrum of excitations becomes linear about $k = \pi$. The EE shows scaling $S(L_A) = \frac{c_{\text{eff}}}{3} \log(L_A)$ with $c_{\text{eff}} = c(\alpha) + c(\mu)$. $c(\mu)$ is the critical contribution that jumps to $\frac{1}{2}$ at μ_c but vanishes away from it. The c_{eff} in our notation is unrelated to the Virasoro central charge of a CFT in general. The anomalous α-dependent contribution $c(\alpha)$ is independent of any $O(1)$ choice of μ other than μ_c. It is close to $\frac{1}{2}$ as $\alpha = 0$ and approaches 0 in a continuous manner as α is increased. Notably the interacting long-range 1D antiferromagnetic Ising model displays very similar behavior of the coefficient c_{eff} as a function of α [76].

$$(ii) \quad A_{ij} = \frac{\cos(\pi d_P(i,j))}{d_P(i,j)^\alpha} \quad \text{and} \quad B_{ij} = \frac{\text{sgn}(i-j)}{d_P(i,j)^\alpha} \quad (5.21)$$

(a)　　　　　　　　(b)　　　　　　　　(c)
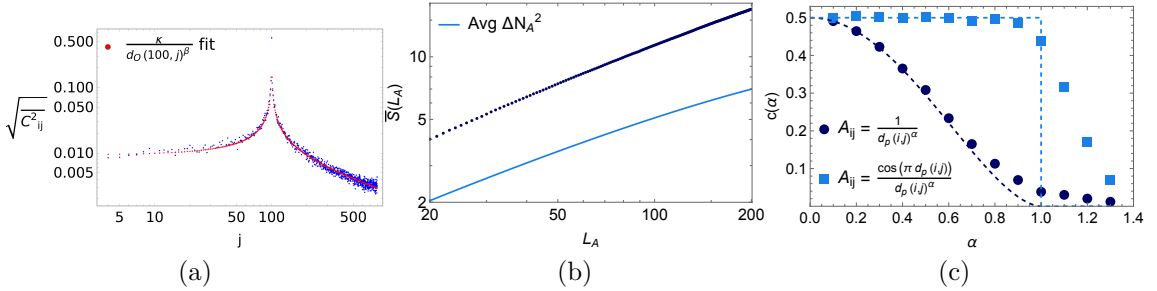
Figure 5.3: Fig 5.3a shows the root-mean square correlator $\sqrt{C_{ij}^2}$ with $i = 100$ for $L = 800$ after averaging over 100 random samples from the power-law ensemble (5.14) with $\alpha = 0.8$ obeying (5.16). Fig 5.3b uses empirically determined parameters m and β for $L = 2000$ in (A.5) and makes a prediction for number fluctuations (orange line) consistent with (5.17) using (A.5). $S(L_A)$ (dots) is for a system of $L = 2000$ averaged over 400 samples for the same α. Note the agreement between the slopes for small subsystem sizes. Fig 5.3c demonstrates $c_{\text{eff}}(\alpha)$ for models shown in (5.20), (5.21), with $\alpha_h = \alpha_p = \alpha$ and $\mu = 0$. The superimposed dashed lines show the analytically computed c_{eff} using block Topelitz symbols.

This model of staggered hopping terms, with $\alpha = \alpha_h = \alpha_p$, has its spectrum shifted such that it cannot be tuned to a gapless point by tuning μ for $\alpha < 1$. Naturally, this model would also have a different low-energy theory. We set $\mu = 0$ and still write $S(L_A) = \frac{c_{\text{eff}}(\alpha)}{3} \log(L_A)$ as a convention. c_{eff} here is a function of α alone. For $\alpha \leq 1$, the numerically obtained c_{eff} is approximately constant and close to $\frac{1}{2}$, and as α increases beyond 1 it goes to 0 (see Fig 5.3c).

We now interpret these numerical results in light of developments in [80], [81] which allow the computation of the leading order terms in $S(L_A)$ in terms of the matrix symbol $G(k)$ of the block Toeplitz correlation matrix:

$$C_A(i-j) = \begin{pmatrix} \delta_{ij} - 2\left\langle c_i^\dagger c_j \right\rangle & 2\left\langle c_i c_j \right\rangle \\ 2\left\langle c_i^\dagger c_j^\dagger \right\rangle & -\delta_{ij} + 2\left\langle c_i^\dagger c_j \right\rangle \end{pmatrix}, \tag{5.22}$$

which is written in terms of the 2×2 matrix $G(k)$ as

$$C_A(i-j) = \frac{1}{2\pi} \int_0^{2\pi} dk \ G(k)e^{ik(i-j)}. \tag{5.23}$$

Similar to the discussion below (5.8), the asymptotic expansion of the determinant of C_A was computed in [80], [81] and it was used to determine that the leading order term in $S(L_A)$ is logarithmic with a coefficient which depends on the discontinuities of the matrix symbol $G(k)$, see Appendix D for details. In general, the analytical value of c_{eff} has an integral representation and for (5.20) we plot it in Fig 5.3c. We find that the analytical prediction for c_{eff} vanishes at $\alpha = 1$ although the numerically determined c_{eff} is nonzero and continues to decay past $\alpha = 1$. For (5.21) the analytical $c_{\text{eff}} = \frac{1}{2}$ when $0 < \alpha < 1$ with a jump to $c_{\text{eff}} \approx 0.437$ at $\alpha = 1$ and $c_{\text{eff}} = 0$ for $\alpha > 1$. The numerically determined c_{eff} is close to $\frac{1}{2}$ for $\alpha < 1$ but decays gradually for $\alpha > 1$.

This apparent discrepancy between numerics and the analytical c_{eff} is resolved with the observation that the scaling of entanglement entropy is an asymptotic statement about L_A. In other words, in an infinite system $S(L_A)$ can continue to grow logarithmically (or otherwise) up to some point and can then transition into its true asymptotic scaling. In the long-range models we consider, even in the absence of true asymptotic logarithmic scaling $S(L_A)$ continues to grow with logarithmic behavior for finite L_A until when the large L_A behavior from the asymptotic expansion of Toeplitz determinants becomes valid. This is also found when one considers a theory near a critical point such that $m \ll 1$, in which one finds from field-theory calculations that $S(L_A) \sim \frac{c}{3} \log(L_A)$ for L_A smaller than the scale set by m^{-1} with $S(L_A)$ saturating beyond that, a scenario validated in lattice models. In case of the gapped long-range models with $\alpha > 1$, the length-scale controlling the transition is not obvious. It is unclear if the logarithmic growth which saturates when c_{eff} calculated from the matrix symbol vanishes, could persist on turning on interactions.

Our examples show that the anomalous scaling of entanglement is quite sensitive to the details of the model. The manner in which such scaling can transition to conventional scaling is non-universal. Given that the isolated divergences of $b(k)$ for $\alpha < 1$ play a crucial technical role for c_{eff} to be nonzero for $\alpha > 1$ as outlined in Appendix D, it is likely that there is no violation of the area-law in the presence of a gap for $\alpha > 1$ for translationally invariant models with a thermodynamic limit. That being said, there could be faster growth of entanglement for finite L and for finite subsystems L_A below a certain scale.

5.4 Summary: Fermionic models with long-range interactions

In this chapter, we examined the behavior of ground-state entanglement entropy in lattice models with long-range couplings and numerically studied several examples of free fermionic models in one spatial dimension. We found a regime of intermediate fractal scaling for disordered models and for a sequence of deterministic Hamiltonians without a continuum limit, as a function of the decay exponent α. For disordered models EE continues to be unbounded for $\alpha > 1$. We provided constructions where the ground state EE approaches maximal volume-law growth consistent with the size of local Hilbert space. For systems with a continuum limit, we found that in the thermodynamic limit, the entanglement entropy is described by the predictions from the effective low-energy theory. The low-energy theory for $\alpha < 2$ may be an exotic one, featuring fractional derivative terms that give rise to algebraic decay of correlations and unbounded entanglement in the presence of a gap. In the translationally invariant models we study, the transition to conventional scaling of entanglement occurs when $\alpha > 1$ and we discuss why likely $\alpha_c = 1$ for this case. There is no common α_c at which conventional entanglement scaling kicks in across all free fermion systems.

This brings us to our main result which is conceptual. Consider an infinite system. Long-range entanglement describes quantum correlations across large spatial distances and is in this sense an IR property. For translationally invariant models with a continuum limit, this implies that entanglement scaling in the IR will constrain the scaling in the UV. Here $S(L_A)$ is precisely translationally invariant and is expected to match the predictions from UV theory at $L_A \ll \xi$, where ξ is the length scale above which the IR scaling sets in. In $d = 1$, an application of strong subadditivity gives[1] $S(\xi) \geq S(l)$ for $l \ll \xi$. The inequality above constrains the range over which the UV scaling can be parametrically faster. For example, assuming $S(\xi) \sim \log(\xi)$ and $S(l) \sim l^\gamma$, the inequality above constrains the power-law growth to be suppressed for domains of size roughly larger than $\log(\xi)^{1/\gamma}$. Further constraints in general systems can probably be deduced on the grounds of smoothness of S and dimensional analysis. There is perhaps a better formulation of these constraints by considering the putative equivalence of field-theoretic renormalization to real-space renormalization schemes like entanglement renormalization [82], [83] that proceed by removing short-distance entanglement along with rescalings.

In $d = 1$, for Poincare-invariant continuum theories the constraints can be made much stronger:

$$\frac{d}{dL_A}\left(L_A \frac{dS(L_A)}{dL_A}\right) \leq 0 \tag{5.24}$$

implies that $S(L_A)$ cannot grow faster than $\log(L_A)$, regardless of some nonlocal description. The concavity of $S(L_A)$ with respect to $\log(L_A)$, which follows from the Poincare invariance of $S(L_A)$, lies at the heart of the entropic c-theorem [84]. Conjectured generalizations of similar restrictions on scaling also exist for higher dimensions

---

[1]Strong subadditivity applied to subsystems corresponding to intervals l_1, l_2 and the union of l_1, l_2 with separating interval of length r gives $S(l_1 + r) + S(l_2 + r) \geq S(l_1) + S(l_2)$ for all l_1, l_2 and r. We set $l_1 = l_2 = l$ and $l + r = \xi$.

[85]. Independent arguments based on crossovers between entanglement and thermal entropies restrict the violations of area law to be at most logarithmic [86] assuming conventional low-temperature thermodynamics. Due to technical considerations, area laws (with potential logarithmic enhancements) are natural in continuum field theories, even nonlocal ones [87], [56] although there are constructions of highly nonlocal theories with volume-law scaling [56], [88]. The logarithmic scaling we find in the smooth long-range free fermionic systems on the lattice follows from these considerations applied to the corresponding IR continuum theories. This reasoning is consistent with results from various nonlocal lattice models [52], [89].

Disordered systems and systems without a continuum limit are not constrained in this manner. To clarify, our statements about the continuum limit do not imply the lack of a continuum field-theoretic description of spatial or ensemble-averages for these models. Nor do our suggestions contradict the findings of entanglement scaling in local disordered models, where the logarithmic scaling obtained after a real-space RG procedure describes the entanglement up to short-distance terms [90].

It would be desirable to put our RG arguments above on a more quantitative footing. Another important task would be to carry out a systematic effective field theory calculation of entanglement entropy in the long-range lattice models discussed in this chapter. As a separate matter, it would be interesting to compare the properties of nonlocal UV-complete quantum field theories with the lattice models considered here. The latter will not have Lorentz-invariant effective theories in general. Similar computations in analytically solvable $d > 1$ models may shed more light on the scaling of entanglement in reasonable nonlocal models.

Chapter 6 Temperature Dependence of Lanczos coefficients

This chapter is based on work-in-progress in collaboration with D. Chakraborty and A. Dymarsky and is reproduced here with the consent of both collaborators.

6.1 Introduction: Krylov complexity

In recent years, the study of Krylov space and Krylov complexity has emerged as a significant avenue for exploring chaotic dynamics in quantum systems. Krylov space, defined as the minimal linear space that contains an operator A during its time evolution, is spanned by nested commutators of the operator with the Hamiltonian $[H, [H, \cdots [H, A] \cdots]]$. Utilizing the recursion method, an orthogonal Krylov basis can be constructed, also leading to the sequence of Lanczos coefficients b_n. This sequence encodes the auto-correlation function $C(t)$ of the operator A, with its asymptotic behavior at large n offering insights into the system's dynamics [15].

Krylov complexity $K(t)$ is the average position of the operator $A(t)$ in the abstract Krylov basis. In some regime, it quantifies the "size" of the operator A as it evolves over time. For a generic chaotic system $K(t)$ is proportional to $e^{\lambda_K t}$ asymptotically. This exponential growth of $K(t)$ is also universal for field theories. It was conjectured in [15] and proved for $\beta = 0$, that the exponent λ_K serves as an upper bound for the growth exponent λ_{OTOC} of out-of-time-ordered correlation functions (OTOCs). Further developments [16] proposed this conjecture as part of a generalized Maldacena-Shenker-Stanford inequality

$$\lambda_{\text{OTOC}} \leq \lambda_K \leq \frac{2\pi}{\beta}. \tag{6.1}$$

Considering systems at a finite inverse temperature β, the Lanczos sequence exhibits β-dependence due to the parametric dependence of the autocorrelation function $C_\beta(t)$ on temperature. In [91], the Lanczos coefficients were promoted to a continuous function of Euclidean time and it was shown that the singularity of $C_\beta(t)$ in Euclidean time was due to delocalization in Krylov space. The dynamics of b_n in Euclidean time is governed by the Toda equations, a completely integrable system. Using related techniques, in Section 6.2 we show that the β-dependence of b_n is described by integrable Hamiltonian dynamics, which has a Lax pair formulation. Specifically, the β-evolution of b_n is described by a pair of systems related to the Toda hierarchy.

In Section 6.3.1, we inspect the β-dependent properties of the spectral function. We describe two mechanisms that induce "staggering" in the Lanczos sequence on introducing β-dependence. We illustrate these ideas through examples such as the XY model and free scalar field theory. In Section 6.3.2, we argue for a universal asymptotic behavior of b_n in typical system for low temperatures. In a finite system, half of the Lanczos coefficients converge to the energy gaps while the rest asymptote to zero. The convergence rate depends on n, with b_n of smaller n converging faster

to their asymptotic values. In Section 6.3.3, we discuss the implications for $K(t)$. We provide numerical evidence that the time-averaged Krylov complexity $\bar{K}$ exponentially decays with β, with the exponent proportional to the system's first energy gap. We conjecture that this behavior of complexity holds for arbitrarily large system sizes.

6.2 Equations of motion and Hamiltonian

The starting point is the Lanczos algorithm, which is used to iteratively build an orthogonal basis in the Krylov space, starting with an initial operator A. Orthogonality is defined with respect to a choice of an inner product, defined in terms of the correlation function. Our goal is to understand temperature dependence of the correlation function and we define the scalar product

$$\langle A, B \rangle_\beta \equiv \mathrm{Tr}\big(A^\dagger \rho_1(\beta) B \rho_2(\beta)\big). \tag{6.2}$$

such that

$$C_\beta(t) \equiv \langle A(0) A(t) \rangle_\beta = \langle A(0), A(t) \rangle_\beta, \tag{6.3}$$

In general $\rho_1(\beta)$ and $\rho_2(\beta)$ are Hermitian positive semi-definite operators that commute with the system's Hamiltonian. In most of this chapter we focus on the Wightman inner product by making the choice

$$\rho_1 = \rho_2 = e^{-\frac{\beta}{2} H}, \tag{6.4}$$

where H is the Hamiltonian of the quantum system. Later in 6.2.3, we will explain how our formalism can be straightforwardly adapted to the choice of other thermal inner products. For an initial operator A_0, we define the Krylov basis recursively

$$A_{n+1} = [H, A_n] - b_{n-1}^2 A_{n-1}, \tag{6.5}$$

where we set $b_{-1} = 0$. The Lanczos coefficients $b_n(\beta)$ are fixed by requiring that the basis is orthogonal,

$$b_n^2(\beta) = \frac{\langle A_{n+1}, A_{n+1} \rangle_\beta}{\langle A_n, A_n \rangle_\beta}. \tag{6.6}$$

Since the norms are non-negative, for convenience, we define $q_n(\beta)$ as follows

$$\delta_{nm} e^{q_n(\beta)} := \langle A_n, A_m \rangle_\beta. \tag{6.7}$$

It is sometimes convenient to work with the orthonormal Krylov basis $\{O_n\}$ defined by

$$O_n := \frac{A_n}{\sqrt{\langle A_n, A_n \rangle_\beta}} = A_n e^{-\frac{q_n(\beta)}{2}}. \tag{6.8}$$

Since the inner product (6.4) is β-dependent, all quantities introduced above, including the Lanczos coefficients $b_n(\beta)$ and the Krylov basis operators O_n are β-dependent.

Our main goal is to understand this temperature dependence. We often will suppress β-dependence in our notations, except where necessary for clarity.

From (6.5) it follows that the action of the Liouvillian $[H, \cdot]$ in the normalized Krylov basis has a tridiagonal representation,

$$M_{nm} := \langle O_n, [H, O_m] \rangle_\beta = \begin{pmatrix} 0 & b_0 & 0 & 0 & \ddots \\ b_0 & 0 & b_1 & 0 & \ddots \\ 0 & b_1 & 0 & b_2 & \ddots \\ 0 & 0 & b_2 & 0 & \ddots \\ \ddots & \ddots & \ddots & \ddots & \ddots \end{pmatrix}. \tag{6.9}$$

A central point is that regardless of the temperature, which defines scalar product in the Krylov space, the Krylov space itself, and the adjoint action of H are temperature independent. It follows that β-dependent matrix M in (6.9) are different representations of the same operator, thus β-dependence is the isospectral deformation of M, which we would like to study.

To that end it is convenient to introduce "temperature evolution," by considering β-dependent operators,

$$A[\beta] := e^{-\frac{\beta}{2} H} A \, e^{-\frac{\beta}{2} H}. \tag{6.10}$$

An important subtlety is that temperature evolution of $A = A_0$ will in most cases move it out of the Krylov space. To see that, we decompose A in the energy eigenbasis

$$A = A^\perp + A_d, \tag{6.11}$$

where A_d and $A^\perp$ stand for diagonal and off-diagonal parts of A, written in the eigenbasis of H, correspondingly. The diagonal operator A_d is in the nullspace of the Liouvillian and therefore all operators A_n defined by (6.5) will share the same diagonal part (up to normalization). On the contrary, diagonal part of $A[\gamma]_d$ is γ-dependent and hence for $\gamma \neq 0$ outside the Krylov space. The same problem will appear for any degenerate energy gaps $\omega_{ij} = E_i - E_j$, and zero energy gap $\omega = 0$ is always maximally degenerate. Keeping this in mind, in full generality we can introduce the superoperator $-\frac{1}{2}\{H, .\}$ acting on the Krylov space as

$$-\frac{1}{2}\{H, O_n\} =: \sum_m T_{nm} O_m + T_n^\perp \implies T_{nm}(\beta) := -\frac{1}{2}\langle O_m, \{H, O_n\} \rangle_\beta, \tag{6.12}$$

where by $T_n^\perp$ we denote the components not contained in the Krylov space.

Our goal would be to derive differential equations describing integrable dynamics of β-dependence of T_{nm} and M_{mn}. We first assume that A has no non-zero matrix elements A_{ij} corresponding to degenerate gaps ω_{ij}, in particular all diagonal matrix elements of A have to be zero. This would ensure that all $T_n^\perp$ vanish. This scenario would normally apply to a chaotic H with no non-zero degenerate gaps, and A with vanishing thermal expectation value at all temperatures, due to a discrete symmetry. We then generalize to include arbitrary H and A.

6.2.1 No degenerate energy gaps

Here we consider the case when $\{H, \cdot\}$ does not move operators outside the Krylov space, which means all $T_n^{\perp}$ vanish. It is easy to see that the matrices $T(\beta), M(\beta)$ commute, as follows from

$$[H, \{H, \, . \, \}] = \{H, [H, \, . \,]\}. \tag{6.13}$$

Next, we temperature-evolve basis operators in Krylov space

$$O_n(\beta) \left[\frac{\beta - \beta_0}{2}\right] \equiv e^{-\frac{(\beta - \beta_0)H}{4}} O_n(\beta) e^{-\frac{(\beta - \beta_0)H}{4}} = \sum_m \left(e^{T(\beta)\frac{\beta - \beta_0}{2}}\right)_{nm} O_m(\beta). \tag{6.14}$$

It is clear that $O_n(\beta) \left[\frac{\beta - \beta_0}{2}\right]$ are mutually orthogonal with respect to the scalar product $\langle \cdot, \cdot \rangle_{\beta_0}$. Thus, the basis $\{O_n(\beta) \left[\frac{\beta - \beta_0}{2}\right]\}$ is related to the basis $\{O_n(\beta_0)\}$ by an orthogonal transformation Q,

$$\sum_m (e^{T(\beta)\frac{\beta - \beta_0}{2}})_{nm} O_m(\beta) = \sum_m Q_{nm}(\beta, \beta_0) O_m(\beta_0). \tag{6.15}$$

Acting on both sides of (6.15) with $[H, \cdot]$, and using $[M, T] = 0$, we obtain

$$M(\beta) = Q(\beta, \beta_0) M(\beta_0) Q^T(\beta, \beta_0). \tag{6.16}$$

Similarly, acting by $-\frac{1}{2}\{H, \cdot\}$ and using (6.12) we obtain

$$T(\beta) = Q(\beta, \beta_0) T(\beta_0) Q^T(\beta, \beta_0). \tag{6.17}$$

As was expected, β-evolution of both M and T is an isospectral deformation and can be written in Lax form. The "evolution" operator Q can be written as $Q(\beta, \beta_0) = U(\beta) U^\dagger(\beta_0)$, where U is an orthogonal matrix. The recursion relation (6.5) implies that the basis element $O_n(\beta)$ is a linear combination of the first n elements of the basis $O_m(\beta_0)$. Hence there is a lower-triangular matrix R^T such that

$$O_n(\beta) = \sum_m (R^{-1})_{nm}^T(\beta, \beta_0) O_m(\beta_0) \tag{6.18}$$

Therefore, (6.15) can be written as follows

$$\sum_m (e^{T(\beta)\frac{\beta - \beta_0}{2}})_{nm} O_m(\beta) = \sum_{m,k} Q_{nm}(\beta, \beta_0) R_{mk}^T(\beta, \beta_0) O_k(\beta), \tag{6.19}$$

which implies

$$e^{T(\beta)\frac{\beta - \beta_0}{2}} = Q(\beta, \beta_0) R^T(\beta, \beta_0), \tag{6.20}$$

where R is an upper triangular matrix. Using (6.17) with (6.20) we find the QR decomposition

$$e^{T(\beta_0)\frac{\beta - \beta_0}{2}} = Q^T(\beta, \beta_0) R(\beta, \beta_0). \tag{6.21}$$

Taking a derivative with respect to β and using (6.17), we obtain

$$\frac{1}{2}T(\beta) = -B(\beta) + \dot{R}(\beta, \beta_0)R^{-1}(\beta, \beta_0), \tag{6.22}$$

where we defined

$$B(\beta) = -Q(\beta, \beta_0)\dot{Q}^T(\beta, \beta_0). \tag{6.23}$$

Notice, that B is independent of β_0. Now using the fact that B is antisymmetric and $\dot{R}R^{-1}$ is upper triangular, (6.22) implies that

$$B(\beta) = \frac{1}{2}(T^+(\beta) - T^-(\beta)), \tag{6.24}$$

where by T^+, T^- we denote the upper-triangular and lower-triangular parts of T, respectively. Finally, taking a derivative of (6.17) and (6.16) with respect to β gives

$$\dot{T} = [B, T], \quad \dot{M} = [B, M], \quad B = \frac{1}{2}(T^+ - T^-). \tag{6.25}$$

The equations (6.25) describe completely integrable dynamics. They govern temperature-dependence of Lanczos coefficients $b_n(\beta)$. This is one of our main results, written in a simplified scenario of no degenerate energy gaps. Similar equations would describe the dependence of b_n on any continuous parameter deforming the scalar product.

Since our main goal is to understand temperature dependence of b_n, or equivalently, $q_n(\beta)$, we would like to parameterize T through the same variables. From (6.12), and using the fact than the unnormalized bases $A_n(\beta)$ and $A_n(\beta_0)$ are related by a lower-triangular matrix with 1 in its diagonal, it follows that the diagonal entries of T are given by

$$h_n \equiv T_{nn} = \dot{q}_n \tag{6.26}$$

One possible strategy is to make use of $[M, T] = 0$ to recursively solve for the entries of T in terms of h_n and the Lanczos coefficients b_n. We may build T_{nm} recursively as follows

$$T_{n,n+(k+2)} = \frac{b_{n-1}T_{n-1,n-1+(k+2)} + b_n T_{n+1,n+1+k} - b_{n+k}T_{n,n+k}}{b_{n+1+k}}. \tag{6.27}$$

The identity (6.27) can be used recursively to determine T. Care must be taken to ensure proper termination condition in the case of finite-dimensional Krylov space. The Lax equations (6.25) can be written as a system of differential equations for b_n, h_n, i.e. for both $q_n(\beta)$ and $\dot{q}_n(\beta)$. To specify a solution, one needs to supply initial conditions not only for b_n, but also for h_n. The former can be evaluated by the Lanczos algorithm at the initial value $\beta = \beta_0$, while for the latter one needs to evaluate the following quantities in the initial Krylov basis at $\beta = \beta_0$

$$h_n(\beta_0) = -\frac{1}{2}\langle O_n(\beta_0), \{H, O_n(\beta_0)\}\rangle_{\beta_0}. \tag{6.28}$$

An explicit example of writing down and solving differential equations for $q_n(\beta)$ is given in subsection (6.2.1).

Finally we can identify the orthogonal matrix $U(\beta)$ introduced above with the matrix that diagonalizing M

$$M(\beta) = U(\beta)\Lambda U^T(\beta). \tag{6.29}$$

Here Λ is β-independent diagonal matrix of eigenvalues, and U satisfies

$$U(\beta) = Q(\beta, \beta_0)U(\beta_0), \qquad \dot{U}(\beta) = B(\beta)U(\beta). \tag{6.30}$$

Relation to Toda chain

There is another way to build a basis for the Krylov space. We start by performing the Lanczos algorithm with the super-operator $-\frac{1}{2}\{H, \cdot\}$ and the initial operator $\tilde{A}_0^{\text{even}} \equiv A_0$:

$$\tilde{A}_{n+1}^{\text{even}} = -\frac{1}{2}\{H, \tilde{A}_n^{\text{even}}\} - \tilde{a}_n^{\text{even}}\tilde{A}_n^{\text{even}} - (\tilde{b}_{n-1}^{\text{even}})^2 \tilde{A}_{n-1}^{\text{even}}, \tag{6.31}$$

where

$$(\tilde{b}_n^{\text{even}})^2 = \frac{\langle \tilde{A}_{n+1}^{\text{even}}, \tilde{A}_{n+1}^{\text{even}} \rangle}{\langle \tilde{A}_n^{\text{even}}, \tilde{A}_n^{\text{even}} \rangle}, \quad \tilde{a}_n^{\text{even}} = \frac{\langle \tilde{A}_n^{\text{even}}, \{H, \tilde{A}_n^{\text{even}}\} \rangle}{\langle \tilde{A}_n^{\text{even}}, \tilde{A}_n^{\text{even}} \rangle}. \tag{6.32}$$

After normalizing A_n^{even} we obtain $\tilde{O}_n^{\text{even}}$. We observe that for Hermitian initial operator A_0, the Krylov basis $\{O_n\}$ splits into alternating Hermitian and anti-Hermitian operators for even and odd n respectively. However, $\{H, \cdot\}$ maps a Hermitian (anti-Hermitian) operator to another Hermitian (anti-Hermitian) operator. This implies that $\{\tilde{O}_n^{\text{even}}\}$ spans only half of the Krylov space, namely the subspace spanned by Hermitian operators. To obtain the rest of the Krylov space, we must perform Lanczos iteration again, but this time starting with the initial operator $\tilde{A}_0^{\text{odd}} \equiv A_1$. This leads to another set of operators $\{\tilde{O}_n^{\text{odd}}\}$ and Lanczos coefficients $\tilde{b}_n^{\text{odd}}, \tilde{a}_n^{\text{odd}}$.

The super-operator $-\frac{1}{2}\{H, \cdot\}$ has a tridiagonal representations $\tilde{T}_{\text{even}}, \tilde{T}_{\text{odd}}$ in these two bases:

$$(\tilde{T}_{\text{even}})_{nm} = -\frac{1}{2}\langle \tilde{O}_n^{\text{even}}, \{H, \tilde{O}_m^{\text{even}}\} \rangle, \tag{6.33}$$

$$(\tilde{T}_{\text{odd}})_{nm} = -\frac{1}{2}\langle \tilde{O}_n^{\text{odd}}, \{H, \tilde{O}_m^{\text{odd}}\} \rangle, \tag{6.34}$$

while $\langle \tilde{O}_n^{\text{odd}}, \{H, \tilde{O}_m^{\text{even}}\} \rangle = \langle \tilde{O}_n^{\text{even}}, \{H, \tilde{O}_m^{\text{odd}}\} \rangle = 0$. Following the same steps as in [91], it is straightforward to show that the temperature evolution of these matrices is governed by Toda equations

$$\dot{\tilde{T}}_i = [\tilde{B}_i, \tilde{T}_i], \quad \tilde{B}_i = \frac{1}{2}(\tilde{T}_i^+ - \tilde{T}_i^-), \quad i = \text{even, odd}. \tag{6.35}$$

We can arrive at this result in a different way. Due to the elements of the Krylov basis $\{O_n\}$ alternating between Hermitian and anti-Hermitian operators for even and odd n respectively, $T_{ij} = 0$ unless $i + j$ is even. Hence, we can split T into a direct sum of even and odd parts

$$(T_{\text{even}})_{ij} = T_{2i,2j} \quad (T_{\text{odd}})_{ij} = T_{2i+1,2j+1}. \tag{6.36}$$

66

We rewrite the equation for $\dot{T}$ (6.25) as two Lax equations

$$\dot{T}_l = [B_l, T_l], \quad B_l = \frac{1}{2}(T_l^+ - T_l^-), \quad l = \text{even}, \text{odd}. \tag{6.37}$$

Therefore the dynamical equations governing even and odd subspaces are fully decoupled. It follows from the Lax representation that the constants of motion are

$$\mathcal{I}_k^l = \frac{1}{k}\operatorname{tr}(T_l^k), \quad l = \text{even}, \text{odd}. \tag{6.38}$$

From the definition of T and using that T and M commute, one finds

$$\mathcal{I}_k^{\text{even}} = \mathcal{I}_k^{\text{odd}}. \tag{6.39}$$

The matrices $T_{\text{even}}, T_{\text{odd}}$ are real-symmetric and can be tri-diagonalized using Lanczos algorithm. Namely, by acting by T_{even} on A_0, and by T_{odd} on A_1 Lanczos algorithm will yield $\tilde{T}_{\text{even}}$ and $\tilde{T}_{\text{odd}}$ respetively. In other words $\tilde{T}_l$, for $l = \text{even}, \text{odd}$, are the matrices $T_{\text{even}}, T_{\text{odd}}$ brought to tridiagonal form by a β-dependent orthogonal transformations P_l,

$$T_l = P_l \tilde{T}_l P_l^T, \quad l = \text{even}, \text{odd}. \tag{6.40}$$

The Lax equations (6.37) are equivalent to the following equations for $\tilde{T}_l$

$$\frac{d}{d\beta}\tilde{T}_l = [\tilde{B}_l, \tilde{T}_l], \quad \tilde{B}_l = \frac{1}{2}(\tilde{T}_l^+ - \tilde{T}_l^-), \quad l = \text{even}, \text{odd}. \tag{6.41}$$

The equations (6.41) describe precisely two Toda chains in Lax form. In terms of the phase space variables $\{\tilde{p}^l = \dot{\tilde{q}}^l, \tilde{q}^l\}$ with the canonical Poisson bracket, the Hamiltonian is

$$\mathcal{H} = \mathcal{I}_2^{\text{even}} + \mathcal{I}_2^{\text{odd}}. \tag{6.42}$$

This describes two decoupled open Toda chains, related only by the initial conditions $\mathcal{I}_k^{\text{even}} = \mathcal{I}_k^{\text{odd}}$ for all k. The same Hamiltonian (6.42) generates the dynamics of the original matrix T. However, the relation between $q_n(\beta)$ and $\tilde{q}_n(\beta)$ is non-universal and complicated. Both Hamiltonians I_k^l and the Poisson brackets look non-trivial in terms of q_n.

Example

As a simple example, let us consider a spin chain of size 2 governed by the Hamiltonian

$$H = -J(\sigma_x^1 \sigma_y^2 + \sigma_y^1 \sigma_x^2) + h(\sigma_y^2 + \sigma_x^1). \tag{6.43}$$

The eigenvalues of this Hamiltonian are

$$E_0 = 0, \ E_1 = 2J, \ E_2 = -J - \sqrt{J^2 + 4h^2}, \ E_3 = -J + \sqrt{J^2 + 4h^2}. \tag{6.44}$$

Starting from the initial operator

$$A_0 = \sigma_y^1 \sigma_z^2. \tag{6.45}$$

and performing the Lanczos algorithm with $\beta = 0$ we find

$$
\begin{align}
A_1 &= 4ih(\sigma_y^1 \sigma_x^2 + \sigma_z^1 \sigma_z^2) + 4iJ\sigma_y^2, \tag{6.46}\\
A_2 &= -16h^2 \sigma_z^1 \sigma_x^2, \tag{6.47}\\
A_3 &= 32i\frac{h^2 J}{2h^2 + J^2}\left((2h^2 + J^2)\sigma_x^1 + hJ\sigma_y^1\sigma_x^2 - 2h^2\sigma_y^2 + hJ\sigma_z^2\sigma_z^2\right), \tag{6.48}
\end{align}
$$

along with Lanczos coefficients

$$
b_0(0) = 2\sqrt{J^2 + 2h^2}, \quad b_1(0) = \frac{4h^2}{\sqrt{2h^2 + J^2}}, \quad b_2(0) = 2\sqrt{\frac{4h^2 J^2 + J^4}{2h^2 + J^2}}. \tag{6.49}
$$

We also evaluate

$$
h_i(0) = -\frac{1}{2}\operatorname{tr}\left(A_i^\dagger\{H, A_i\}\right)/\operatorname{tr}\left(A_i^\dagger A_i\right), \tag{6.50}
$$

resulting in

$$
h_0(0) = h_2(0) = 0, \quad h_1(0) = -h_3(0) = \frac{2h^2 J}{2h^2 + J^2}. \tag{6.51}
$$

The Krylov space is 4-dimensional. Let us write

$$
T^{\text{even}} = \begin{pmatrix} h_0 & t_{02} \\ t_{02} & h_2 \end{pmatrix}, \qquad T^{\text{odd}} = \begin{pmatrix} h_1 & t_{13} \\ t_{13} & h_3 \end{pmatrix}, \tag{6.52}
$$

$$
t_{02} = \frac{b_0}{b_1}(h_1 - h_0), \quad t_{13} = \frac{b_0^2(h_1 - h_0) + b_1^2(h_2 - h_1)}{b_1 b_2}, \tag{6.53}
$$

where we used (6.27) to determine the off-diagonal entries of matrix T in terms of b_i, h_i.

The Lax equations $\dot{T} = [B, T]$, $\dot{M} = [B, M]$ become the following system of differential equations

$$
\dot{h}_0 = -\dot{h}_2 = \frac{b_0^2}{b_1^2}(h_0 - h_1)^2, \quad \dot{h}_1 = -\dot{h}_3 = \frac{b_2^2}{b_1^2}(h_2 - h_3)^2, \tag{6.54}
$$

$$
\dot{b}_0 = \frac{1}{2}b_0(h_1 - h_0), \quad \dot{b}_1 = \frac{1}{2}b_1(h_2 - h_1), \quad \dot{b}_2 = \frac{1}{2}b_2(h_3 - h_2). \tag{6.55}
$$

Taking advantage of the fact that the quantities $\operatorname{tr}(M^2)$ and $\operatorname{tr}\left((T^{\text{even}})^k\right) = \operatorname{tr}\left((T^{\text{odd}})^k\right)$ for $k = 1, 2$ are conserved, we find the general solution parametrized by $c, \kappa, \beta_0, \beta_1, \lambda$,

$$
h_0 = \frac{c}{2} + \kappa \tanh(\kappa(\beta - \beta_0)), \tag{6.56}
$$

$$
h_2 = \frac{c}{2} - \kappa \tanh(\kappa(\beta - \beta_0)), \tag{6.57}
$$

$$
h_1 = \frac{c}{2} + \kappa \tanh(\kappa(\beta - \beta_1)), \tag{6.58}
$$

$$
h_3 = \frac{c}{2} - \kappa \tanh(\kappa(\beta - \beta_1)), \tag{6.59}
$$

68

$$b_0 = \frac{\lambda}{\sqrt{\cosh\left(\kappa(\beta + \beta_1 - 2\beta_0)\right)\operatorname{sech}\left(\kappa(\beta - \beta_1)\right) + 1}}, \tag{6.60}$$

$$b_1 = \frac{\lambda\,\operatorname{sech}(\kappa(\beta - \beta_1))|\sinh(\kappa(\beta_1 - \beta_0))|}{\sqrt{\cosh\left(\kappa(\beta + \beta_1 - 2\beta_0)\right)\operatorname{sech}\left(\kappa(\beta - \beta_1)\right) + 1}}, \tag{6.61}$$

$$b_2 = \frac{\lambda\cosh(\kappa(\beta - \beta_0))\operatorname{sech}(\kappa(\beta - \beta_1))}{\sqrt{\cosh\left(\kappa(\beta + \beta_1 - 2\beta_0)\right)\operatorname{sech}\left(\kappa(\beta - \beta_1)\right) + 1}}. \tag{6.62}$$

Given the initial values $b_i(0), h_j(0)$ (6.49,6.51), the integration constants can be evaluated to be

$$c = 0, \ \lambda = 2\sqrt{2J^2 + 4h^2}, \ \kappa = -J, \ \beta_0 = 0, \ \beta_1 = -\frac{1}{J}\operatorname{arctanh}\frac{2h^2}{2h^2 + J^2}. \tag{6.63}$$

This completes the derivation of $b_n(\beta)$.

Asymptotically, as $\beta \to \infty$ we find that $b_0 \to |E_1 - E_0|$, $b_1 \to 0$, $b_2 \to |E_3 - E_2|$. This is a pattern that we explore in generality in section 6.3.2.

We note that in this small-dimensional example, $T_{\text{even}} = \tilde{T}_{\text{even}}$, $T_{\text{odd}} = \tilde{T}_{\text{odd}}$, so this system is exactly the same as two conventional Toda chains of size two, with dynamical variables $\{q_i, h_i\}$ satisfying conventional Poisson brackets. This is no longer true for Krylov spaces of larger size: the Poisson brackets between $\{q_i, h_i\}$ become complicated.

6.2.2 General initial operator

For a general initial operator with non-vanishing diagonal matrix elements A_{ii}, even if non-zero gaps ω_{ij} are non-degenerate, zero gap is degenerate. This will alter derivation of the preceding section. Most importantly, Krylov spaces for different β are different. However it is possible to keep track of the diagonal parts of operators separately. We modify the definition (6.12) to

$$T_{nm}(\beta) = -\frac{1}{2}\langle O_n, \{H, O_m\}\rangle_\beta - \frac{1}{2}a_m\langle O_n, \{H, e^{-\mu(\beta,\beta_0)}d(\beta_0)\}\rangle_\beta, \tag{6.64}$$

$$d(\beta_0) \equiv \frac{\operatorname{diag} A}{\sqrt{\langle \operatorname{diag} A, \operatorname{diag} A\rangle_{\beta_0}}}, \qquad e^{2\mu(\beta,\beta_0)} \equiv \langle d, d\rangle_\beta, \tag{6.65}$$

where, up to normalization, d is the diagonal part of A – the projection of A on the nullspace of $[H, \cdot]$ (we assume energy spectrum is non-degenerate). In (6.64) basis operators O_n are β-dependent. Vector a_n is the normalized null vector of the Liouvillian M, and consequently also the null vector of T. Explicitly, a_n can be written in terms of Lanczos coefficients

$$a_n(\beta) = \begin{cases} (-1)^k \left(\prod_{l=0}^{l=k-1} \frac{b_{2l}(\beta)}{b_{2l+1}(\beta)} \right) a_0(\beta), & n = 2k, \\ 0, & n = 2k+1, \end{cases} \tag{6.66}$$

and $a_0(\beta)$ is given by

$$a_0(\beta) = \frac{\langle d, O_0\rangle_\beta}{\sqrt{\langle d, d\rangle_\beta}}. \tag{6.67}$$

69

By these modifications, T becomes a representation of $-\frac{1}{2}\{H,\cdot\}$ projected on the Krylov space with the direction corresponding to the degenerate eigenvalue of M subtracted, while the evolution of the initial operator outside this space is governed by functions $a_n(\beta)$ and $\mu(\beta)$. From (6.64) it follows that the temperature evolution operator acting on the Krylov basis can be expressed as

$$e^{-\frac{(\beta-\beta_0)H}{4}}O_n(\beta)e^{-\frac{(\beta-\beta_0)H}{4}} = \sum_m (e^{T(\beta)\frac{\beta-\beta_0}{2}+\mu(\beta,\beta_0)a^T(\beta)a(\beta)})_{nm}O_m(\beta). \tag{6.68}$$

Similarly to (6.21), we consider the QR decomposition:

$$e^{T(\beta_0)\frac{\beta-\beta_0}{2}+\mu(\beta,\beta_0)a(\beta_0)a^T(\beta_0)} = Q^T(\beta,\beta_0)R(\beta,\beta_0). \tag{6.69}$$

The matrix T and its null-vector a evolve as

$$T(\beta) = Q(\beta,\beta_0)T(\beta_0)Q^T(\beta,\beta_0), \quad a(\beta) = Q(\beta,\beta_0)a(\beta_0). \tag{6.70}$$

Taking a derivative of (6.69) with respect to β we find that the Lax equations (6.25) continue to hold with a generalized B:

$$B = \frac{1}{2}(T^+ - T^-) + \dot{\mu}((aa^T)^+ - (aa^T)^-), \tag{6.71}$$

where we note that, due to definition (6.65), $\dot{\mu}(\beta) \equiv \frac{\partial}{\partial\beta}\mu(\beta,\beta_0)$ is independent of β_0. Just like before, the equations for the odd and even subspaces decouple

$$\dot{T}_l = [B_l, T_l], \quad l = \text{even, odd}, \tag{6.72}$$

$$B_{\text{even}} = \frac{1}{2}(T^+_{\text{even}} - T^-_{\text{even}}) + \dot{\mu}((aa^T)^+_{\text{even}} - (aa^T)^-_{\text{even}}), \quad B_{\text{odd}} = \frac{1}{2}(T^+_{\text{odd}} - T^-_{\text{odd}}). \tag{6.73}$$

These equations do not determine the function $\dot{\mu}(\beta)$, which must be evaluated independently from its definition (6.65).

This dynamics has a Hamiltonian description. To see this, we could consider the tridiagonal representation $\tilde{T}_l$. These continue to satisfy the same type of Lax equation

$$\dot{\tilde{T}}_l = [\tilde{B}_l, \tilde{T}_l], \quad l = \text{even, odd}, \tag{6.74}$$

with

$$\tilde{B}_{\text{even}} = \frac{1}{2}(\tilde{T}^+_{\text{even}} - \tilde{T}^-_{\text{even}}) + \dot{\mu}((\tilde{a}\tilde{a}^T)^+_{\text{even}} - (\tilde{a}\tilde{a}^T)^-_{\text{even}}), \quad B_{\text{odd}} = \frac{1}{2}(\tilde{T}^+_{\text{odd}} - \tilde{T}^-_{\text{odd}}). \tag{6.75}$$

Here $\tilde{a}$ is the normalized null-vector of $\tilde{T}_{\text{even}}$. From this we can infer that the full Hamiltonian describes two decoupled systems

$$\mathcal{H} = \mathcal{H}_{\text{even}} + \mathcal{H}_{\text{odd}}, \tag{6.76}$$

where the odd subspace continues to evolve according to the usual Toda dynamics with the Hamiltonian

$$\mathcal{H}_{\text{odd}} = \mathcal{I}_2^{\text{odd}} = \frac{1}{2}\text{tr}(T^2_{\text{odd}}), \tag{6.77}$$

and the even part is modified to

$$\mathcal{H}_{\text{even}} = \mathcal{I}_2^{\text{even}} + \dot{\mu}\,\mathcal{H}', \quad \mathcal{H}' = \sum c_k\,\mathcal{I}_k^{\text{even}}. \tag{6.78}$$

The coefficients c_k introduced in (6.78) are the coefficients that appear in the characteristic polynomial of T_{even}. They can be evaluated as

$$c_k = \frac{1}{k!}\frac{\partial^k}{\partial\lambda^k}\det(\lambda - T(\beta_0))|_{\lambda=0} \tag{6.79}$$

The determinant of T_{even} is written in general in terms of I_k as

$$\mathcal{C} = \sum_{k=1}^{n} k c_k \mathcal{I}_k^{\text{even}}. \tag{6.80}$$

$\mathcal{C}$ vanishes on-shell due to the zero mode of T_{even}. A calculation (see Appendix F) shows that

$$c_k = \frac{2}{\frac{\partial\mathcal{C}}{\partial\mathcal{I}_1^{\text{even}}}}\frac{\partial\mathcal{C}}{\partial\mathcal{I}_k^{\text{even}}}, \tag{6.81}$$

allowing (6.78) to be rewritten as, (where "*os*" stands for on-shell)

$$\mathcal{H}' = \frac{2\mathcal{C}}{\frac{\partial\mathcal{C}}{\partial\mathcal{I}_1^{\text{even}}}}\Bigg|_{os}. \tag{6.82}$$

Example

Consider again the spin chain of section 6.2.1

$$H = -J(\sigma_x^1\sigma_y^2 + \sigma_y^1\sigma_x^2) + h(\sigma_y^2 + \sigma_x^1). \tag{6.83}$$

Starting from the initial operator

$$A_0 = \sigma_z^1\sigma_z^2, \tag{6.84}$$

and performing the Lanczos algorithm with $\beta = 0$ we find

$$\begin{align}
A_1 &= 4ih(\sigma_z^1\sigma_x^2 - \sigma_y^1\sigma_z^2), \tag{6.85}\\
A_2 &= 8hJ(\sigma_x^1 + \sigma_y^2) + 16h^2\sigma_y^1\sigma_x^2, \tag{6.86}
\end{align}$$

$$\tag{6.87}$$

along with Lanczos coefficients

$$b_0(0) = 2\sqrt{2}|h|, \quad b_1(0) = 2\sqrt{2h^2 + J^2}. \tag{6.88}$$

We also evaluate

$$h_i(0) = -\frac{1}{2}\operatorname{tr}\left(A_i^\dagger\{H, A_i\}\right) / \operatorname{tr}\left(A_i^\dagger A_i\right), \tag{6.89}$$

71

and

$$e^{2\mu(\beta,0)} \equiv \langle d, d \rangle_\beta, \tag{6.90}$$

resulting in

$$h_0(0) = \frac{2h^2 J}{4h^2 + J^2}, \quad h_1(0) = J, \quad h_2(0) = \frac{2h^2 J + J^3}{4h^2 + J^2}, \tag{6.91}$$

$$e^{2\mu(\beta,0)} = \frac{2J^2 e^{\beta J} \cosh(\beta\Delta) + \Delta^2 \left(e^{-2\beta J} + 1\right)}{2\left(\Delta^2 + J^2\right)}, \quad \Delta \equiv \sqrt{4h^2 + J^2}. \tag{6.92}$$

The Krylov space is 3-dimensional. Let us write

$$T^{\text{even}} = \begin{pmatrix} h_0 & t_{02} \\ t_{02} & h_2 \end{pmatrix}, \qquad T^{\text{odd}} = \begin{pmatrix} h_1 \end{pmatrix}, \tag{6.93}$$

$$t_{02} = \frac{b_0}{b_1}(h_1 - h_0), \tag{6.94}$$

where we used (6.27) to determine the off-diagonal entry of matrix T in terms of b_i, h_i. The Lax equations $\dot{T} = [B, T]$, $\dot{M} = [B, M]$ give the following system of differential equations

$$\dot{h}_0 = -\dot{h}_2 = \frac{b_0^2}{b_1^2}(h_0 - h_1)^2 + \dot{\mu}\frac{2b_0^2}{b_0^2 + b_1^2}(h_0 - h_1), \quad \dot{h}_1 = 0, \tag{6.95}$$

$$\dot{b}_0 = \frac{1}{2}b_0(h_1 - h_0) - \dot{\mu}\frac{b_0 b_1^2}{b_0^2 + b_1^2}, \quad \dot{b}_1 = \frac{1}{2}b_1(h_2 - h_1) + \dot{\mu}\frac{b_0^2 b_1}{b_0^2 + b_1^2}. \tag{6.96}$$

Taking advantage of the fact that the quantities $\text{tr}(M^2)$ and $\text{tr}\left((T^{\text{even}})^k\right) = \text{tr}\left((T^{\text{odd}})^k\right)$ for $k = 1, 2$ are conserved, we find the general solution parametrized by c, C, λ

$$h_0 = c\frac{Ce^{c\beta - 2\mu(\beta,0)}}{1 + Ce^{c\beta - 2\mu(\beta,0)}}, \tag{6.97}$$

$$h_1 = c, \tag{6.98}$$

$$h_2 = c\frac{1}{1 + Ce^{c\beta - 2\mu(\beta,0)}}, \tag{6.99}$$

$$b_0^2 = \frac{\lambda^2 C}{C + e^{2\mu(\beta,0) - c\beta}}, \tag{6.100}$$

$$b_1^2 = \frac{\lambda^2}{1 + Ce^{c\beta - 2\mu(\beta,0)}}. \tag{6.101}$$

Given the initial values $b_i(0), h_j(0)$ (6.88,6.91), the integration constants can be evaluated to be

$$c = J, \ \lambda = 2\sqrt{4h^2 + J^2}, \ C = \frac{2h^2}{J^2 + 2h^2}. \tag{6.102}$$

This completes the derivation of $b_n(\beta)$.

6.2.3 Case of degeneracies and Generalizations

Here we consider systems with degeneracies in the energy differences. The simplest example is the quantum harmonic oscillator (see Appendix E). This treatment works for all initial operators and general inner products (6.2) with a real parameter β where $\rho_1(\beta), \rho_2(\beta)$ are Hermitian, positive semi-definite operators that commute with the Hamiltonian. Let J be the self-adjoint super-operator such that $e^{J\beta}A = \rho_1(\beta)A\rho_2(\beta)$ for all operators A. For the Wightman inner product we have $J = -\frac{1}{2}\{H, \cdot\}$.

We start by extending the Krylov space with an additional set of orthonormal operators which span the operator space. Let N denote the size of Krylov space and $N' \geq N$ the size of the extended Krylov space. There are several equivalent ways to do this. The resulting normalized operators O_i with $i < N$ are fixed, but there is freedom in the choice of O_i for $i \geq N$, stemming from the freedom to rotate O_i among themselves for $i \geq N$. One way to accomplish this is to lift all the degeneracies by introducing a small parameter ϵ, perform the Lanczos algorithm, normalize the operators and send $\epsilon \to 0$ in the end. Another way to accomplish this, is to perform Lanczos algorithm with the operator $[H, \cdot] + \epsilon J$, and send $\epsilon \to 0$ at the end.

We define the extended matrix T' similar to (6.12), but with i, j running through the entire extended Krylov space

$$T'_{ij} = \langle O_i, JO_j \rangle_\beta, \quad 0 \leq i, j \leq N' - 1. \tag{6.103}$$

The superoperator J is an endomorphism of the extended Krylov space, and using the same steps as in section 6.2.1 we obtain the Lax equation

$$\dot{T}' = [B', T'], \quad B' = \frac{1}{2}((T')^+ - (T')^-). \tag{6.104}$$

Let us denote by T_K the submatrix of T_{ij} with $0 \leq i, j \leq N - 1$ in order to write T' in the block form:

$$T' = \begin{pmatrix} T_K & t \\ t^T & T_E \end{pmatrix}. \tag{6.105}$$

From (6.104) we obtain the following equation for T_K

$$\dot{T}_K = [B_K, T_K] + tt^T, \quad B = \frac{1}{2}(T_K^+ - T_K^-). \tag{6.106}$$

We can also write the equation as follows

$$\dot{T}_K = [B_K, T_K] - T_K^2 + Y, \tag{6.107}$$

where

$$Y_{ij} = \langle JO_i, JO_j \rangle. \tag{6.108}$$

6.2.4 Exact Solutions

For a generic system in the absence of symmetry reasons, T and hence B will be a full-matrix with roughly $O(N^2)$ components. This makes the task of obtaining exact

solutions of (6.25) daunting. There are special choices of T that offer a way to solve for the b_n's through (6.25), though most of the solutions in question may not be physical Lanczos coefficients. A way of obtaining exact solutions could be through postulating an ansatz for the diagonal elements T_{nn} in terms of $\{q_n\}$. Another way could be through the choice of an even function f, such that $T = f(M)$. The evenness requirement ensures compatibility in multiplicity of eigenvalues of T and M, consistent with T being a direct sum of odd and even parts. An interesting choice is $f(M) = \alpha M^{2k}$ for a positive integer k. The equation $\dot{M} = [B, M]$ then becomes an instance of the Toda hierarchy.

The case with $T = -\frac{1}{2}\alpha M^2$ is particularly convenient. T becomes direct sum of two coupled Toda chains T_{odd} and T_{even} which allows one to solve exactly for $T(\beta)$. The equation $\dot{M} = [B, M]$ reduces to

$$\dot{b}_n(\beta) = -\frac{\alpha}{2}b_n(\beta)(b_{n+1}^2(\beta) - b_{n-1}^2(\beta)). \tag{6.109}$$

This is the integrable system studied by Kac and Van Moerbeke [92]. The separable polynomial solutions to these equations are given by

$$b_n(\beta) = \alpha\sqrt{\frac{n+1}{\beta - \beta_0}}. \tag{6.110}$$

The autocorrelation function corresponding to this solutions is the Gaussian

$$C_\beta(t) = e^{-\frac{\alpha^2 t^2}{2(\beta - \beta_0)}}, \tag{6.111}$$

which for $\alpha > 0$ has physical behavior. For large β, $C_\beta(t)$ decays more slowly and the spectral function becomes localized, consistent with the large β limit for $C_\beta(t)$ in a physical system.

6.3 General Properties of Lanczos Coefficients

6.3.1 Properties of the Measure

In practice a lot can be said about the general properties of temperature dependence of Lanczos coefficients by considering the spectral representation of the Wightman function:

$$C_\beta(t) = \int e^{i(E_1 - E_2)t}e^{-\beta\frac{E_1 + E_2}{2}}\rho(E_1, E_2)|\langle E_1| A |E_2\rangle|^2 dE_1 dE_2, \tag{6.112}$$

where $\rho(E_1, E_2)$ is the joint density of eigenvalues. It is useful to change variables to $E = \frac{1}{2}(E_1 + E_2)$ and $\omega = E_1 - E_2$ to write

$$C_\beta(t) = \int (g(\omega, \beta) + \kappa(\beta)\delta(\omega))e^{i\omega t}d\omega \equiv \int \Phi(\omega)e^{i\omega t}\,d\omega \tag{6.113}$$

where

$$g(\omega, \beta) = \int e^{-\beta E}\rho\big(E+\frac{\omega}{2}\big)\rho\big(E-\frac{\omega}{2}\big)|A(E,\omega)|^2 dE \ , \ \ \kappa(\beta) = \int e^{-\beta E}\rho(E)|A(E,0)|^2 dE \tag{6.114}$$

The asymptotic growth rate of Lanczos coefficients is governed by the large-frequency asymptotics of the measure $\Phi(\omega)$, [15], and it follows that a key ingredient is the β-dependence of the asymptotic decay of the measure induced from the E integral. However, the large-ω behavior of $\Phi(\omega)$ is not enough to characterize the details of the Lanczos sequence.

In this section, we describe a number of general factors that determine the behavior of the spectral function $\Phi(\omega)$ as β is varied, and hence comment on universal behavior of Lanczos coefficients in systems with a discrete spectrum. These factors include the relation between β and the saddle point location E^* in the integrand defining $g(\omega, \beta)$, the size of $\kappa(\beta)$ and the suppression of the $|A(E, \omega)|^2$ for small ω due to the presence of a finite gap Δ in the energy spectrum of a the system.

Reference [15] showed that the slowest possible asymptotic decay for large β is $\Phi(\omega) \sim e^{-\frac{\beta}{2}|\omega|}$ in the case of the Wightman function. A number of results show that this slowest possible decay is saturated and results in the behavior of $b_n \sim \frac{\pi n}{\beta}$. At $\beta = 0$, the linear growth of Lanczos coefficients for local operators in discrete systems is associated with chaotic systems, because they are expected to saturate the bound $\Phi(\omega) \le Ce^{-\gamma\omega}$ consistent with locality. In field theory, the singularity of $C_\beta(t)$ at $t = i\frac{\beta}{2}$ implies the exponential decay above and the asymptotic growth $b_n \sim \frac{\pi n}{\beta}$ provided the dependence on n is smooth. An important point is to bridge the gap between these regimes discussed in the literature based on an analysis of (6.113).

In the large-system limit and local operators, $|A(E, \omega)|^2$ is typically expected to decay with a factor of $e^{-S(E)}$ and any other E-dependence will be subleading. Collecting the factors of ρ in (6.114), we find that $g(\beta, \omega)$ to be determined mainly by the E integral about the saddle-point E^*, defined by $S'(E^*) = \beta$, provided such E^* exists. The ω dependence of the integrand of $g(\omega, \beta)$ will be dominated by the contribution of the slice $|A(E^*, \omega)|^2$, which for small β probes contributions from the high-energy parts of the spectrum. For systems (such as a spin-chain) where $\rho'(E)$ changes sign and $\rho(E)$ decays after some E, at large enough β, E^* may not exist, and instead the ω-dependence would come from the lower limit of E in the integral defining g. Consistency with the asymptotic $e^{-\beta\frac{|\omega|}{2}}$ would imply constraints on the $|A(E^*, \omega)|^2$ along the ω-direction.

Another perspective is the following: for an infinite system with zero ground state energy the limits in defining g are

$$g(\omega, \beta) = \int_{\frac{|\omega|}{2}}^\infty e^{-\beta E}\rho\big(E + \frac{\omega}{2}\big)\rho\big(E - \frac{\omega}{2}\big)|A(E, \omega)|^2 dE, \qquad (6.115)$$

and this integral can be rewritten with the shift $\tilde{E} = E - \frac{|\omega|}{2}$

$$g(\omega, \beta) = e^{-\beta\frac{|\omega|}{2}} \int_0^\infty e^{-\beta\tilde{E}}\rho\big(\tilde{E} + |\omega|\big)\rho\big(\tilde{E} + |\omega|\big)|A(\tilde{E} + |\frac{\omega}{2}|, \omega)|^2 d\tilde{E}. \qquad (6.116)$$

Once again, a saddle point analysis of the integral in terms of the variables $\tilde{E}$ could be used to identify $\tilde{E}^*(\beta)$ which contributes most of the ω-dependence. If the ω-dependence coming from this region in (6.116) is slower than the $e^{-\beta\frac{|\omega|}{2}}$ coming from

the shift, that would explain the emergence of the field-theory answer and the asymptotic $\frac{\pi n}{\beta}$ growth. Such a mechanism is likely at play for local operators in integrable lattice models with a good field theory limit, where for small β, $g(\omega)$ decays *faster* than exponential. For large β, the low-energy matrix elements contribute and their slower ω-decay gets dominated by the exponential decay coming from the shift in (6.116). This can be made firmer if $|A(E, \omega)|^2$ vanishes beyond some $|\omega_{\max}|$, like in free integrable models. In that case the $e^{-\frac{\beta|\omega|}{2}}$ decay dominating for intermediate $\omega < \omega_{\max}$ will determine the moments and b_n.

The contribution of $\kappa(\beta)$ to the spectral sum, i.e. $C_\beta(0)$, relative to $g(\omega, \beta)$ will typically increase with β. This follows from the exponential (in β) suppression of exponentially many high-energy states, which diminish the contribution of $\kappa(\beta)$ to the moments for small β. The contribution of $\kappa(\beta)$ may be missed in the thermodynamic limit depending on the operators in question and the order of limits. However, for systems with a discrete spectrum, in the extreme $\beta\Delta \to \infty$ where $\Delta = E_1 - E_0$ is the first energy gap, the Wightman function will project onto the element $|A_{00}|^2$. In practice, g will typically decay faster as a function of β than κ, and $\kappa(\beta)$ will contribute to the moments at a $O(1)$ value of β. This is because only a finite region around E^* (or E_0) will contribute significantly to both κ and g. Of course, there could be systems in which the $\kappa(\beta)$ could be non-negligible, despite being a non-increasing function of β and we find such an example in massive XY model where the spin auto-correlation function has a t-independent piece equal to the magnetization.

The κ term has the effect of rescaling all but the zeroth moment by a factor of $\frac{1}{1+\kappa}$. This suggests that the Lanczos coefficients for $\kappa \neq 0$ could be related to the Lanczos coefficients for $\kappa = 0$. That is indeed the case. There exists the following relationship between the Lanczos coefficients $\tilde{b}_n$ at $\kappa = 0$ and b_n at non-zero κ:

$$b_{2n+1}^2 b_{2n+2}^2 = \tilde{b}_{2n+1}^2 \tilde{b}_{2n+2}^2, \quad \text{for} \quad n = 0, 1, 2... \tag{6.117}$$

$$b_{2n}^2 + b_{2n+1}^2 = \tilde{b}_{2n}^2 + \tilde{b}_{2n+1}^2, \quad \text{for} \quad n = 0, 1, 2... \tag{6.118}$$

And by definition,

$$b_0^2 = \frac{\int w^2 g(\omega)d\omega}{\kappa + \int g(\omega)d\omega}. \tag{6.119}$$

These suggest that b_n for even n are shifted relative to $\tilde{b}_n$ for odd n. For example, the effect of κ given $\tilde{b}_n$ smoothly depends on n and $\tilde{b}_n = \alpha n + o(n)$,

$$b_n = \tilde{b}_n + (-1)^n c_n, \tag{6.120}$$

where $c_n > 0$ for $n > 0$ can be shown to be slowly decaying to 0 with n. At large β, $g(\omega)$ becomes localized around $\omega = 0$ and, for typical A, κ dominates over the second moment of g and b_0 tends to 0. While the mathematical relation between b_n and $\tilde{b}_n$ continues to hold, in this range of β the Lanczos coefficients will become sensitive to the spectrum and for small n, the Lanczos coefficients will begin approaching their $\beta \to \infty$ value. The asymptotics for Lanczos coefficients are positive energy gaps and 0's in alternating odd-even pattern. We will address this in details in 6.3.2.

Yet another deformation, independent of κ is when $\beta\Delta \gg 1$ and the $e^{-\beta\Delta}$ factor in (6.114) suppresses the contribution of $|A(E,\omega)|^2$ as $\omega \to 0$. This could depend on whether the integrand in $g(\omega, \beta)$ gets a large contribution in the vicinity of $E \gtrapprox \Delta$. This would result in $g(\omega)$ approximately vanishing in the vicinity of $\omega = 0$. In free-field theory, $g(\omega)$ for a local field $\phi(x)$ will vanish exactly for $|\omega| \leq m$ where m is the mass for $\phi(x)$. $g(\omega)$ having a "gap" around $\omega = 0$ will be another source of staggering in the Lanczos coefficients. It may be possible to describe the Lanczos coefficients in this case through the use of the auxiliary measure described in the appendix G but one can deduce staggering from the fact that the difference of asymptotic value of b_n's for odd and even n has to be equal to the size of the gap in $g(\omega)$. In the case $\kappa = 0$, for small n the b_n's again converge to the positive gaps in alternating pattern, but this time b_0 converges to Δ. Including the effect of κ causes this staggering to "shift" such that the even b_n's vanish.

So far, the focus was on the behavior of Lanczos coefficients for $n \leq O(S)$, which survives in the thermodynamic limit. The Krylov space dimension N is $O(e^{2S})$ and for n/N finite, the behavior of the Lanczos coefficients is governed by the UV physics, i.e the b_n's are sensitive to the fact that the measure is a sum of Dirac mass points. Numerics show that on increasing β, b_n's continue to decay with the profile determined by the spectrum of M with the Lanczos coefficients showing progressively larger fluctuations about the mean. The transition to the UV behavior is controlled by the so-called Lanczos plateau where b_n is approximately equal to a constant b. The Lanczos plateau can still be described by the properties of the continuous measure $\Phi(\omega)$: if $\Phi(\omega) = 0$ for $\omega > \omega_{\max}$ (which necessarily exists in finite sytems), then $b = \frac{\omega_{max}}{2}$ and assuming smooth behavior for the growth $b_n \sim b(n)$, the n^* at which $b_n = b$ will be given by $n^* = b^{-1}(\frac{\omega_{\max}}{2})$. Hence, provided β is not extremely large such that the $\beta \to \infty$ answer kicks in throughout the entire Lanczos chain, $\Phi(\omega)$ will get more localized and the growth of moments will be suppressed by β-dependent factor. Thus the rate of growth of b_n's will slow down and n^* will increase. When $b_n \sim \frac{\pi n}{\beta}$, then $n^* \propto \beta$.

Above, we mentioned a few factors describing the deformation of the measure $\Phi(\omega)$ as β increases, including factors that go beyond asymptotic decay of $\Phi(\omega)$. As evidence, we plot the Lanczos coefficients for the XY model (see (A.38)) in thermodynamic limit along the Ising line at the critical point $h = 1, \gamma = 1$ as well as at a point with gap, $h = 1.1$ and $\gamma = 1$. At the critical point, for positive β the Lanczos coefficients show the $\frac{\pi n}{\beta}$ behavior with staggering due to the presence of nonzero κ (which is decreasing with β in this case). On increasing β, the plateau shifts to infinity and the field theory answer emerges see Fig 6.2b. At $h = 1.1$ there is a range of positive β, where the linear Lanczos growth emerges in presence of staggering from both κ and gap in measure due to $\Delta = \epsilon_0$ until saturation see Fig 6.1a. When $\beta\Delta \gg 1$, for small n the Lanczos coefficients begin to converge to gaps corresponding to lowest energy sums cf. 6.3.2 probed by the operator and b_1, $b_4 \dots$ converge to $2\epsilon_0$.

We now consider the Lanczos coefficients of free scalar field theory, which are plotted numerically for $d = 3$ and $m = 10$ in 6.2a. There is staggering for all β due to the presence of a mass gap m in the measure $\Phi(\omega)$, which sets the magnitude of

this staggering. In the large β limit and for small n, the subsequence b_{2n+1} is close to 0, while b_{2n} converge to the mass m, consistent with the results of section 6.3.2. The singularity of $C(t)$ in Euclidean time still implies asymptotic linear in n growth of b_n. In Appendix G we explain how this is captured by considering the combination $b_{2n} + b_{2n+1}$ for $n \gg 1$. Note the staggering pattern is different from that of XY model because $\kappa = 0$ here.

We illustrate these deformations using a toy model of $\Phi(\omega)$ in (A.30). This toy model takes into account the presence of a gap in the measure as $\omega \to 0$, the universal asymptotic $e^{-\beta \frac{|\omega|}{2}}$ decay, as well as an upper bound where $\Phi(\omega)$ gets cut off. This model accurately captures the behavior of Lanczos coefficients in both XY model and free scalar theory (for different values of its parameters). In particular, the Lanczos coefficients of the transverse spin operator in the XY model, in the regime of finite β (but $\beta\Delta$ not too large), is described by a finite value of $\omega_{\max}$ and $\Delta = 2\epsilon_0$, where ϵ_0 is the energy gap of a single particle state. Meanwhile, the behavior of massive free scalar field theory is captured by $\omega_{\max} \to \infty$ and $\Delta = m$. In the case of scalar field theory, the agreement with the Lanczos coefficients holds to a high degree of numerical precision because this toy measure is a very accurate approximation for the true $\Phi(\omega)$ in scalar field theory, especially for $d = 3$. We use this agreement to find an answer for b_n's in scalar field theory valid for $\beta\Delta \gg 1$ and small n:

$$
\begin{aligned}
b_{2n} &= \Delta + \frac{2n}{\beta} + \frac{(2n)^2}{2\beta^2 \Delta} + O\Big(\frac{1}{\beta^3 \Delta^2}\Big) \\
b_{2n+1} &= \frac{2n+1}{\beta} + \frac{(2n+1)^2}{2\beta^2 \Delta} + O\Big(\frac{1}{\beta^3 \Delta^2}\Big).
\end{aligned}
\tag{6.121}
$$

This expansion gets $o(n)$ corrections depending on the number of spacetime dimensions d and is consitent with the expansion computed in [93]. Beyond certain n the expansion (6.121) receives significant corrections from the subleading terms such that the asymptotic in n behavior kicks in

$$
\begin{aligned}
b_{2n} + b_{2n+1} &= \frac{4\pi n}{\beta} + o(n). \\
b_{2n} - b_{2n+1} &\approx m,
\end{aligned}
\tag{6.122}
$$

see appendix G for a discussion.

6.3.2 Large β asymptotics of the flow

A remarkable property of the Toda flow and its generalizations is that they offer an alternative perspective on the spectral theorem for symmetric matrices [94], [95]. We will illustrate this principle for the specific case of β evolution of T and M. Let us first consider the case when $\dot{\mu} = 0$. In that case the eigenvalues of T, λ_k are determined by the energy sums: $\lambda_k = -\frac{1}{2}(E_i + E_j)$. As $\beta \to \infty$, T converges to the diagonal matrix of its eigenvalues.

To see this, we first note that under the flow T remains a symmetric matrix and hence $T_{ii} < \max_k \lambda_k$. Therefore for any partial sums of diagonal elements $\sum_{i=0}^{l} T_{ii}$
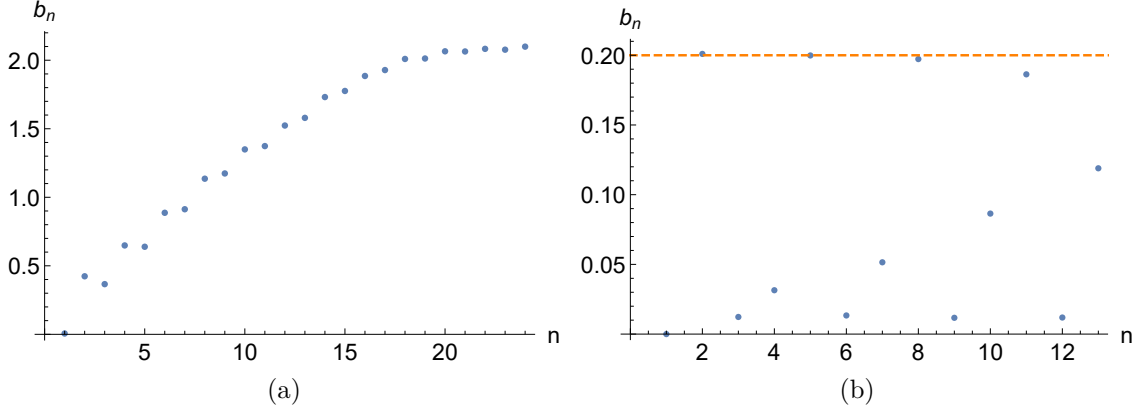
Figure 6.1: Lanczos coefficients for the XY model (see appendix H) at parameters $\gamma = 1$ and $h = 1.1$ (Ising limit) and $\beta = 25$ (left) and $\beta = 3000$ (right). In 6.1a, the "average" $\frac{\pi n}{\beta}$ dependence, until reaching saturation, is deformed by the presence of both κ and presence of gap in measure due to gap in spectrum. In 6.1b, for small n, the b_n are converging to the energy gaps. Orange dashed line is at $2\epsilon_0$, the energy gap connecting the vacuum to two-particle states in the free-fermion representation.

for finite l exists, and consequently the $\lim_{\beta \to \infty} T_{ii}$ exists. Now we notice that the β derivative of the partial sum is given by

$$\frac{d(\sum_{i=0}^{l} T_{ii})}{d\beta} = \sum_{j \leq l, k > l} T_{jk}^2 \tag{6.123}$$

For the $\lim_{\beta \to \infty} T_{ii}$ to exist all T_{jk} for $j \neq k$ have to vanish as $\beta \to \infty$. This shows how T converges to the diagonal matrix of its eigenvalues. In principle, T could converge to any diagonal matrix but the stable fixed-point of this flow is given by the diagonal matrix with the ordering $T_{kk} = \lambda_k$ such that $\lambda_0 = \lambda_1 > \lambda_2 = \lambda_3 \ldots$, where $\lambda_0 = -\frac{1}{2}(E_0 + E_1)$. Because the non-diagonal energy sums are symmetric in their two indices, each eigenvalue of T appears twice and $\lambda_{2k} = \lambda_{2k+1}$.

The Lanczos coefficients in this limit can be obtained using the following components of $[T, M]$:

$$[T, M]_{k,k+1} = b_i(\lambda_k - \lambda_{k+1}) \tag{6.124}$$

For this to vanish we must have $b_i = 0$ or $\lambda_i = \lambda_{i+1}$. The latter condition is satisfied for all even i so the b_{2i}'s do not have to vanish. To satisfy the former conditions, we find that all the $b_{2i+1} = 0$. Hence, strictly at the $\beta \to \infty$ limit, M becomes block diagonal, consisting of 2×2 blocks. This helps us deduce the even Lanczos coefficients by noticing that the diagonal matrix M^2 has $M_{2k,2k}^2 = M_{2k+1,2k+1}^2 = b_{2k}^2$. Then using the fact that T and M^2 share common eigenvectors, it follows that $b_{2k} = |E_i - E_j|$ given that $\lambda_{2k} = -\frac{1}{2}(E_i + E_j)$.

The situation is altered in a slight way in the case when $\dot{\mu} \neq 0$. By construction, T has a 0 eigenvalue in addition to the remaining eigenvalues proportional to non-diagonal energy sums. Asymptotically $\dot{\mu} = -E_0$ and that has the effect of shifting

$\lambda_0 = 0$ and $\lambda_1 = \lambda_2 > \lambda_3 = \lambda_4 > \ldots$, such that λ_i for $i \geq 1$ are proportional to the non-diagonal energy sums in decreasing order. The ordering argument for Lanczos coefficients follows as before such that for initial operators with nonzero diagonals, the even Lanczos coefficients vanish in the large β limit and the odd Lanczos coefficients converge to (positive) energy gaps.

Regarding the rate of convergence, inspecting the expression for $A_n(\beta)$ in energy eigenbasis would suggest that b_n's should converge exponentially to their infinite β values when

$$\beta \min_k \ (\lambda_k - \lambda_{k+1}) \gg 1 \tag{6.125}$$

similarly to what is known for Toda case [96]. In practice, the convergence of b_n's depends on n and we argue that b_n for small n will converge to the gaps faster with a rate related to $\beta\Delta$, where $\Delta = E_1 - E_0$. To see this we remind ourselves that this limit emerges when the spectral measure is a sum of discrete delta functions successively exponentially suppressed

$$\Phi(\omega) = |A_{00}|^2 \delta(\omega) + e^{-\beta\Delta} |A_{01}|^2 \delta(\omega - \Delta) + \ldots, \tag{6.126}$$

where we order the terms by the magnitude of the coefficients of the delta functions. The moments μ_{2n} for small n are largely determined by the location of the delta functions whose coefficients are leading in this ordering. However as n becomes large enough μ_{2n} will begin probing the tails of the spectral function $\Phi(\omega)$, despite it being exponentially suppressed. Provided that for larger ω the coefficients of successive delta functions don't decrease too rapidly, the asymptotic growth of μ_{2n} could still be well-approximated using a continuous approximation to Φ. Finally, while we provided this argument without considering the degeneracy in the spectrum of M, combining the arguments of this section with the construction in 6.2.3 would suggest the same convergence in the extended space.

6.3.3 K-Complexity

The mean position of the operator $O(t)$ in the Krylov chain is given by the Krylov complexity $K(t)$, defined as

$$K(t) = \sum_{n=0}^{n=N-1} n |\langle O_n, O(t) \rangle_\beta|^2. \tag{6.127}$$

When $K(t)$ receives most of its contributions from the Lanczos sequence in the region $n \leq O(S)$, it serves as a good measure of the spatial operator size. In this regime, if b_n is a smooth function of n, $K(t)$ can be calculated in the continuum limit using the discrete Schrödinger equation for the wavefunctions:

$$-i\frac{d}{dt}\langle O_n, O(t)\rangle_\beta = b_n \langle O_{n+1}, O(t)\rangle_\beta + b_{n-1}\langle O_{n+1}, O(t)\rangle_\beta. \tag{6.128}$$

We have identified certain β-dependent deformations of the Lanczos coefficients that induce odd-even staggering without altering the asymptotic slope. Numerical
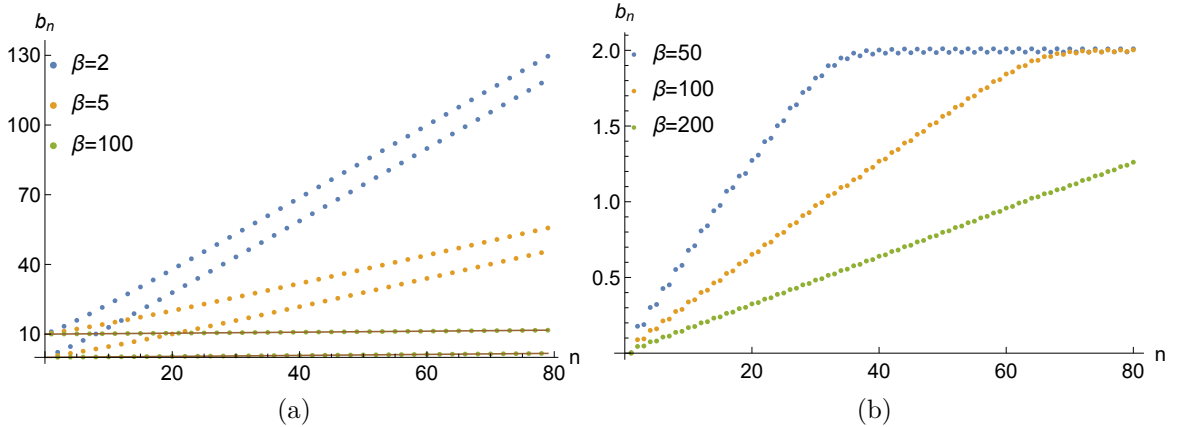
Figure 6.2: In 6.2a, the Lanzcos coefficients are shown for free scalar field-theory with mass $m = 10$ and different β. As β increases, b_n for even n approach 0 and for odd n they approach m at rate given by (6.121). For larger n they continue to grow linearly satisfying (6.122). The solid line superimposed with $\beta = 100$ values display the fit with (6.121). In 6.2b we show the emerging field theory behavior for b_n for the Ising critical point ($\gamma = 1$ and $h = 1$) in the 1D quantum XY chain.

evidence presented in [97] supports the results of a continuum limit calculation with staggering, where (6.128) is transformed into a Dirac equation. This suggests that for sufficiently large times $t > t_0$

$$K(t) \sim e^{\frac{2\pi}{\beta}(t-t_0)}, \tag{6.129}$$

where t_0 is a characteristic time scale, and it is assumed that b_n asymptotically grow as $b_n \approx \frac{\pi n}{\beta}$. In infinite systems, even in the large $\beta\Delta$ case, in the regime where the initial b_n start converging to gaps, (6.129) is expected to hold provided that our arguments are valid and that the asymptotic growth is maintained. The effect of half of the b_n approaching 0 will be to induce oscillatory behavior in the early growth of $K(t)$. This can be seen by considering a perturbation of M at infinite β, which will be a direct sum of 2×2 blocks of nonzero b_n. From the discussion presented in section 6.3.1, we can infer that for free scalar field theory, $K(t)$ will transition from an oscillatory behavior

$$K(t) \approx \sin^2(mt) \tag{6.130}$$

at early times $t \propto \beta$ for fixed m, to the asymptotic behavior (6.129), consistent with the numerics presented in [93].

In finite systems for fixed β, $K(t)$ slows down after this exponential growth (or polynomial growth if b_n grow slower than linearly), but it continues to grow for $O(e^{2S}) > t > O(S)$. This regime is primarily determined by the spectrum of M, which also determines the b_n for $n > O(S)$ and causes their "ringdown". As discussed in section 6.3.1, at large β, this ringdown becomes distorted, leading to a large deviation about the mean.

Increasing β in finite systems slows down the growth of complexity. When there is large staggering due to $\beta\Delta \gg 1$, or when the growth of b_n is significantly modified by the convergence of b_n to gaps, $K(t)$ may not exhibit obvious growth. In this regime, $K(t)$ will show only oscillatory behavior due to the finite number of contributing modes. Since it is challenging to characterize the time-dependence of $K(t)$ further, we examine the infinite time average or mean position of $O(t)$ in the Krylov chain after time-averaging:

$$\overline{K}(\beta) = \lim_{t\to\infty} \frac{1}{T} \int_0^T K(t)dt = \sum_{n,k} n|U_{0k}|^2 |U_{nk}|^2, \tag{6.131}$$

where $\overline{K}$ has been expanded as sum over the overlap (see (6.29)) between the Krylov basis indexed by n and the eigenvectors of M indexed by k

In the large β limit, the overlap $|U_{0k}|^2$ will localize towards $\omega_k = 0$, responsible for the localization of the measure $\Phi(\omega)$. This suggests that $\overline{K}$ should decay with β. For operators with no projections on the nullspace of Liouvillian, $\lim_{\beta\to\infty} \overline{K}(\beta) = \frac{1}{2}$, while for operators with a nonzero diagonal in energy basis, $\lim_{\beta\to\infty} \overline{K}(\beta) = 0$. $\overline{K}$ can be estimated using analytical tools in some cases [98], and we leave the task of analytically predicting $\overline{K}(\beta)$ for future work. In spin-chains, we numerically find that for large enough β, $\overline{K} \sim Nr(\beta)$, where $r(\beta) \approx ce^{-\frac{\Delta\beta}{2}}$ at large β, as illustrated in Figure 6.3. At intermediate β, $r(\beta)$ likely receives polynomial corrections to the exponential decay. We conjecture that such behavior will persist to larger system sizes. This suggests that by tuning β, the mean position $\overline{K}(\beta)$ can display various scalings as a function of system size.

6.4 Summary: Temperature dependence and large-β asymptotics

In this chapter we studied the temperature dependence of Lanczos coefficients inherited through a temperature-dependent inner product for operators. First, we cast this temperature dependence as an integrable system of equations related to the Toda hierarchy. For initial operators with no diagonal components in the energy basis this dynamics is described in terms of two Toda chains, while for a generic operator, one of the Toda chains is modified.

We also directly analyzed how the spectral measure of generic systems could evolve as a function of temperature. Through this analysis we identified two distinct mechanisms that cause the cause "staggering" in the Lanczos sequence. One source of staggering is the off-diagonal part $g(\omega, \beta)$ of the measure Φ (6.113) developing a gap around $\omega = 0$. Another source is the presence of a diagonal term $\sim \delta(\omega)$ in the measure Φ with a large contribution to the spectral sum. We illustrate the former mechanism by a toy model (appendix G) with tunable parameters.

Additionally, we described universal features of the Lanczos chain at low temperatures $\beta \to \infty$. Specifically, in a finite-dimensional Krylov space, as $\beta \to \infty$, half of the Lanczos coefficients vanish while the other half converge to positive energy gaps, with the b_n's for smaller n converging more quickly to their asymptotic values. This feature appears to persist in the thermodynamic limit.
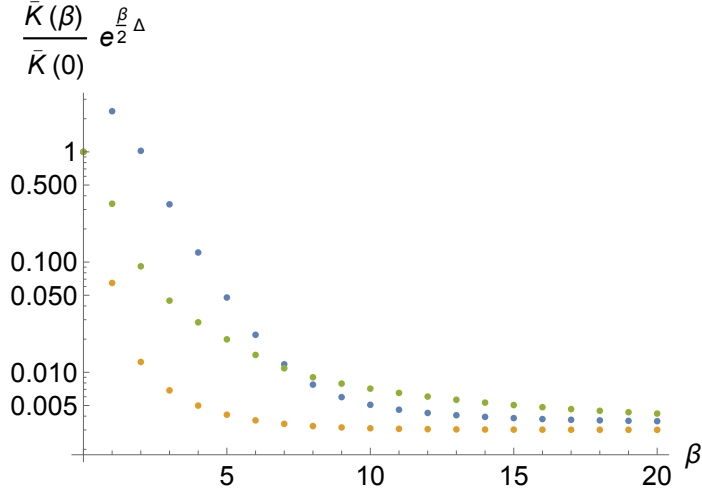
Figure 6.3: The quantity $\frac{\bar{K}(\beta)}{\bar{K}(0)}e^{\frac{\beta}{2}\Delta}$ is plotted against β for the integrable Ising (blue), Heisenberg (orange) and non-integrable Ising (green) models for initial operators with non-zero diagonal in the energy eigenbasis. The parameters have been fine-tuned so that the gap $\Delta \cong 3.46$ is the same for the three models. The saturation for large β indicates a universal exponential behavior of the time-average complexity $\frac{\bar{K}(\beta)}{\bar{K}(0)} \propto e^{-\beta\frac{\Delta}{2}}$.

We argued that the time-averaged Krylov complexity decreases exponentially at large β as $\bar{K}(\beta) \sim e^{-\Delta\beta/2}$, up to polynomial corrections, where Δ is the first energy gap. We conjecture that this behavior persists for arbitrarily large system sizes.

These results pave the way for a more systematic understanding of how temperature affects Krylov space and complexity. Future directions include:

1. The Lax equations (6.72) have been studied in the literature. It would be interesting to identify solutions that describe the Lanczos coefficients of realistic physical systems

2. The equations of motion (6.72) could be used to numerically calculate temperature-dependent Lanczos coefficients. This can be done perturbatively given knowledge of the Lanczos coefficients at some fixed β. To accomplish this a study of numerical stability of the equations is needed.

3. An important step would be to study the Krylov complexity $K(t)$ as the inverse temperature β is tuned to large values. Fresh analytical tools to incorporate the effects of staggering could give new analytical solutions describing the true behavior of $K(t)$ in systems with a gap. In particular, is $K(t)$ always a decreasing function of β for generic system in the limit of large N? How can the generalized MSS bound be formulated in the $\beta \to \infty$ limit in systems where the Lanczos coefficients converge to gaps?

4. The Lanczos algorithm has historically been a tool to numerically obtain extremal eigenvalues. Our analysis of the large β behavior of Lanczos algorithm suggests that it can be used to find the energy gaps related to low-lying energies of the Hamiltonian. This could be especially promising with the combined use of quantum algorithms with Krylov methods on quantum devices.

Chapter 7 Conclusion

In this dissertation, we studied topics in high-energy physics through the lens of information theory.

In Chapter 3, we developed a connection between error-correcting codes and Narain CFTs. This unites and generalizes previous constructions relating Narain CFTs to binary and $\mathbb{F}_4$ codes [8, 29] [32], as well as codes over $\mathbb{Z}_p$ [33]. The torus partition function of the CFT is given in terms of the code enumerator polynomial, which has properties that guarantee the modular invariance of the partition function. In this way, one can rephrase and solve modular bootstrap constraints in terms of polynomials.

We provided explicit constructions for all (conjectural) optimal Narain theories for $c \leq 8$, [27]. By averaging over codes, we showed the existence of theories at large central charge c whose spectral gap Δ^* scales linearly $\Delta^* \propto c/(2\pi e)$, with the coefficient being maximal, as conjectured in [23].

From this construction, and its generalizations [11], it is apparent that any Narain CFT can be constructed from codes. This provides a powerful framework to systematically study the space of Narain CFTs. In Chapter 4 we used the code formalism to study the Narain CFTs at the points of enhanced symmetry, described by A, D, E affine Lie algebras at level 1. The problem of classifying modular invariants and calculating fusion rules can be phrased fully in terms of 2-dimensional codes. We proceeded to evaluate the Poincaré series of the vacuum character in each case.

In Chapter 5 we turned our attention to the entanglement entropy of 1-dimensional fermionic chains. Specifically, we studied fermionic chains with long-range interactions, where the hopping and pairing terms fall-off with distance as a power-law with exponent α. For systems with a smooth continuum limit, the scaling of the entanglement entropy at the thermodynamic limit is determined by the low-energy effective theory and is described by area law.

For disordered models, as well as for non-disordered Hamiltonians without a smooth continuum limit, the scaling of entanglement entropy is not constrained in this way. These systems exhibit a regime of intermediate fractal scaling, whose exponent is a continuous function of α. There is no universal critical value α_c at which the scaling of entanglement across all free fermion systems transitions to the conventional scaling.

In chapter 6 we studied the temperature-dependence of Lanczos coefficients and Krylov complexity. The temperature dependence of the Lanczos coefficients is described by an integrable system of equations related to the Toda hierarchy. For initial operators with vanishing diagonal in the energy basis, this evolution is described in terms of two decoupled Toda chains, while for a general operator, one of the Toda chains is modified.

We proceeded to identify two mechanisms that cause "staggering" in the Lanczos sequence. These mechanisms are best described in terms of the spectral measure $\Phi(\omega)$. One cause of staggering is the off-diagonal part of the measure developing a

gap at $\omega = 0$. The other source is the presence of a diagonal term in the measure, proportional to $\sim \delta(\omega)$.

In addition, we identified universal properties of the Lanczos coefficients at low temperatures. In a finite-dimensional Krylov space, as $\beta \to \infty$, half of the Lanczos coefficients vanish while the other half converge to positive energy gaps. The Lanczos coefficients that appear early in the chain converge much faster to their asymptotic values that the later ones. We show numerical evidence that this feature persists in the thermodynamic limit. We also show numerical evidence that the time-averaged Krylov complexity decreases exponentially at large inverse temperature β as $\bar{K}(\beta) \sim e^{-\Delta\beta/2}$, up to polynomial corrections, where Δ is the first energy gap. We believe that this behavior persists for arbitrarily large system sizes.

Appendices

Appendix A: Shortest vector bound

Let us consider a two-dimensional Euclidean lattice Λ with the scalar product g_2. Using rotation and up to an overall rescaling basis vectors can be chosen to be 1 and $\tau = \tau_1 + i\tau_2$, where we introduced complex coordinates on $\mathbb{R}^2$. In other words

$$g_2 = \Lambda^T \Lambda, \qquad \Lambda = \alpha \begin{pmatrix} 1 & \tau_1 \\ 0 & \tau_2 \end{pmatrix}, \tag{A.1}$$

and α is some scalar factor. Using $GL(2, \mathbb{Z})$ transformations, together with an appropriate rotation and rescaling, we can bring τ to belong to fundamental domain

$$|\tau_1| \leq 1/2, \quad \tau_2 \geq 0, \quad |\tau| \geq 1. \tag{A.2}$$

In this case the shortest vector is $\alpha(1, 0)^T$ and its norm is α^2. From (A.1) we find $\alpha^4 = \det g_2 / \tau_2^2$ and from (A.2) we know $\tau_2^2 \geq 3/4$. We therefore find the bound

$$\alpha^2 \leq \frac{2}{\sqrt{3}} \sqrt{\det g_2}, \tag{A.3}$$

which in many cases is conservative. Applying that to (3.25) we obtain (3.26).

Appendix B: Fractal Scaling in Disordered Models

The exponent γ can be inferred from (5.16) as a function of β, though the derivation of β as a function of α is a task to be done. Let us assume that the density of ground state is $\frac{1}{L} \text{Tr}(\overline{C}) = \frac{1}{2}$. This mild assumption follows from the symmetry of averaged single-particle Hamiltonian about zero. This leads to $\frac{1}{L} \text{Tr}(\overline{C}^2) = \frac{1}{2}$. Since the diagonal elements scale differently than the off-diagonal ones, let $\overline{C_{ii}^2} = m$. This fixes normalization κ as:

$$\kappa = \frac{\frac{1}{2} - m}{2(H_{2\beta}(L-1) - \frac{H_{2\beta-1}(L-1)}{L})} \tag{A.4}$$

Where $H_j(n)$ is the generalized Harmonic number of order j. Plugging in the same κ and m, in expression of $\overline{N}_A^2$

$$\Delta \overline{N}_A^2 = (\frac{1}{2} - m)(L_A - \frac{H_{2\beta}(L_A - 1)L_A - H_{2\beta-1}(L_A - 1)}{H_{2\beta}(L-1) - \frac{H_{2\beta-1}(L-1)}{L}}) \tag{A.5}$$

In (A.5) an accurate estimate is provided, consistent with the scaling of $\overline{S}(L_A)$ on plugging in the numerically obtained β and m see Fig. 5.3b. The undetermined value

of m does not alter scaling of entanglement but changes the coefficient. For finite L and arbitrary β (A.5) does not give a simple power-law. However, for $1 < 2\beta < 2$ and large enough L_A and L, $\overline{N}_A^2$ scales as $L_A^{2-2\beta}$.

For the $\alpha = 0$ limit, $\beta = 0$, and this computation gives the accurate estimate of $\overline{N}_A^2$ as $\frac{L_A}{4} - \frac{L_A L}{4(L^2-L)}$. In fact, the leading order expression for $S(L_A) = L_A \log(2)$ follows directly from analytic continuation (in n) of $\text{Tr}(C_A^n) \approx L_A 2^{-(n+1)}$, neglecting correlations among the elements of C_A for $L_A \ll L$ and likewise for $(\mathbb{I} - C_A)$.

Appendix C: A Ground State With Maximal Entanglement Entropy

Consider a system of even size L with the interaction Hamiltonian

$$H = \sum_{i,j=1}^{L} V_{ij} c_i^\dagger c_j, \quad V_{ij} = V(i-j), \quad V(r) = \delta_{r,\frac{L}{2}} + \delta_{r,-\frac{L}{2}}. \tag{A.6}$$

The single-particle eigenvalues are

$$a_k = \sum_{j=1}^{L} V(j) e^{ij\frac{2\pi k}{L}} = (-1)^k. \tag{A.7}$$

The correlation matrix is given by

$$C(r) = \frac{1}{L} \sum_{j=1}^{L} e^{2\pi i \frac{rj}{L}} \Theta(-a_j) = \frac{1}{L} \sum_{j \text{ odd}} e^{2\pi i \frac{rj}{L}} \tag{A.8}$$
$$= \frac{1}{2}(\delta_{r,0} - \delta_{r,\frac{L}{2}} - \delta_{r,-\frac{L}{2}}).$$

For a subsystem A of size $L/2$ or smaller, the correlation matrix is diagonal $C_A = \frac{1}{2}\mathbb{I}$. This implies maximal growth of entanglement entropy

$$S(L_A) = L_A \log 2. \tag{A.9}$$

Appendix D: Block Toeplitz Matrix

The correlation matrix (5.22) is a block Toeplitz matrix, which can be written as

$$C_A(i-j) = \frac{1}{2\pi} \int_0^{2\pi} dk \, G(k) e^{ik(i-j)}, \tag{A.10}$$

where the matrix symbol is

$$G(k) = \frac{1}{\lambda(k)} \begin{pmatrix} \alpha(k) + \mu & ib(k) \\ -ib(k) & -\alpha(k) - \mu \end{pmatrix}. \tag{A.11}$$

We apply the method of [81] to obtain c_{eff} from this block-matrix symbol. We parametrize the latter as

$$G(k) = \cos \phi_k \sigma_z + \sin \phi_k \sigma_y. \tag{A.12}$$

We define the coefficient of the logarithmic term to be $c_{\text{eff}}/3$. It is determined by the discontinuities of the symbol. Let $\{k_n\}$, be the values of k at which the symbol is discontinuous. Then, c_{eff} is given by the integral

$$c_{\text{eff}} = \frac{3}{\pi^2} \sum_n \int_{\cos \xi_n}^1 dx \; \log \frac{1-x}{1+x} \log \frac{\sqrt{1-x^2}}{\sqrt{x^2 - \cos^2 \xi_n} + \sin \xi_n}, \tag{A.13}$$

where

$$\xi_n = \frac{\delta \phi_{k_n}}{2}, \tag{A.14}$$

and $\delta \phi_{k_n}$ is the discontinuity of ϕ_k at $k = k_n$.

For (5.20), and $\alpha_h = \alpha_p = \alpha$, there is only one discontinuity at $k = 0$

$$\delta \phi_0 = \begin{cases} \pi(1-\alpha) & 0 \le \alpha < 1 \\ 0 & \alpha \ge 1 \end{cases}. \tag{A.15}$$

On tuning μ to the critical value $\mu = -a(\pi)$, a second discontinuity arises at $k = \pi$, such that $\delta \phi_\pi = \pi$. In this case, the integral (A.13) results to $c_{\text{eff}} = \frac{1}{2}$.

For (5.21), and $\alpha_h = \alpha_p = \alpha$, the discontinuity is again at $k = 0$

$$\delta \phi_0 = \begin{cases} \pi & 0 \le \alpha < 1 \\ 2 \arctan \frac{\pi}{2 \log 2} & \alpha = 1 \\ 0 & \alpha > 1 \end{cases}. \tag{A.16}$$

This leads to $c_{\text{eff}} = \frac{1}{2}$ for $\alpha < 1$ and $c_{\text{eff}} \approx 0.437$ for $\alpha = 1$.

Appendix E: Quantum Harmonic Oscillator

Consider the quantum harmonic oscillator $H = \omega(\frac{1}{2} + a^\dagger a)$ with initial operator $A_0 = x$. The Krylov space is two-dimensional $A_0 = x$, $A_1 = -ip$, with Lanczos coefficient $b_0 = \omega$.

The matrix T_K as defined in (6.107) is

$$T_K = \omega \coth \frac{\beta \omega}{2} \begin{pmatrix} 1 & 0 \\ 0 & 1 \end{pmatrix}. \tag{A.17}$$

This means that $B = 0$ and the equation (6.107) becomes

$$\dot{T}_K = -T_K^2 + Y. \tag{A.18}$$

The matrix Y can be calculated independently from

$$Y_{ij} = \frac{1}{4} \langle \{H, x\}, \{H, x\} \rangle \delta_{ij} = \omega^2 \frac{\cosh(\beta \omega)}{\cosh(\beta \omega) - 1} \delta_{ij}. \tag{A.19}$$

It is now straightforward to confirm that equation (A.18) is satisfied.

Appendix F: Modified Toda Dynamics

The constants c_i in terms of the eigenvalues of T_{even} are

$$c_i = 2(-1)^{i+1}\frac{e_{n-i}(\{\lambda_j\})}{e_{n-1}(\{\lambda_j\})}, \tag{A.20}$$

where e_i denotes the elementary homogeneous symmetric polynomial of order i. Due to one of the eigenvalues vanishing, we have the following constraint

$$\mathcal{C} = \sum_{k=1}^{n} kc_k \mathcal{I}_k^{\text{even}} = 0. \tag{A.21}$$

Let us define the generating function

$$G(z) = \det(1 + zT_{\text{even}}) = e^{z\mathcal{I}_1^{\text{even}}}e^{-z^2\mathcal{I}_2^{\text{even}}}e^{z^3\mathcal{I}_3^{\text{even}}}\cdots. \tag{A.22}$$

We can write the elementary polynomials as follows

$$e_i = \frac{1}{i!}G^{(i)}(0). \tag{A.23}$$

The constraint can be written as

$$\mathcal{C} \equiv \frac{1}{n!}G^{(n)}(0). \tag{A.24}$$

Note that it vanishes on-shell $\mathcal{C}|_{os} = 0$.

We can calculate

$$\frac{\partial}{\partial \mathcal{I}_i}G(z) = (-1)^{i+1}z^i G(z). \tag{A.25}$$

Therefore

$$\frac{\partial \mathcal{C}}{\partial \mathcal{I}_i} = (-1)^{i+1}\frac{d^n}{dz^n}(z^i G(z))|_{z=0} = n!e_{n-i}(-1)^{i+1}. \tag{A.26}$$

We can write

$$c_i = \frac{2}{\frac{\partial \mathcal{C}}{\partial \mathcal{I}_1}}\frac{\partial \mathcal{C}}{\partial \mathcal{I}_i}. \tag{A.27}$$

The Hamiltonian can now be written as

$$\mathcal{H}' = \frac{2}{\frac{\partial \mathcal{C}}{\partial \mathcal{I}_1}\Big|_{os}}\sum \frac{\partial \mathcal{C}}{\partial \mathcal{I}_i}\Big|_{os}\mathcal{I}_i. \tag{A.28}$$

The same flow is generated by the following function, since it has the same gradient as $\mathcal{H}$ on the surface of constraint

$$\mathcal{H}' = \frac{2\mathcal{C}}{\frac{\partial \mathcal{C}}{\partial \mathcal{I}_1}\Big|_{os}}. \tag{A.29}$$

Appendix G: A Toy Model for $\Phi(\omega)$

Here we consider a toy model of an orthogonality measure, which captures the generic features of Lanczos coefficients that come into play with β-dependence. To avoid extraneous factors of 2, we make the shift $\beta \to 2\beta$ and the measure is:

$$\Phi(\omega) = \begin{cases} \frac{1}{\mathcal{N}} e^{-\beta|\omega|} + \kappa\delta(\omega), & \text{if } \Delta < |\omega| < \omega_{\max} \\ 0, & \text{otherwise} \end{cases}, \qquad (A.30)$$

where the normalization is

$$\mathcal{N} = \frac{2\left(e^{-\beta\Delta} - e^{-\beta\omega_{\max}}\right)}{\beta}. \qquad (A.31)$$

First we consider the case when $\kappa = 0$ such that Δ models the presence of a "gap" where the measure vanishes, which in this case arises from the spectral gap in density of states relevant for large β. $\omega_{\max}$ is a hard cutoff for the measure arising from presence of maximum energy in a finite system. The even moments are given by (while the odd moments vanish)

$$\mu_{2n} = \frac{e^{\beta(\Delta+\omega_{\max})}\left(\Gamma(2n+1, \beta\Delta) - \Gamma\left(2n+1, \beta\omega_{\max}\right)\right)}{\beta^{2n}(e^{\beta\omega_{\max}} - e^{\beta\Delta})} \qquad (A.32)$$

Let's consider the case with $\Delta = 0$ first. The saddle point expression of μ_{2n} approximately matches the $\omega_{\max} \to \infty$ answer, and we find that for $2n < \beta\omega_{\max}$, $\mu_{2n} \approx \frac{2n!}{\beta^{2n}}$. For $2n > \beta\omega_{\max}$, using the leading order asymptotics of the Gamma functions, we find that $\mu_{2n} \approx \frac{\beta\omega_{\max}^{2n+1}}{2n}e^{-\beta\omega_{max}}$

Thus, for $\Delta = 0$,

$$\mu_{2n} \approx \begin{cases} \frac{2n!}{\beta^{2n}}, & \text{for } 2n < \beta\omega_{\max} \\ \frac{\beta\omega_{\max}^{2n+1}}{2n}e^{-\beta\omega_{\max}} & \text{for } 2n > \beta\omega_{\max} \end{cases} \qquad (A.33)$$

For $n < n^* = \frac{\beta\omega_{\max}}{\pi}$, the Lanczos coefficents go as $b_n \approx \frac{\pi}{2\beta}n$, and for $n > n^*$, $b_n \approx \frac{\pi}{2\beta}n^*$. The saturation of Lanczos coefficients can be inferred from the following bound

$$\mu_{2n} \geq b_0^2 b_1^2 \dots b_{n-1}^2, \qquad (A.34)$$

since indefinite growth of b_n's would be incompatible with the asymptotic growth of μ_{2n} for $2n > \beta\omega_{\max}$. The inequality above does not fix the proportionality constants in n^*, which instead is fixed by continuity of b_n with its asymptotic value.

In general, a full analysis for the case incorporating the effects of the gap Δ can be carried out when the recurrence coefficents for the measure $\Phi(\sqrt{\omega})/\sqrt{\omega}$ ($\omega > 0$) is known [99]. Nonetheless [99], this will generically cause an even-odd splitting of b_n's such that in terms of variables $\lim_{n\to\infty} b_{2n} = b_e$ and $\lim_{n\to\infty} b_{2n+1} = b_o$, $b_e - b_o = \Delta$. For this model the sum $b_e + b_o$ will coincide for any choice of Δ, as it is set by $\omega_{\max}/2$.

The mathematical argument is summarized in the following. The true interval of orthogonality which determines the support of the continuous part of the measure

$\Phi(\omega)$ is in general fixed by the limiting values (as $n \to \infty$) of recursion coefficients. Consider the more general recursion relation:

$$P_{n+1}(\omega) = P_n(\omega) - a_n P_n(\omega) - b_{n-1}^2 P_{n-1}(\omega). \tag{A.35}$$

The true interval of orthogonality of an arbitrary measure $\Phi(\omega)$ is given by $[a - 2b, a + 2b]$ where

$$\lim_{n\to\infty} a_n = a \quad \text{and} \quad \lim_{n\to\infty} b_n = b. \tag{A.36}$$

In general, for an even measure $\Phi(\omega)$, $a_n = 0$ so it follows that if the support of the bounded measure is $[-\omega_{\max}, \omega_{\max}]$, then $b = \frac{\omega_{\max}}{2}$. Now, to describe the case with Δ, one instead considers the auxilliary orthogonality measure $\Phi(\sqrt{\omega})/\sqrt{\omega}$ with the interval of orthogonality $[\Delta^2, \omega_{\max}^2]$. The recursion with respect to this measure becomes

$$P'_{n+1}(\omega) = P'_n(\omega) - a'_n P_n(\omega) - b_{n-1}'^2 P'_{n-1}(\omega) \tag{A.37}$$

Where the relations $a'_n = b_{2n}^2 + b_{2n+1}^2$ and $b_{n-1}'^2 = b_{2n}^2 b_{2n+1}^2$ can be inferred. Now from (A.36), it follows that $b_e - b_o = \Delta$ and $b_e + b_o = \omega_{\max}$. Thus knowledge of a'_n and b'_n may be used to obtain b_n. Nonzero Δ implies even-odd splitting for the Lanczos coefficients, see Fig A.1a for illustration in toy model. To see that we note that the difference of their limiting values must match Δ.

In practice for the toy model and also for free scalar field theory, we find that $b_{2n} - b_{2n+1}$ quickly converges to a value close to Δ (m in scalar field theory). The sum $b_{2n} + b_{2n+1} \approx \frac{4\pi n}{\beta} + o(n)$ for large enough $n >> \beta\Delta$. This convergence could be understood through the following way: the asymptotics of the recurrence coefficients of the auxilliary measure, a'_n and b'_n are determined by the asymptotic decay of the auxilliary measure. The asymptotic decay of the auxilliary measure as $\omega_{\max} \to \infty$ is independent of the choice of Δ and therefore for large n, the moments of the auxilliary measure approach the moments of the auxillary measure as $\Delta = 0$. The asymptotic a'_n and b'_n of course will still retain an imprint of Δ such that the difference $a'_n - b'_{n-1}$ converges to the Δ^2. However the sum $a'_n + b'_{n-1}$ will approach the same limit, just like in the case of $\omega_{\max}$ where it follows from the theorem mentioned above. As an illustration of this, see Fig A.1b.
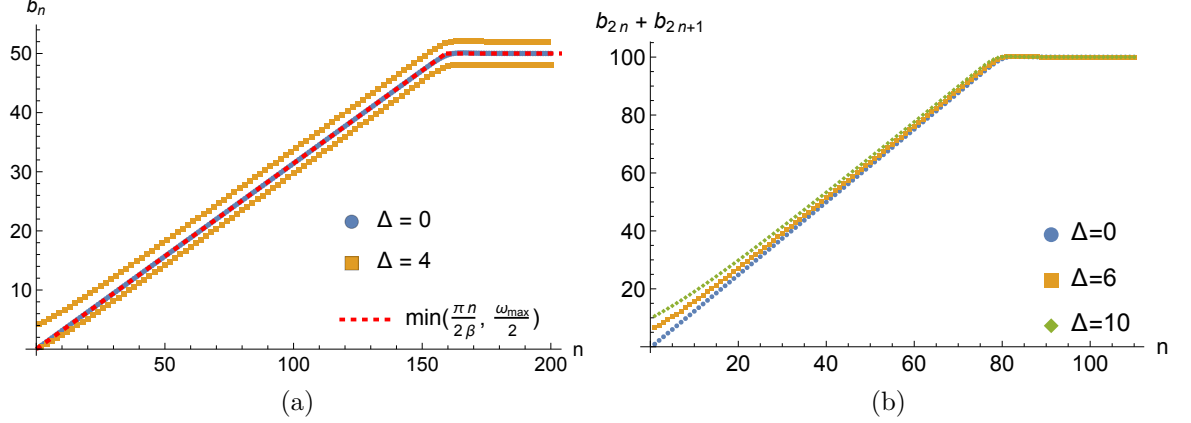
Figure A.1: Lanczos coefficients corresponding to the orthogonality measure (A.30) for $\beta = 5$ and $\omega_{max} = 100$. (a) Compares the Lanczos coefficents for the gapless case with the case when $\Delta = 3$. (b) shows the convergence of $b_{2n} + b_{2n+1}$ for different values of Δ with n.

Appendix H: XY model

Consider the integrable XY model with periodic boundary conditions, described by the Hamiltonian:

$$H = \sum_{j=1}^{N}[(1+\gamma)S_j^x S_{j+1}^x + (1-\gamma)S_j^y S_{j+1}^y] - h\sum_{j=1}^{N} S_j^z. \tag{A.38}$$

We consider the limit where $N \to \infty$.

Define the following auto-correlation function at inverse temperature β:

$$C_\beta(t) = \langle S_0^z S_0^z \rangle = \frac{\text{tr}\{e^{-\beta H/2}S_0^z e^{-\beta H/2}S_0^z(t)\}}{\text{tr}(e^{-\beta H})}. \tag{A.39}$$

The Hamiltonian (A.38) can be diagonalized by the Jordan-Wigner transformation. The quasi-particles energies are

$$\epsilon_k = \sqrt{(\cos k - h)^2 + \gamma^2 \sin^2 k}. \tag{A.40}$$

In addition, define

$$\lambda_k = \frac{1}{2}\arctan\frac{\gamma \sin k}{\cos k - h}. \tag{A.41}$$

Note that in all formulas of this section, we make the choice $\arctan(x) \in (0, \pi]$.

The auto-correlation function is given by [100]

$$C_\beta(t) = m_z^2 + \left[\frac{1}{2\pi}\int_0^\pi dk\ \cos(\epsilon_k t)\text{sech}\left(\frac{1}{2}\beta\epsilon_k\right)\right]^2 + \left[\frac{1}{2\pi}\int_0^\pi dk\ \cos(2\lambda_k)\sin(t\epsilon_k)\text{sech}\left(\frac{1}{2}\beta\epsilon_k\right)\right]^2,$$
$$\tag{A.42}$$

where
$$m_z \equiv \langle S_0^z \rangle_\beta = -\frac{1}{2\pi} \int_0^\pi dk \; \cos\left(\arctan\frac{\gamma \sin k}{\cos k - h}\right).$$ (A.43)

In order to calculate the moments, we first Taylor expand as follows

$$\frac{1}{2\pi} \int_0^\pi dk \; \cos(\epsilon_k t) \operatorname{sech}\left(\frac{1}{2}\beta\epsilon_k\right) = \sum_{n=0}^\infty u_{2n} t^{2n},$$ (A.44)

$$\frac{1}{2\pi} \int_0^\pi dk \; \cos(2\lambda_k) \sin(t\epsilon_k) \operatorname{sech}\left(\frac{1}{2}\beta\epsilon_k\right) = \sum v_n t^{2n},$$ (A.45)

where the expansion coefficients are

$$u_{2n} = \frac{(-1)^n}{2\pi} \frac{\epsilon_k^{2n} \operatorname{sech}\left(\frac{1}{2}\beta\epsilon_k\right)}{(2n)!},$$ (A.46)

$$v_{2n} = \frac{(-1)^n}{2\pi} \frac{\epsilon_k^{2n} \operatorname{sech}\left(\frac{1}{2}\beta\epsilon_k\right) \cos(2\lambda_k)}{(2n+1)!}.$$ (A.47)

The moments are now given by

$$\mu_{2n} = \frac{1}{M_0} \left(m_z^2 \delta_{n,0} + n! \sum_{i=0}^n (u_i u_{n-i} + v_i v_{n-i}) \right),$$ (A.48)

where M_0 is a constant chosen such that $\mu_0 = 1$.

Bibliography

[1] James M. Bardeen, B. Carter, and S. W. Hawking. The Four laws of black hole mechanics. *Commun. Math. Phys.*, 31:161–170, 1973.

[2] Jacob D. Bekenstein. Generalized second law of thermodynamics in black-hole physics. *Phys. Rev. D*, 9:3292–3300, Jun 1974.

[3] Juan Maldacena. The large-n limit of superconformal field theories and supergravity. *International Journal of Theoretical Physics*, 38(4):1113–1133, 1999.

[4] Shinsei Ryu and Tadashi Takayanagi. Holographic derivation of entanglement entropy from the anti–de sitter space/conformal field theory correspondence. *Physical Review Letters*, 96(18), May 2006.

[5] Mark Van Raamsdonk. Building up spacetime with quantum entanglement. *Gen. Rel. Grav.*, 42:2323–2329, 2010.

[6] Ahmed Almheiri, Xi Dong, and Daniel Harlow. Bulk locality and quantum error correction in ads/cft. *Journal of High Energy Physics*, 2015(4), April 2015.

[7] Fernando Pastawski, Beni Yoshida, Daniel Harlow, and John Preskill. Holographic quantum error-correcting codes: toy models for the bulk/boundary correspondence. *Journal of High Energy Physics*, 2015(6), June 2015.

[8] Anatoly Dymarsky and Alfred Shapere. Quantum stabilizer codes, lattices, and cfts. *Journal of High Energy Physics*, 2021(3):1–84, 2021.

[9] Phil Saad, Stephen H. Shenker, and Douglas Stanford. Jt gravity as a matrix integral. *arXiv:1903.11115*, 2019.

[10] Alexander Maloney and Edward Witten. Averaging over narain moduli space. *Journal of High Energy Physics*, 2020(10), October 2020.

[11] Ofer Aharony, Anatoly Dymarsky, and Alfred D. Shapere. Holographic description of narain cfts and their code-based ensembles. *arXiv:2310.06012*, 2023.

[12] Douglas Stanford and Leonard Susskind. Complexity and shock wave geometries. *Physical Review D*, 90(12), December 2014.

[13] Adam R. Brown, Daniel A. Roberts, Leonard Susskind, Brian Swingle, and Ying Zhao. Holographic complexity equals bulk action? *Physical Review Letters*, 116(19), May 2016.

[14] Juan Maldacena, Stephen H. Shenker, and Douglas Stanford. A bound on chaos. *Journal of High Energy Physics*, 2016(8), August 2016.

[15] Daniel E. Parker, Xiangyu Cao, Alexander Avdoshkin, Thomas Scaffidi, and Ehud Altman. A universal operator growth hypothesis. *Phys. Rev. X*, 9:041017, Oct 2019.

[16] Alexander Avdoshkin, Anatoly Dymarsky, and Michael Smolkin. Krylov complexity in quantum field theory, and beyond. *JHEP*, 06:066, 2024.

[17] John Horton Conway and Neil James Alexander Sloane. *Sphere packings, lattices and groups*, volume 290. Springer Science & Business Media, 2013.

[18] Philippe Di Francesco, Pierre Mathieu, and David Sénéchal. Conformal field theory. 1999.

[19] K. S. Narain, M. H. Sarmadi, and Edward Witten. A Note on Toroidal Compactification of Heterotic String Theory. *Nucl. Phys. B*, 279:369–379, 1987.

[20] Nikolaos Angelinos, Debarghya Chakraborty, and Anatoly Dymarsky. Optimal narain cfts from codes. *Journal of High Energy Physics*, 2022(11), November 2022.

[21] Simeon Hellerman. A universal inequality for CFT and quantum gravity. *Journal of High Energy Physics*, 2011(8), aug 2011.

[22] Thomas Hartman, Christoph A Keller, and Bogdan Stoica. Universal spectrum of 2d conformal field theory in the large c limit. *Journal of High Energy Physics*, 2014(9):1–29, 2014.

[23] Anatoly Dymarsky and Alfred Shapere. Comments on the holographic description of narain theories. *Journal of High Energy Physics*, 2021(10), oct 2021.

[24] Thomas Hartman, Dalimil Mazáč, and Leonardo Rastelli. Sphere packing and quantum gravity. *Journal of High Energy Physics*, 2019(12):48, 2019.

[25] Henry Cohn and Noam Elkies. New upper bounds on sphere packings i. *Annals of Mathematics*, pages 689–714, 2003.

[26] Nima Afkhami-Jeddi, Henry Cohn, Thomas Hartman, David de Laat, and Amirhossein Tajdini. High-dimensional sphere packing and the modular bootstrap. *arXiv:2006.02560*, 2020.

[27] Nima Afkhami-Jeddi, Henry Cohn, Thomas Hartman, and Amirhossein Tajdini. Free partition functions and an averaged holographic duality. *Journal of High Energy Physics*, 2021(1):1–43, 2021.

[28] Gabriele Nebe, Eric M Rains, and Neil James Alexander Sloane. *Self-dual codes and invariant theory*, volume 17. Springer, 2006.

[29] Anatoly Dymarsky and Alfred Shapere. Solutions of modular bootstrap constraints from quantum codes. *Physical Review Letters*, 126(16):161602, 2021.

[30] Louise Dolan, Peter Goddard, and P Montague. Conformal field theories, representations and lattice constructions. *Communications in mathematical physics*, 179(1):61–120, 1996.

[31] Matthew Buican, Anatoly Dymarsky, and Rajath Radhakrishnan. Quantum codes, cfts, and defects. *arXiv:2112.12162*, 2021.

[32] Anatoly Dymarsky and Adar Sharon. Non-rational narain cfts from codes over f4. *Journal of High Energy Physics*, 2021(11):1–34, 2021.

[33] Shinichiro Yahagi. Narain cfts and error-correcting codes on finite fields. *arXiv:2203.10848*, 2022.

[34] Yuma Furuta. Relation between spectra of narain cfts and properties of associated boolean functions. *arXiv:2203.11643*, 2022.

[35] Johan Henriksson, Ashish Kakkar, and Brian McPeak. Codes, lattices, and cfts at higher genus. *arXiv:2112.05168*, 2021.

[36] Johan Henriksson, Ashish Kakkar, and Brian McPeak. Narain cfts and quantum codes at higher genus. *arXiv:2205.00025*, 2022.

[37] Nima Afkhami-Jeddi, Henry Cohn, Thomas Hartman, and Amirhossein Tajdini. Free partition functions and an averaged holographic duality. *arXiv:2006.04839*, 2020.

[38] Scott Collier and Alexander Maloney. Wormholes and spectral statistics in the Narain ensemble. *JHEP*, 03:004, 2022.

[39] Mikhail Vasil'evich Kozlov. The correcting capacities of linear codes. In *Doklady Akademii Nauk*, volume 186, pages 275–278. Russian Academy of Sciences, 1969.

[40] John Pierce. Limit distribution of the minimum distance of random linear codes. *IEEE Transactions on Information Theory*, 13(4):595–599, 1967.

[41] Salvatore Torquato and Frank H Stillinger. New conjectural lower bounds on the optimal density of sphere packings. *Experimental Mathematics*, 15(3):307–331, 2006.

[42] Philippe Delsarte. An algebraic approach to the association schemes of coding theory. *Philips Res. Rep. Suppl.*, 10, 1973.

[43] Refat Ismail, Ashish Kakkar, and Anatoly Dymarsky. A quantum annealing approach to the minimum distance problem of quantum codes. *arXiv:2404.17703*, 4 2024.

[44] Alexander Maloney and Edward Witten. Quantum gravity partition functions in three dimensions. *Journal of High Energy Physics*, 2010(2), February 2010.

[45] Viraj Meruliya and Sunil Mukhi. Ads3 gravity and rcft ensembles with multiple invariants. *Journal of High Energy Physics*, 2021(8), August 2021.

[46] Debarghya Chakraborty and Nikolaos Angelinos. Entanglement entropy in ground states of long-range fermionic systems. *arXiv:2302.06743*, 2024.

[47] J. Eisert, M. Cramer, and M. B. Plenio. Colloquium: Area laws for the entanglement entropy. *Rev. Mod. Phys.*, 82:277–306, Feb 2010.

[48] Don N. Page. Average entropy of a subsystem. *Phys. Rev. Lett.*, 71:1291–1294, Aug 1993.

[49] Alexei Kitaev and John Preskill. Topological entanglement entropy. *Physical Review Letters*, 96(11), mar 2006.

[50] Mukund Rangamani and Tadashi Takayanagi. *Holographic Entanglement Entropy*. Springer International Publishing, 2017.

[51] J. Ignacio Cirac, David Pé rez-García, Norbert Schuch, and Frank Verstraete. Matrix product states and projected entangled pair states: Concepts, symmetries, theorems. *Reviews of Modern Physics*, 93(4), dec 2021.

[52] Thomas Koffel, M. Lewenstein, and Luca Tagliacozzo. Entanglement entropy for the long-range ising chain in a transverse field. *Physical Review Letters*, 109(26), dec 2012.

[53] Davide Vodola, Luca Lepori, Elisa Ercolessi, Alexey V. Gorshkov, and Guido Pupillo. Kitaev chains with long-range pairing. *Physical Review Letters*, 113(15), oct 2014.

[54] Miguel F. Paulos, Slava Rychkov, Balt C. van Rees, and Bernardo Zan. Conformal invariance in the long-range ising model. *Nuclear Physics B*, 902:246–291, jan 2016.

[55] Noam Chai, Anatoly Dymarsky, and Michael Smolkin. Model of persistent breaking of discrete symmetry. *Physical Review Letters*, 128(1), jan 2022.

[56] Wei Li and Tadashi Takayanagi. Holography and entanglement in flat spacetime. *Physical Review Letters*, 106(14), apr 2011.

[57] Tomotaka Kuwahara and Keiji Saito. Area law of noncritical ground states in 1d long-range interacting systems. *Nature Communications*, 11(1), sep 2020.

[58] M B Hastings. An area law for one-dimensional quantum systems. *Journal of Statistical Mechanics: Theory and Experiment*, 2007(08):P08024–P08024, aug 2007.

[59] Itai Arad, Alexei Kitaev, Zeph Landau, and Umesh Vazirani. An area law and sub-exponential algorithm for 1d systems. *arXiv:1301.1162*, 2013.

[60] G Vitagliano, A Riera, and J I Latorre. Volume-law scaling for the entanglement entropy in spin-1/2 chains. *New Journal of Physics*, 12(11):113049, nov 2010.

[61] Javier Rodríguez-Laguna, Jérôme Dubail, Giovanni Ramírez, Pasquale Calabrese, and Germán Sierra. More on the rainbow chain: entanglement, space-time geometry and thermal states. *Journal of Physics A: Mathematical and Theoretical*, 50(16):164001, March 2017.

[62] Ingo Peschel. Calculation of reduced density matrices from correlation functions. *Journal of Physics A: Mathematical and General*, 36(14):L205–L208, mar 2003.

[63] Pasquale Calabrese and John Cardy. Entanglement entropy and conformal field theory. *Journal of Physics A: Mathematical and Theoretical*, 42(50):504005, dec 2009.

[64] B.-Q. Jin and V. E. Korepin. Quantum spin chain, toeplitz determinants and the fisher–hartwig conjecture. *Journal of Statistical Physics*, 116(1-4):79–95, aug 2004.

[65] Dimitri Gioev and Israel Klich. Entanglement entropy of fermions in any dimension and the widom conjecture. *Physical Review Letters*, 96(10), mar 2006.

[66] Brian Swingle. Entanglement entropy and the fermi surface. *Physical Review Letters*, 105(5), jul 2010.

[67] Chunxiao Liu, Xiao Chen, and Leon Balents. Quantum entanglement of the sachdev-ye-kitaev models. *Physical Review B*, 97(24), jun 2018.

[68] M. Fannes, B. Haegeman, and M. Mosonyi. Entropy growth of shift-invariant states on a quantum spin chain. *Journal of Mathematical Physics*, 44(12):6005, 2003.

[69] S. Farkas and Z. Zimborá s. On the sharpness of the zero-entropy-density conjecture. *Journal of Mathematical Physics*, 46(12):123301, dec 2005.

[70] Lev Vidmar, Lucas Hackl, Eugenio Bianchi, and Marcos Rigol. Entanglement entropy of eigenstates of quadratic fermionic hamiltonians. *Physical Review Letters*, 119(2), jul 2017.

[71] Patrycja Łydż ba, Marcos Rigol, and Lev Vidmar. Eigenstate entanglement entropy in random quadratic hamiltonians. *Physical Review Letters*, 125(18), oct 2020.

[72] Ranjan Modak and Tanay Nag. Many-body dynamics in long-range hopping models in the presence of correlated and uncorrelated disorder. *Phys. Rev. Res.*, 2:012074, Mar 2020.

[73] Róbert Juhász. Testing the validity of random-singlet state for long-range hopping models through the scaling of entanglement entropy. *Phys. Rev. B*, 105:014206, Jan 2022.

[74] Alexander D. Mirlin, Yan V. Fyodorov, Frank-Michael Dittes, Javier Quezada, and Thomas H. Seligman. Transition from localized to extended eigenstates in the ensemble of power-law random banded matrices. *Phys. Rev. E*, 54:3221–3230, Oct 1996.

[75] A. D. Mirlin and F. Evers. Multifractality and critical fluctuations at the anderson transition. *Phys. Rev. B*, 62:7920–7933, Sep 2000.

[76] Davide Vodola, Luca Lepori, Elisa Ercolessi, and Guido Pupillo. Long-range ising and kitaev models: phases, correlations and edge modes. *New Journal of Physics*, 18(1):015001, dec 2015.

[77] Andrea Solfanelli, Stefano Ruffo, Sauro Succi, and Nicolò Defenu. Logarithmic, fractal and volume-law entanglement in a kitaev chain with long-range hopping and pairing. *Journal of High Energy Physics*, 2023(5), May 2023.

[78] Subir Sachdev. Quantum phase transitions. *Physics World*, 12(4):33, apr 1999.

[79] L. Lepori, D. Vodola, G. Pupillo, G. Gori, and A. Trombettoni. Effective theory and breakdown of conformal symmetry in a long-range quantum chain. *Annals of Physics*, 374:35–66, nov 2016.

[80] Filiberto Ares, José G. Esteve, Fernando Falceto, and Amilcar R. de Queiroz. Entanglement in fermionic chains with finite-range coupling and broken symmetries. *Physical Review A*, 92(4), oct 2015.

[81] Filiberto Ares, José G. Esteve, Fernando Falceto, and Amilcar R. de Queiroz. Entanglement entropy in the long-range kitaev chain. *Phys. Rev. A*, 97:062301, Jun 2018.

[82] G. Vidal. Entanglement renormalization. *Physical Review Letters*, 99(22), nov 2007.

[83] Jutho Haegeman, Tobias J. Osborne, Henri Verschelde, and Frank Verstraete. Entanglement renormalization for quantum fields in real space. *Physical Review Letters*, 110(10), mar 2013.

[84] H Casini and M Huerta. A c-theorem for entanglement entropy. *Journal of Physics A: Mathematical and Theoretical*, 40(25):7031–7036, jun 2007.

[85] Hong Liu and Márk Mezei. A refinement of entanglement entropy and the number of degrees of freedom. *Journal of High Energy Physics*, 2013(4), apr 2013.

[86] Brian Swingle and T. Senthil. Universal crossovers between entanglement entropy and thermal entropy. *Physical Review B*, 87(4), jan 2013.

[87] Sergey N. Solodukhin. Entanglement entropy of black holes. *Living Reviews in Relativity*, 14(1), oct 2011.

[88] Noburo Shiba and Tadashi Takayanagi. Volume law for the entanglement entropy in non-local QFTs. *Journal of High Energy Physics*, 2014(2), feb 2014.

[89] A. Bermudez, L. Tagliacozzo, G. Sierra, and P. Richerme. Long-range heisenberg models in quasiperiodically driven crystals of trapped ions. *Physical Review B*, 95(2), jan 2017.

[90] G. Refael and J. E. Moore. Entanglement entropy of random quantum critical points in one dimension. *Physical Review Letters*, 93(26), dec 2004.

[91] Anatoly Dymarsky and Alexander Gorsky. Quantum chaos as delocalization in krylov space. *Phys. Rev. B*, 102:085137, Aug 2020.

[92] M Kac and Pierre van Moerbeke. On an explicitly soluble system of nonlinear differential equations related to certain toda lattices. *Advances in Mathematics*, 16, 1975.

[93] Hugo A. Camargo, Viktor Jahnke, Keun-Young Kim, and Mitsuhiro Nishida. Krylov complexity in free and interacting scalar field theories with bounded power spectrum. *Journal of High Energy Physics*, 2023(5), May 2023.

[94] Jürgen Moser. Finitely many mass points on the line under the influence of an exponential potential – an integrable system. In J. Moser, editor, *Dynamical Systems, Theory and Applications*, volume 38, pages 467–497. 1975.

[95] L.C. Li P. Deift and C. Tomei. Toda flows with infinitely many variables. *Journal of Functional Analysis*, 64, 1985.

[96] T. Nanda P. Deift and C. Tomei. Ordinary differential equations and the symmetric eigenvalue problem. *Journal on Numerical Analysis*, 20, 1983.

[97] Anatoly Dymarsky and Michael Smolkin. Krylov complexity in conformal field theory. *Phys. Rev. D*, 104:L081702, Oct 2021.

[98] Debarghya Chakraborty, Refat Ismail, and Anatoly Dymarsky. Asymptotics of krylov space, work in progress.

[99] Theodore S Chihara. *An Introduction to Orthogonal Polynomials*. Dover, 2011.

[100] Th. Niemeijer. Some exact calculations on a chain of spins 1/2. *Physica*, 36, 1967.

Vita

Nikolaos Angelinos

Place of Birth:

- Athens, Greece

Education:

- University of Crete, Heraklion, Greece
  M.A. in Physics, May. 2019

- University of Crete, Heraklion, Greece
  B.S. in Physics, August 2014

Professional Positions:

- Graduate Teaching Assistant, University of Kentucky, Fall 2019–Spring 2023

Honors

- Huffaker Travel Grant 2023

- MacAdam Fellowship, University of Kentucky, 07/2023–06/2024

Publications & Preprints:

- "Temperature dependence of Lanczos coefficients"
  N. Angelinos, D. Chakraborty, A. Dymarsky,
  Manuscript under preparation

- "Entanglement Entropy in Ground States of Long-Range Fermionic Systems"
  D. Chakraborty, N. Angelinos
  arXiv:2302.06743

- "Optimal Narain CFTs from codes"
  N. Angelinos, D. Chakraborty, A. Dymarsky
  JHEP 11 (2022) 118

- "Critical scaling of the AC conductivity and momentum dissipation",
  N. Angelinos, E. Kiritsis, F. Peña-Benitez
  Phys.Rev.Res. 3 (2021) 1, 013028